Gravitino Phenomenology with MG/ME at colliders

arXiv:1010.4255 [EPJC71(2011)], K.Hagiwara(KEK), KM, Y.Takaesu
arXiv:1101.1289 [appear in EPJC], KM, Y.Takaesu(KEK)
arXiv:1105.????, KM, B.Oexl(VUB), Y.Takaesu(KEK); KM, P. de Aquino(UCL)

Kentarou Mawatari

Vrije Universiteit Brussel

Theoretiche Natuurkunde (TENA)
Elementaire Deeltjes Fysica (ELEM)
Inter-univ. Institute for High Energies (IIHE)

MG Spring 2011 @ Fermilab, 06/05/2011

New phenomenology group at the Vrije U. Brussel

- A 5-year GOA (Geconcentreerde Onderzoeksactie) project on "Supersymmetric models and their signatures at the LHC"
    - Ben Craps, Alexander Sevrin, Alberto Mariotti (theory) - F. 9th floor
    - Catherine De Clercq, Jorgen D'Hondt (experiment) - G. 0th and 1st floor
    - Fabio Maltoni (pheno) - UCL/CP3
- The main goal of the project is
    - to establish a complete chain from fundamental theory to experiment.
    - to use this chain to study possible signatures of SUSY models at the LHC.
- New phenomenology members since last fall
    - Kentarou Mawatari (from U. Heidelberg) -Project leader
    - Phillip Grajek (from KEK, Japan) -PD
    - Bettina Oexl (from U. Tuebingen) -PhD
- Contact to
    - http://we.vub.ac.be/dntk/onderzoek/GOAindex.htm
    - pheno@vub.ac.be

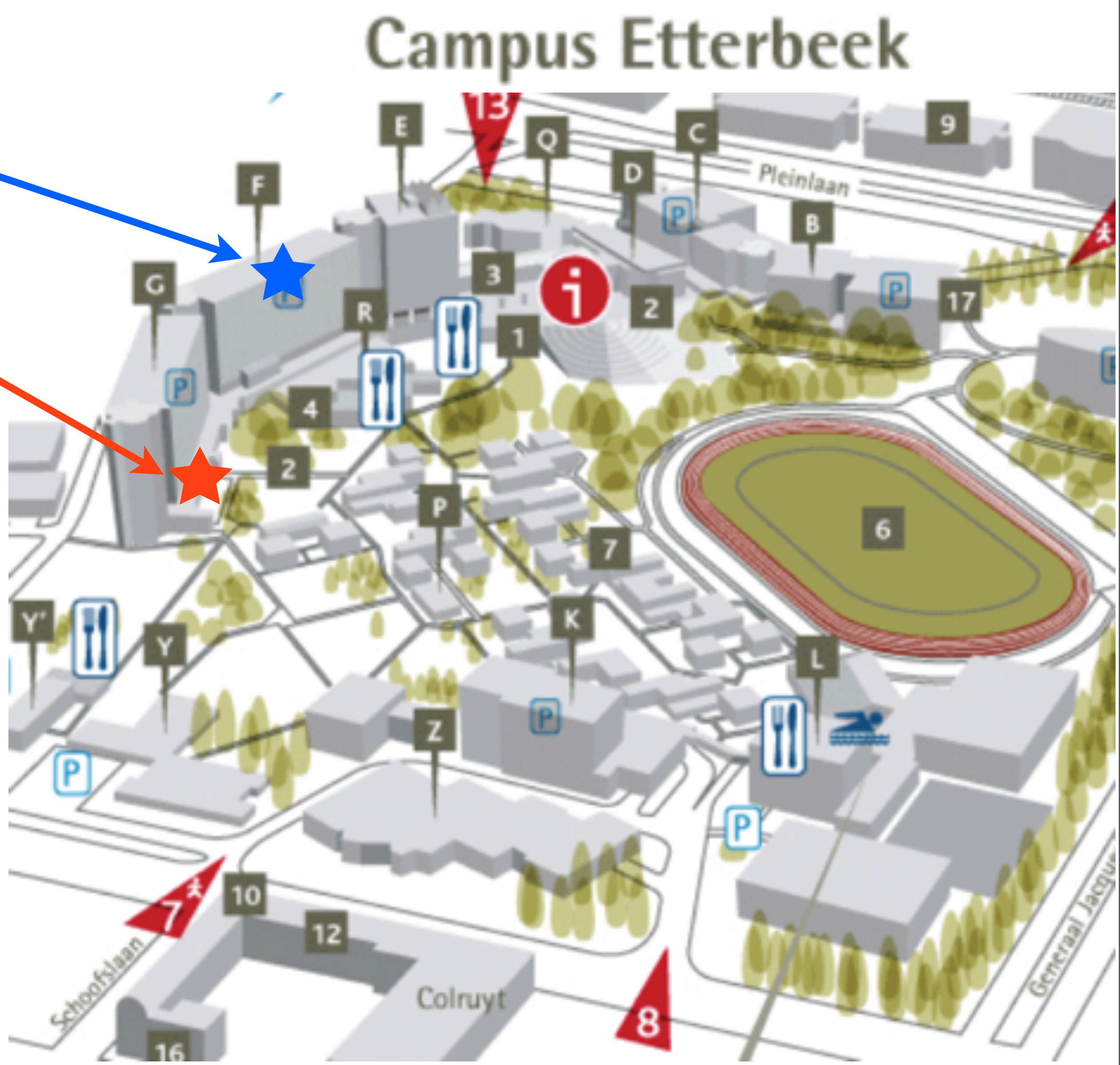

New phenomenology group at the Vrije U. Brussel

- A 5-year GOA (Geconcentreerde Onderzoeksactie) project on "Supersymmetric models and their signatures at the LHC"
  - Ben Craps, Alexander Sevrin, Alberto Mariotti (theory) - F. 9th floor
  - Catherine De Clercq, Jorgen D'Hondt (experiment) - G. 0th and 1st floor
  - Fabio Maltoni (pheno) - UCL/CP3
- The main goal of the project is
  - to establish a complete chain from fundamental theory to experiment.
  - to use this chain to study possible signatures of SUSY models at the LHC.
- New phenomenology members since last fall
  - Kentarou Mawatari (from U. Heidelberg) -Project leader
  - Phillip Grajek (from KEK, Japan) -PD
  - Bettina Oexl (from U.Tuebingen) -PhD
- Contact to
  - http://we.vub.ac.be/dntk/onderzoek/GOAindex.htm
  - pheno@vub.ac.be

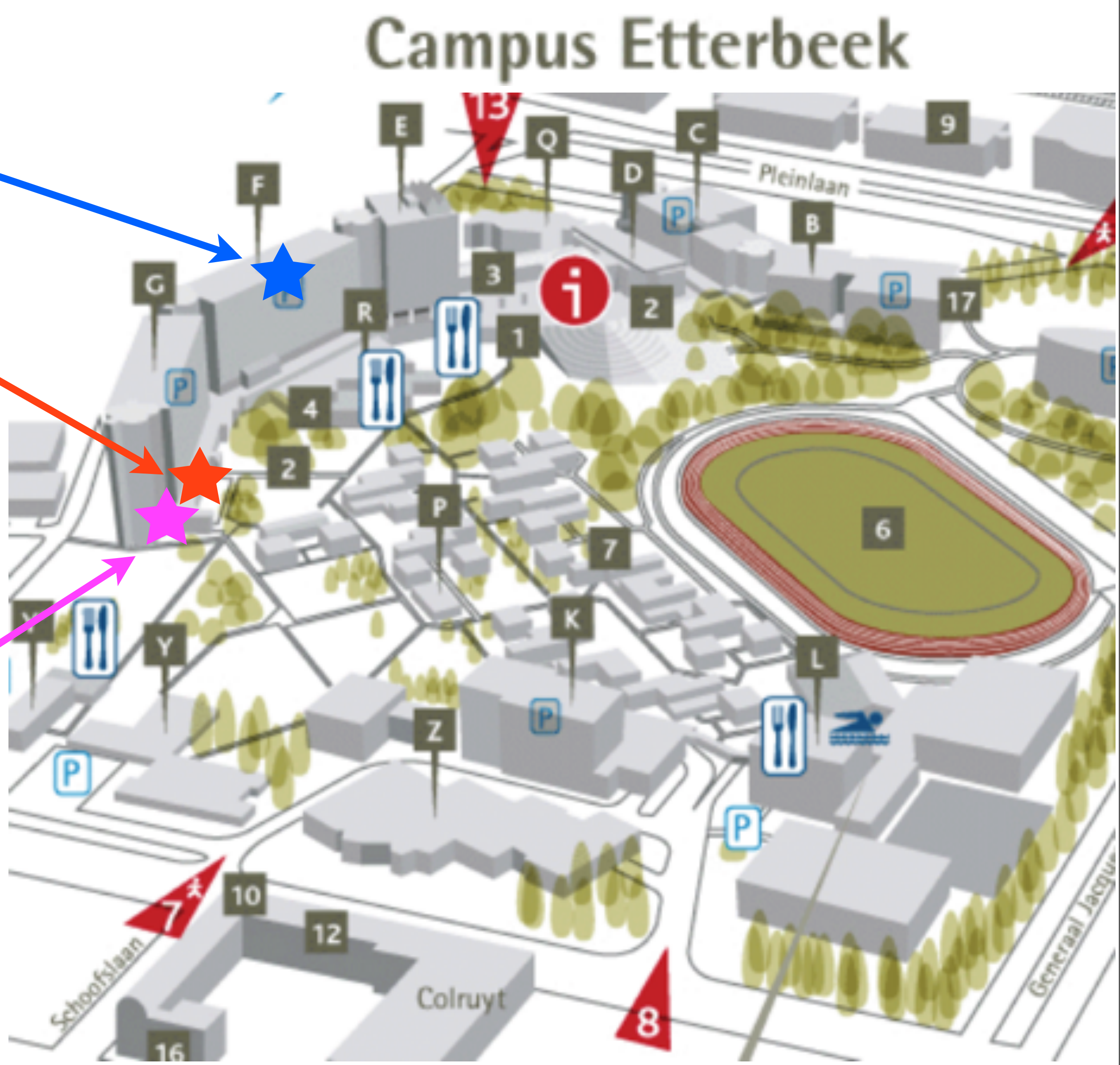

VUB pheno activities

- Phenomenological tool oriented:

MadGraph 2010 : BSM and more

from Monday 04 October 2010 at **08:00** to Friday 08 October 2010 at **18:00** (Europe/Brussels)
at VUB

Description *MadGraph team meeting of Fall 2010 for core developers and collaborators. The main focus will be on BSM tools and physics projects (SUSY in particular).*

- Theory oriented:

Vrije Universiteit Brussel

Gauge Mediated Supersymmetry Breaking workshop

2-3 December 2010 *VUB*

Europe/Brussels timezone

Overview
Timetable
Registration
Registration Form
List of registrants
Accommodation
How to reach the VUB

Supersymmetry is a compelling candidate for beyond the Standard Model physics. With the start of the Large Hadron Collider at CERN it is crucial to study phenomenological signatures of supersymmetry breaking at low scale. In this context gauge mediated supersymmetry breaking has recently been the subject of renewed interest and important developments.

This workshop will bring together experts in the field, with the aim of stimulating discussions and ideas in this fast developing area.

List of confirmed speakers:

Steven Abel, Matthew Buican, Matthew Dolan, Emilian Dudas, Gabriele Ferretti, Mark Goodsell, Zohar Komargodski, Kentarou Mawatari, Moritz McGarrie, Andrea Romanino.

Outlines

- **Gravitino**
  - What is a gravitino?
  - Mass of the gravitino
- **Phenomenology with MG/ME**
  - HELAS and MadGraph/MadEvent
    with gravitino/goldstinos
  - The gravitino-goldstino equivalence
- **at Colliders**
  - Collider signatures for a gravitino LSP
    with gluino NLSP, neutralino NLSP, slepton NLSP, ...

Outlines

theory

- **Gravitino**
  - What is a gravitino?
  - Mass of the gravitino
- **Phenomenology with MG/ME**
  - HELAS and MadGraph/MadEvent with gravitino/goldstinos
  - The gravitino-goldstino equivalence
- **at Colliders**
  - Collider signatures for a gravitino LSP with gluino NLSP, neutralino NLSP, slepton NLSP, ...

Outlines

- **Gravitino**
  - What is a gravitino?
  - Mass of the gravitino
- **Phenomenology with MG/ME**
  - HELAS and MadGraph/MadEvent with gravitino/goldstinos
  - The gravitino-goldstino equivalence
- **at Colliders**
  - Collider signatures for a gravitino LSP with gluino NLSP, neutralino NLSP, slepton NLSP, ...

theory

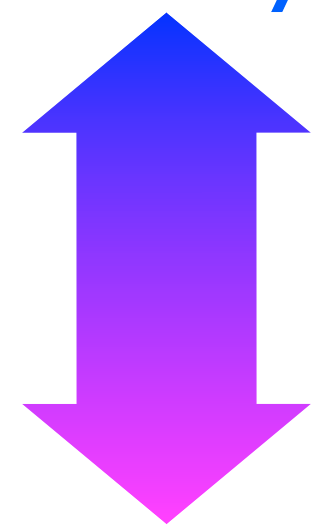

phenomenology

Outlines

- **Gravitino**
  - What is a gravitino?
  - Mass of the gravitino
- **Phenomenology with MG/ME**
  - HELAS and MadGraph/MadEvent with gravitino/goldstinos
  - The gravitino-goldstino equivalence
- **at Colliders**
  - Collider signatures for a gravitino LSP with gluino NLSP, neutralino NLSP, slepton NLSP, ...

Gravitinos

- spin-3/2 superpartners of gravitons in local supersymmetric extensions to the Standard Model (Supergravity).
- If SUSY breaks spontaneously, gravitinos absorb massless spin-1/2 goldstinos and become massive by the super-Higgs mechanism.

Massive gravitinos

Massive gravitinos

- SU(2)xU(1) gauge symmetry

Massive gravitinos

- SU(2)xU(1) gauge symmetry

  ➡ spontaneously broken

(spin)

+1

0 (Goldstone boson)

-1

Higgs mechanism

W, Z bosons

Massive gravitinos

- SU(2)xU(1) gauge symmetry

➡ spontaneously broken

(spin)

------ +1

------ 0 (Goldstone boson)

------ -1 Higgs mechanism

W, Z bosons

➡ discovered in 1983

➡ established the EW theory

Massive gravitinos

- SU(2)xU(1) gauge symmetry

➡ spontaneously broken

(spin)
+1
0 (Goldstone boson)
-1

Higgs mechanism
W, Z bosons

➡ discovered in 1983

➡ established the EW theory

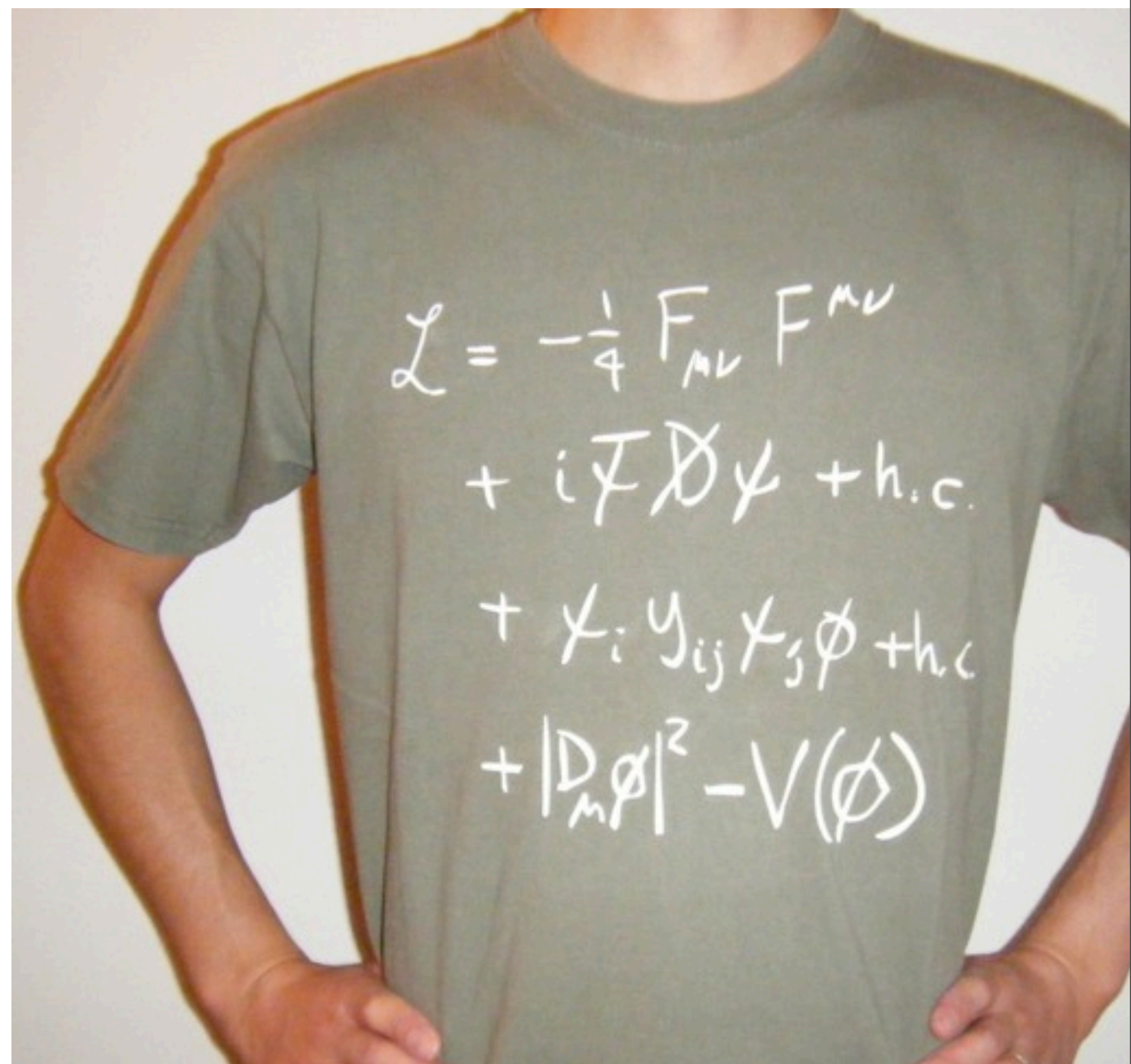

Massive gravitinos

- SU(2)xU(1) gauge symmetry

➡ spontaneously broken

(spin)

------ +1

------ 0 (Goldstone boson)

------ -1 Higgs mechanism

W, Z bosons

➡ discovered in 1983

➡ established the EW theory

Massive gravitinos

- SU(2)xU(1) gauge symmetry

  ➡ spontaneously broken

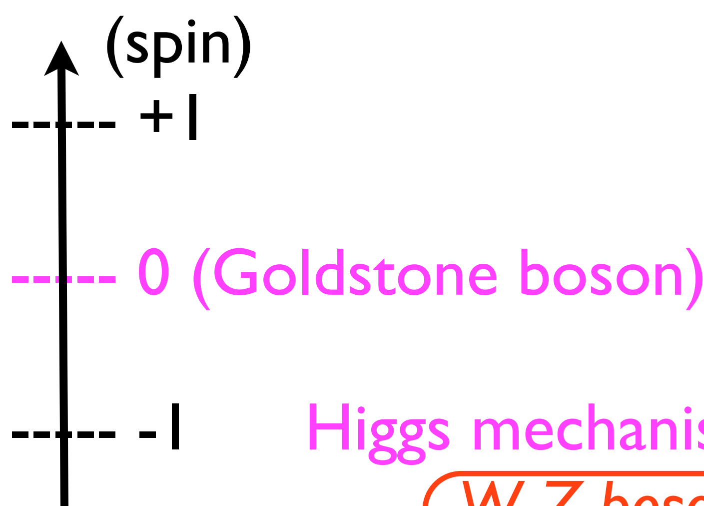

Higgs mechanism

W, Z bosons

  ➡ discovered in 1983

  ➡ established the EW theory

- Local supersymmetry

Massive gravitinos

- SU(2)xU(1) gauge symmetry

  ➡ spontaneously broken

  (spin)
  ------ +1
  ------ 0 (Goldstone boson)
  ------ -1 Higgs mechanism
  W, Z bosons

  ➡ discovered in 1983

  ➡ established the EW theory

- Local supersymmetry

  ➡ spontaneously broken

  (spin)
  ------ +3/2
  ------ +1/2
  (Goldstino)
  ------ -1/2
  super-Higgs mechanism
  ------ -3/2 *Massive gravitinos*

Massive gravitinos

- SU(2)xU(1) gauge symmetry

➡ spontaneously broken

(spin)
------ +1
------ 0 (Goldstone boson)
------ -1
Higgs mechanism
W, Z bosons

➡ discovered in 1983

➡ established the EW theory

- Local supersymmetry

➡ spontaneously broken

(spin)
------ +3/2
------ +1/2
(Goldstino)
------ -1/2
super-Higgs mechanism
------ -3/2
Massive gravitinos

➡ discover in 201? (??)

➡ establish supergravity !!

Massive gravitinos

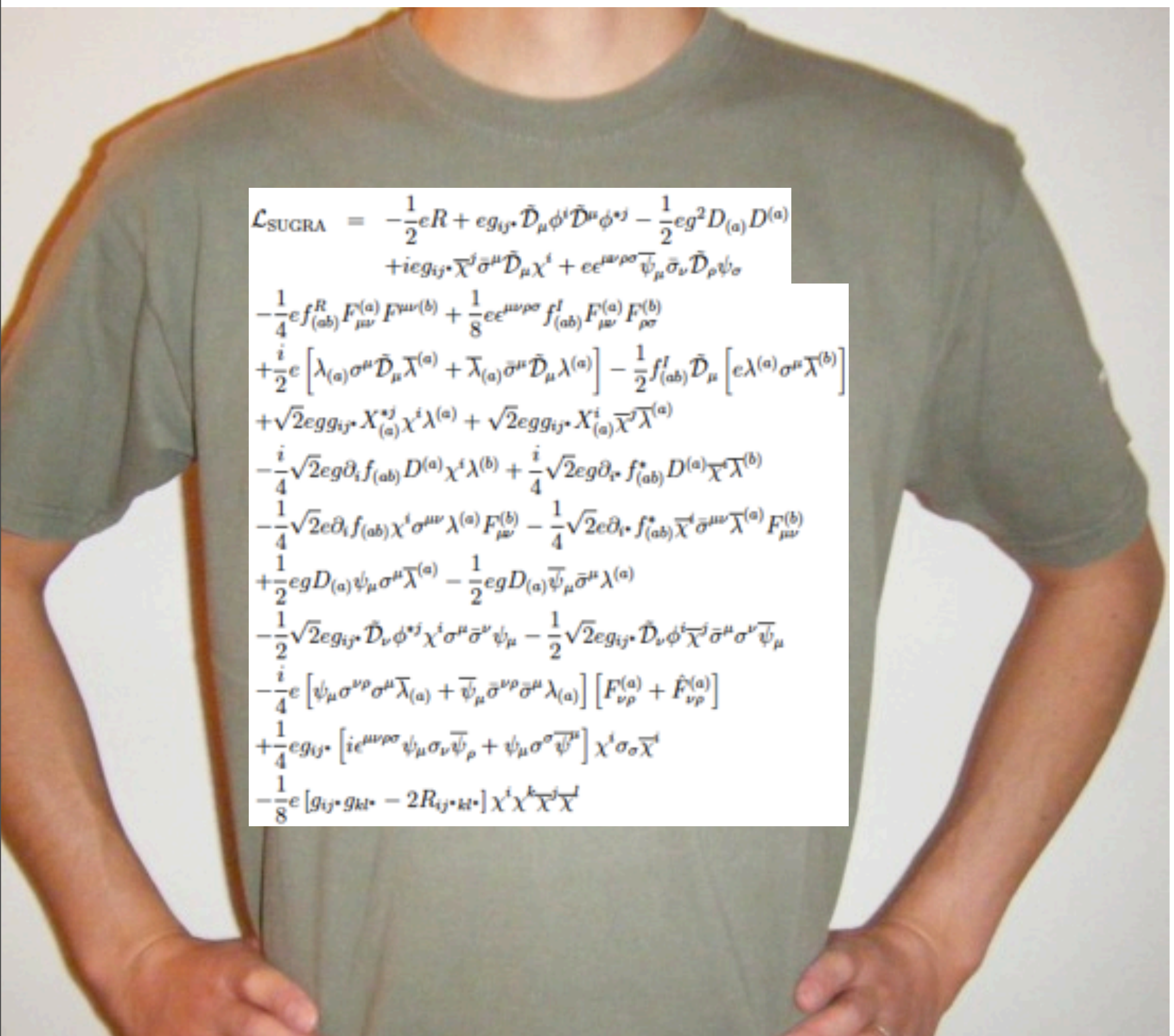

- Local supersymmetry

➡ spontaneously broken

(spin)

+3/2

+1/2

(Goldstino)

-1/2

super-Higgs mechanism

-3/2 *Massive gravitinos*

➡ discover in 201? (??)

➡ establish supergravity !!

Massive gravitinos

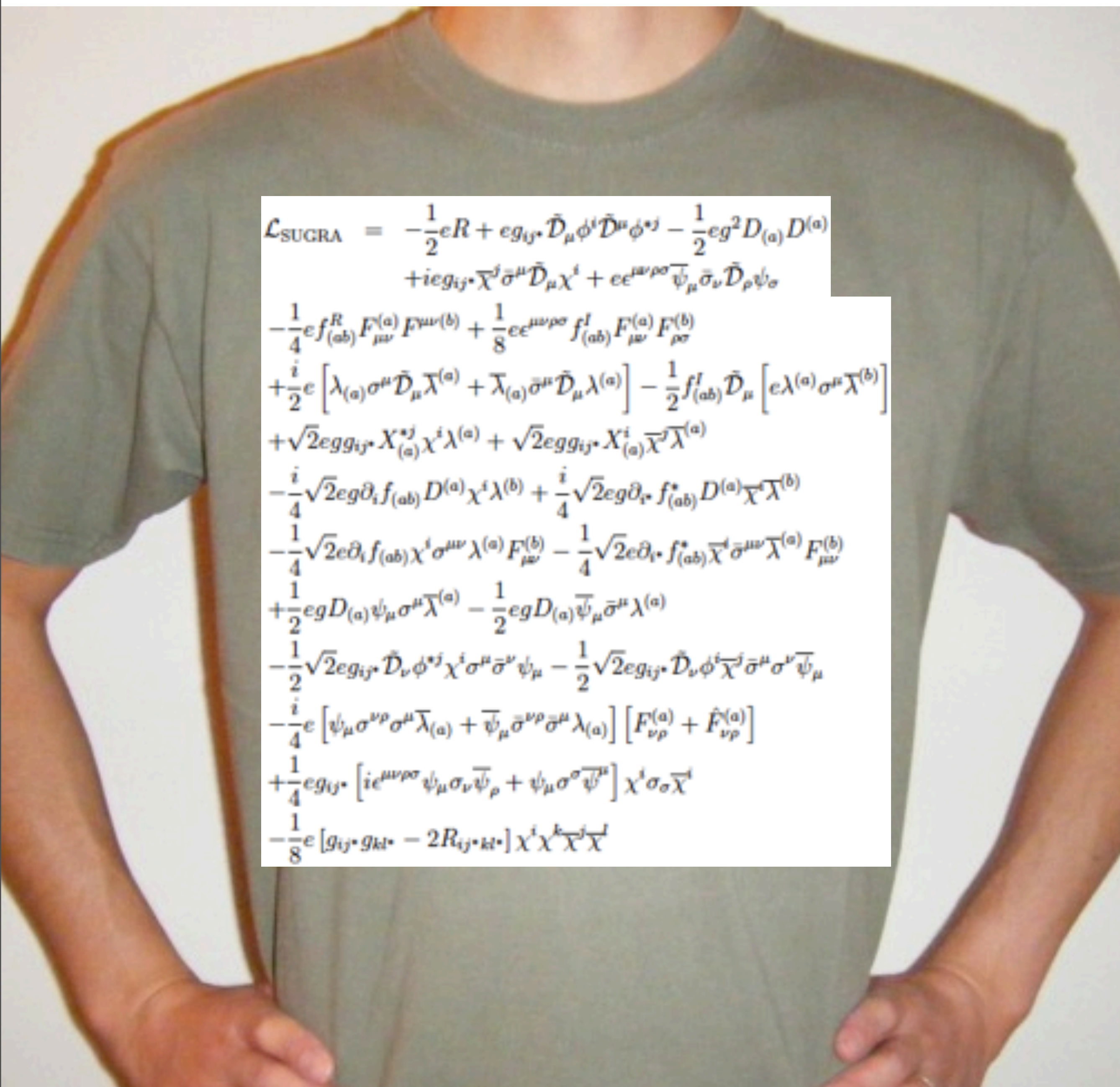

Massive gravitinos

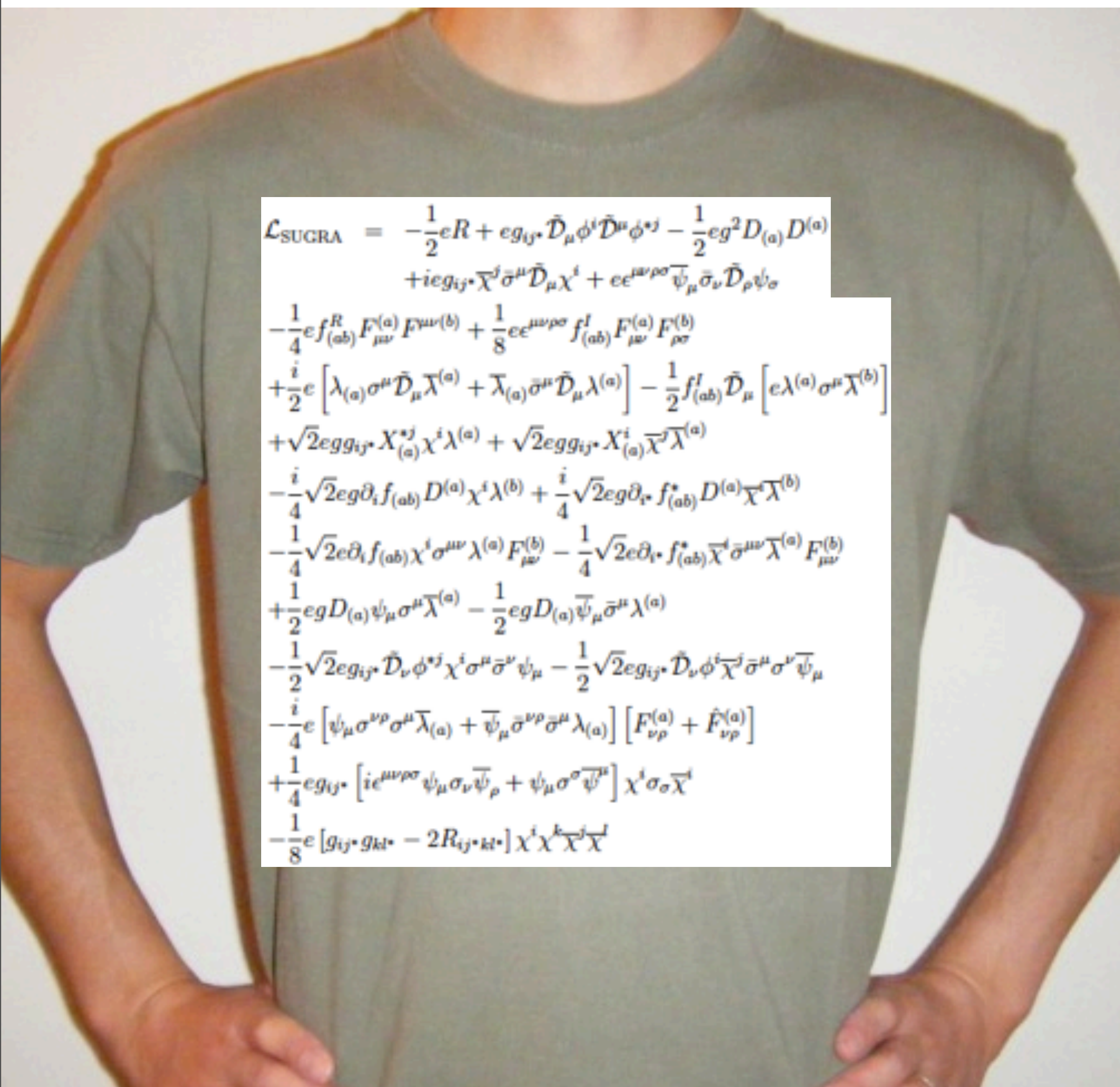

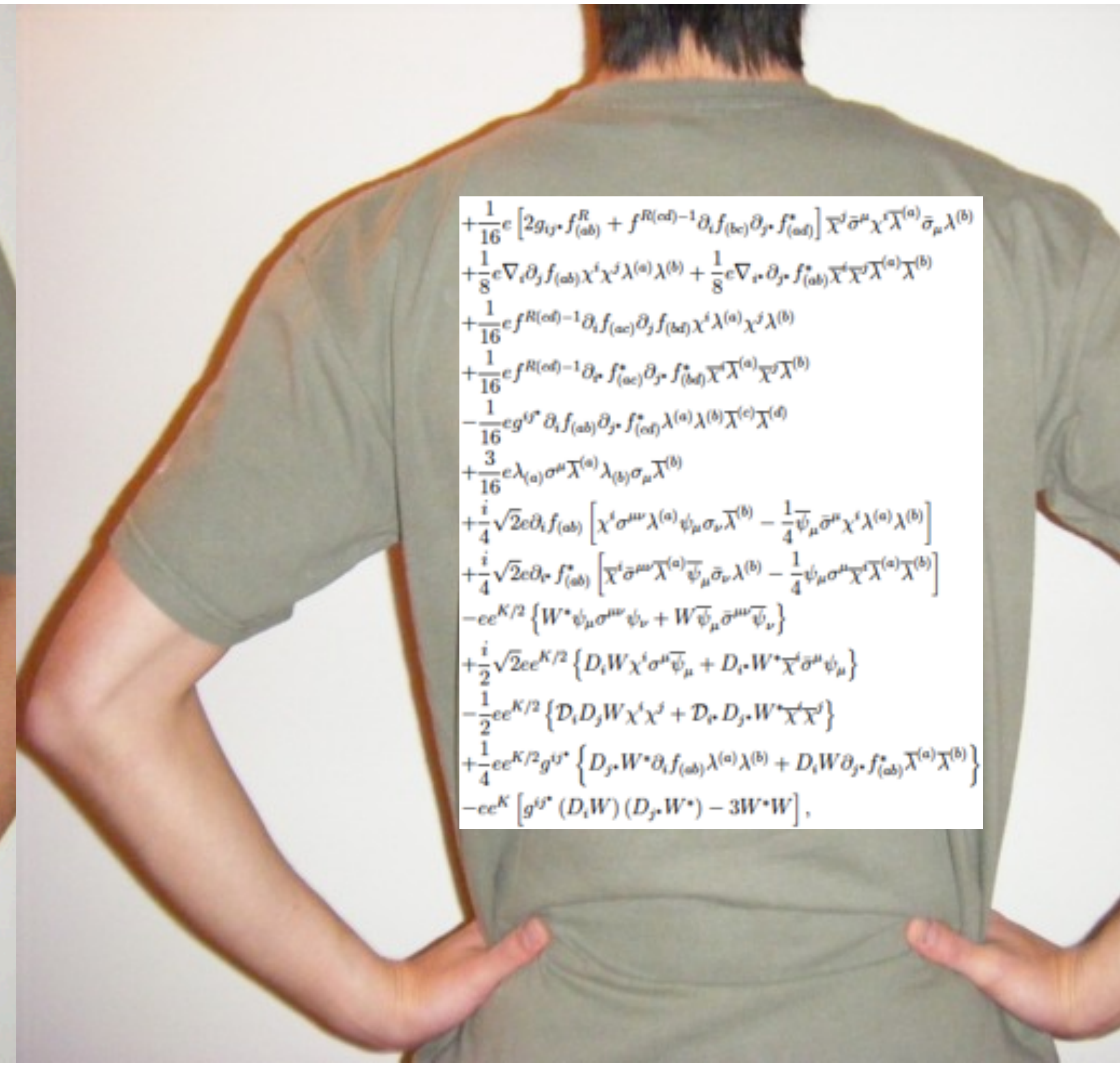

* copied from T.Moroi, hep-ph/9503210.

Mass of the gravitino

- related to the SUSY breaking scale as well as the Planck scale

$$m_{3/2} \sim (M_{\rm SUSY})^2/M_{\rm Pl}$$

- This implies that the gravitino can take a wide range of mass, depending on the SUSY breaking scale, from eV up to scales beyond TeV, and provide rich phenomenology in particle physics as well as in cosmology.

Cosmological constrains for the LSP gravitino

- The next-to-lightest SUSY particles (NLSP) may affect the big-ban nucleosynthesis (BBN) if their lifetimes are longer than ~0.1 sec.
- The lifetime of the NLSP is approximately proportional to $(m_{3/2})^2$.

Kawasaki, Kohri, Moroi, Yotsunagi, PRD(2008)

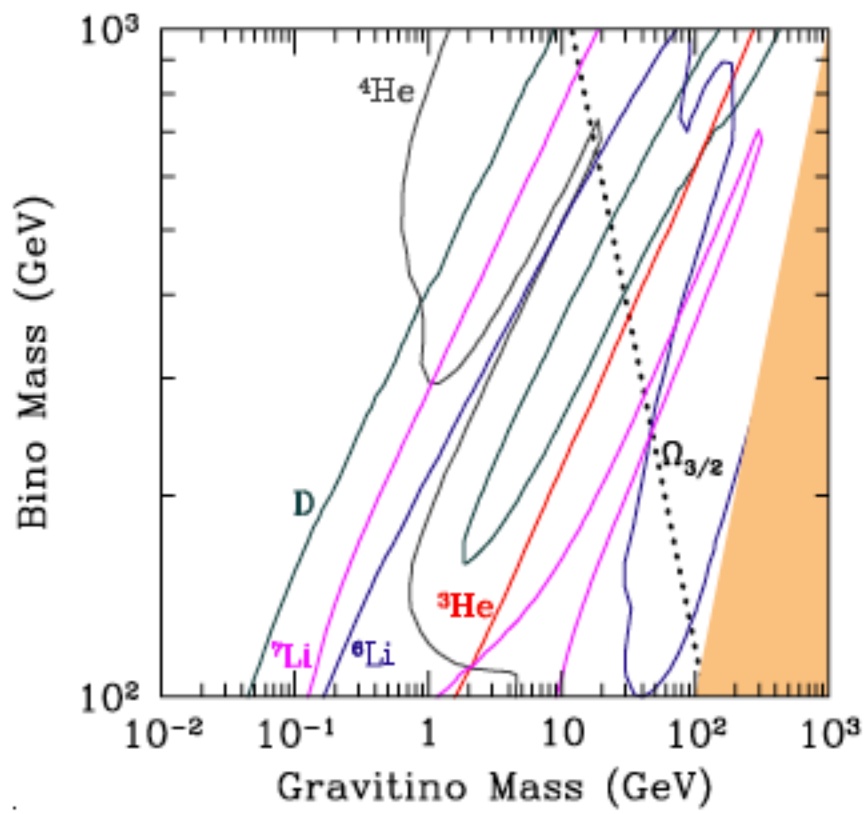

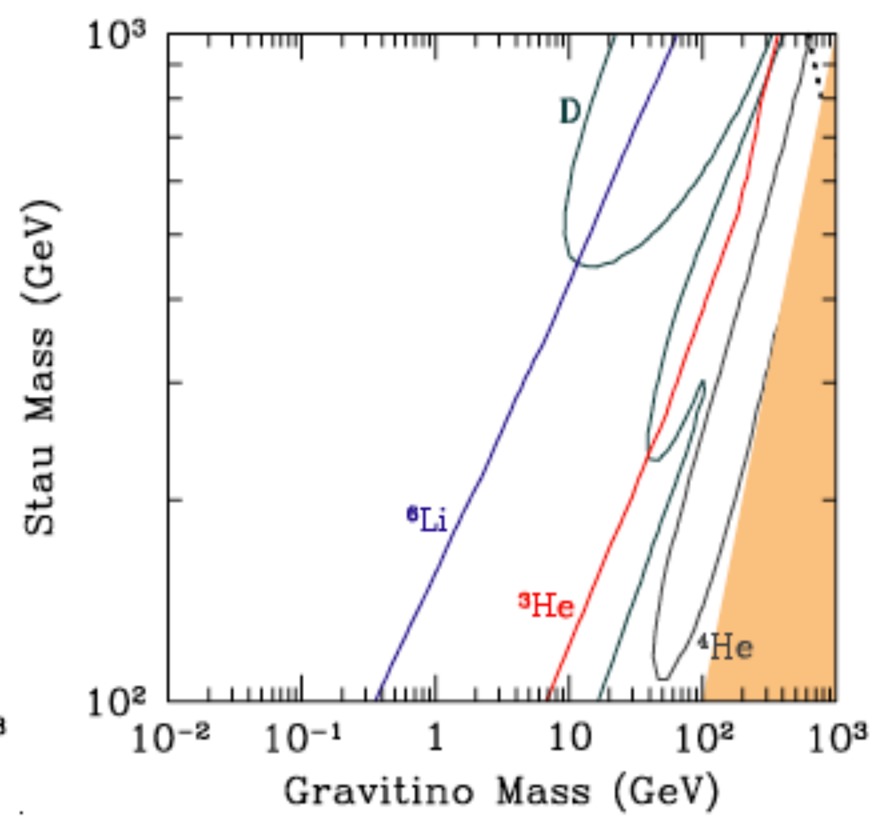

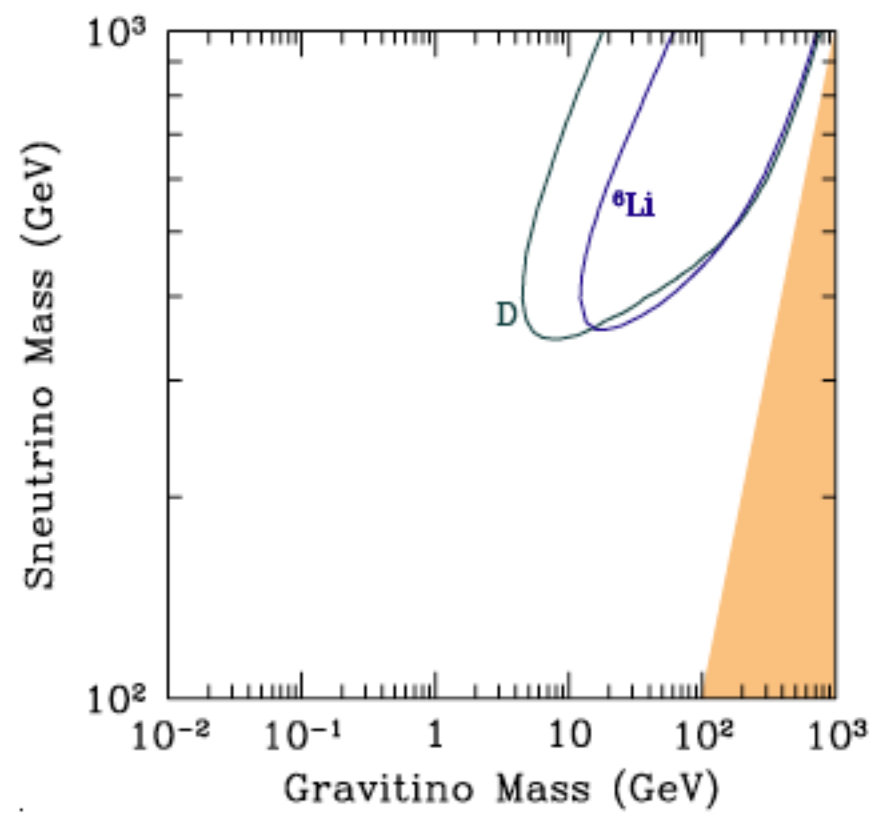

Collider phenomenology for a gravitino LSP

- The low-scale SUSY breaking can naturally happen in gauge-mediated SUSY breaking scenarios, where the gravitino is often the LSP and can play an important role even for collider signatures.
- The phenomenology depends so much on what is the NLSP.
  - In the minimal model of gauge mediation, the lightest neutralino and the lighter stau are often the NLSP.
  - A chargino, sneutrino, gluino, and squark can also be NLSP in, e.g., general gauge mediation models, split SUSY models, ...

HELAS and MadGraph/MadEvent with gravitinos/goldstinos

- Although the gravitino can play an important role even in collider signatures when it is the LSP, there is few Monte Carlo event generators which can treat them.
- "HELAS and MadGraph with spin-3/2 particles (gravitinos)"
  K. Hagiwara (KEK), K. Mawatari (VUB), Y. Takaesu (KEK); EPJC71(2011) [arXiv:1010.4255]
- "HELAS and MadGraph with goldstinos"
  K. Mawatari (VUB), Y. Takaesu (KEK); appear in EPJC [arXiv:1101.1289]
  - We added new HELAS fortran subroutines for massive spin-3/2 gravitinos and goldstinos and their interactions, and implemented them into MadGraph/MadEvent (MG/ME) so that arbitrary amplitudes with external gravitinos/goldstinos can be generated automatically.
  - MG/ME v4,5 supports spin-0, 1/2, 1, and 2.
    [HELAS and MG/ME w/ spin-2 particles by Hagiwara, Kanzaki, Q.Li, KM, EPJC(2008)]

The effective interaction Lagrangian relevant to the gravitino phenomenology

- The effective interaction Lagrangian:

$$\mathcal{L}_{\rm int} = -\frac{i}{\sqrt{2}\,\overline{M}_{\rm Pl}}\left[\bar{\psi}_\mu \gamma^\nu \gamma^\mu P_L f^i \left(D_\nu \phi_L^i\right)^* - \bar{f}^i P_R \gamma^\mu \gamma^\nu \psi_\mu \left(D_\nu \phi_L^i\right)\right] - \frac{i}{8\overline{M}_{\rm Pl}} \bar{\psi}_\mu [\gamma^\nu, \gamma^\rho] \gamma^\mu \lambda^{(\alpha)a} F_{\nu\rho}^{(\alpha)a},$$

  - The covariant derivative:

$$D_\mu = \partial_\mu + i g_s T_3^a A_\mu^a + i g T_2^a W_\mu^a + i g' Y B_\mu$$

  - The field-strength tensors for each gauge group:

$$F_{\mu\nu}^{(3)a} = \partial_\mu A_\nu^a - \partial_\nu A_\mu^a - g_s f_3^{abc} A_\mu^b A_\nu^c,$$
$$F_{\mu\nu}^{(2)a} = \partial_\mu W_\nu^a - \partial_\nu W_\mu^a - g f_2^{abc} W_\mu^b W_\nu^c,$$
$$F_{\mu\nu}^{(1)a} = \partial_\mu B_\nu - \partial_\nu B_\mu,$$

The effective interaction Lagrangian relevant to the gravitino phenomenology

- The effective interaction Lagrangian:

$$\mathcal{L}_{\rm int} = \boxed{-\frac{i}{\sqrt{2}\,\overline{M}_{\rm Pl}}\left[\bar{\psi}_\mu \gamma^\nu \gamma^\mu P_L f^i \left(D_\nu \phi_L^i\right)^* - \bar{f}^i P_R \gamma^\mu \gamma^\nu \psi_\mu \left(D_\nu \phi_L^i\right)\right]} - \frac{i}{8\overline{M}_{\rm Pl}}\bar{\psi}_\mu[\gamma^\nu,\gamma^\rho]\gamma^\mu \lambda^{(\alpha)a} F^{(\alpha)a}_{\nu\rho},$$

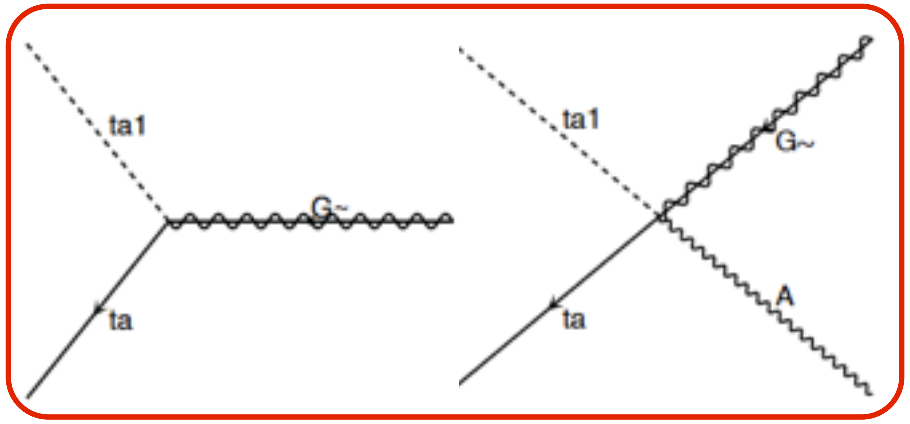

  - The covariant derivative:

$$D_\mu = \partial_\mu + i g_s T_3^a A_\mu^a + i g T_2^a W_\mu^a + i g' Y B_\mu$$

  - The field-strength tensors for each gauge group:

$$F^{(3)a}_{\mu\nu} = \partial_\mu A^a_\nu - \partial_\nu A^a_\mu - g_s f_3^{abc} A^b_\mu A^c_\nu,$$

$$F^{(2)a}_{\mu\nu} = \partial_\mu W^a_\nu - \partial_\nu W^a_\mu - g f_2^{abc} W^b_\mu W^c_\nu,$$

$$F^{(1)a}_{\mu\nu} = \partial_\mu B_\nu - \partial_\nu B_\mu,$$

The effective interaction Lagrangian relevant to the gravitino phenomenology

- The effective interaction Lagrangian:

$$\mathcal{L}_{\text{int}} = \boxed{-\frac{i}{\sqrt{2}\,\overline{M}_{\text{Pl}}}\left[\bar{\psi}_\mu \gamma^\nu \gamma^\mu P_L f^i \left(D_\nu \phi_L^i\right)^* - \bar{f}^i P_R \gamma^\mu \gamma^\nu \psi_\mu \left(D_\nu \phi_L^i\right)\right]}$$

$$\boxed{-\frac{i}{8\overline{M}_{\text{Pl}}}\bar{\psi}_\mu [\gamma^\nu, \gamma^\rho] \gamma^\mu \lambda^{(\alpha)a} F^{(\alpha)a}_{\nu\rho}},$$

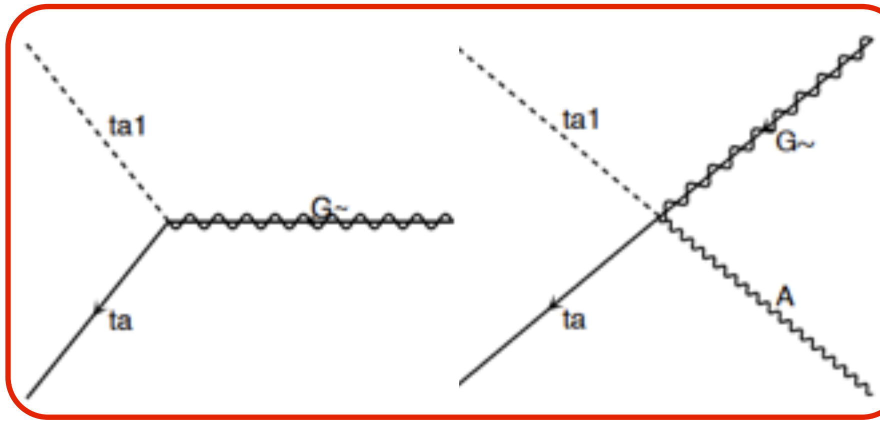

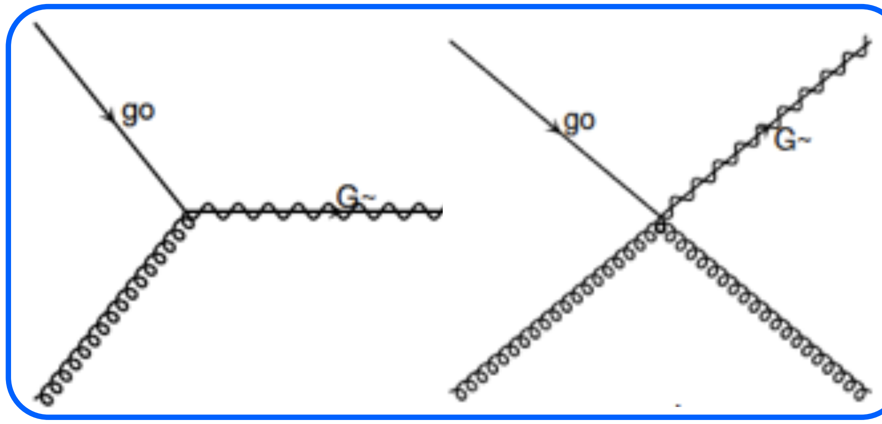

  - The covariant derivative:

$$D_\mu = \partial_\mu + i g_s T_3^a A_\mu^a + i g T_2^a W_\mu^a + i g' Y B_\mu$$

  - The field-strength tensors for each gauge group:

$$F^{(3)a}_{\mu\nu} = \partial_\mu A_\nu^a - \partial_\nu A_\mu^a - g_s f_3^{abc} A_\mu^b A_\nu^c,$$

$$F^{(2)a}_{\mu\nu} = \partial_\mu W_\nu^a - \partial_\nu W_\mu^a - g f_2^{abc} W_\mu^b W_\nu^c,$$

$$F^{(1)a}_{\mu\nu} = \partial_\mu B_\nu - \partial_\nu B_\mu,$$

The effective interaction Lagrangian for a goldstino

- In the high energy limit $E >> m_{3/2}$, the spin-3/2 gravitino field can be replaced by the spin-1/2 goldstino as

$$\psi_\mu \sim \sqrt{2/3}\,\partial_\mu \psi / m_{3/2}$$

- The effective interaction Lagrangian in non-derivative form:

$$\mathcal{L}_{\rm int} = \frac{i(m^2_{\phi^i} - m^2_{f^i})}{\sqrt{3}\,\overline{M}_{\rm Pl}\, m_{3/2}} \left[\bar{\psi} P_L f^i (\phi^i_L)^* - \bar{f}^i P_R \psi\, \phi^i_L\right] - \frac{m_\lambda}{4\sqrt{6}\,\overline{M}_{\rm Pl}\, m_{3/2}} \bar{\psi}[\gamma^\mu, \gamma^\nu] \lambda^{(\alpha)a} F^{(\alpha)a}_{\mu\nu}$$

  - The ψ-f-ϕ-A_μ vertex is absent.
  - The couplings are proportional to the mass splitting inside the supermultiplet.
  - The couplings are inversely proportional to the SUSY-breaking scale through the gravitino mass

$$m_{3/2} = \langle F \rangle / \sqrt{3}\,\overline{M}_{\rm Pl}$$

The effective interaction Lagrangian for a goldstino

- In the high energy limit $E \gg m_{3/2}$, the spin-3/2 gravitino field can be replaced by the spin-1/2 goldstino as

$$\psi_\mu \sim \sqrt{2/3}\,\partial_\mu \psi / m_{3/2}$$

- The effective interaction Lagrangian in non-derivative form:

$$\mathcal{L}_{\rm int} = \boxed{\frac{i(m^2_{\phi^i} - m^2_{f^i})}{\sqrt{3}\,\overline{M}_{\rm Pl}\, m_{3/2}} [\bar{\psi} P_L f^i (\phi^i_L)^* - \bar{f}^i P_R \psi\, \phi^i_L\,]} \\ - \frac{m_\lambda}{4\sqrt{6}\,\overline{M}_{\rm Pl}\, m_{3/2}} \bar{\psi}[\gamma^\mu, \gamma^\nu] \lambda^{(\alpha)a} F^{(\alpha)a}_{\mu\nu}$$

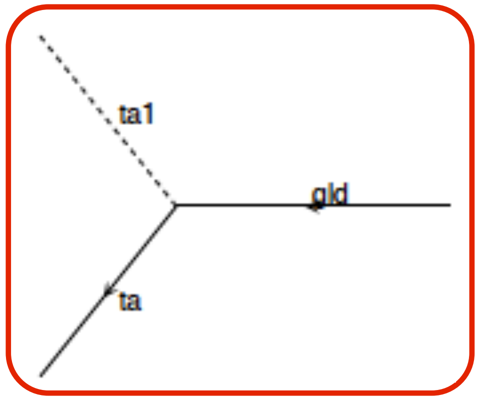

  - The ψ-f-ϕ-A_μ vertex is absent.
  - The couplings are proportional to the mass splitting inside the supermultiplet.
  - The couplings are inversely proportional to the SUSY-breaking scale through the gravitino mass

$$m_{3/2} = \langle F \rangle / \sqrt{3}\,\overline{M}_{\rm Pl}$$

The effective interaction Lagrangian for a goldstino

- In the high energy limit $E \gg m_{3/2}$, the spin-3/2 gravitino field can be replaced by the spin-1/2 goldstino as

$$\psi_\mu \sim \sqrt{2/3}\,\partial_\mu \psi / m_{3/2}$$

- The effective interaction Lagrangian in non-derivative form:

$$\mathcal{L}_{\rm int} = \boxed{\frac{i(m^2_{\phi^i} - m^2_{f^i})}{\sqrt{3}\,\overline{M}_{\rm Pl}\, m_{3/2}} \left[\bar{\psi} P_L f^i (\phi^i_L)^* - \bar{f}^i P_R \psi\, \phi^i_L\right]}$$
$$\boxed{- \frac{m_\lambda}{4\sqrt{6}\,\overline{M}_{\rm Pl}\, m_{3/2}} \bar{\psi}[\gamma^\mu, \gamma^\nu] \lambda^{(\alpha)a} F^{(\alpha)a}_{\mu\nu}}$$

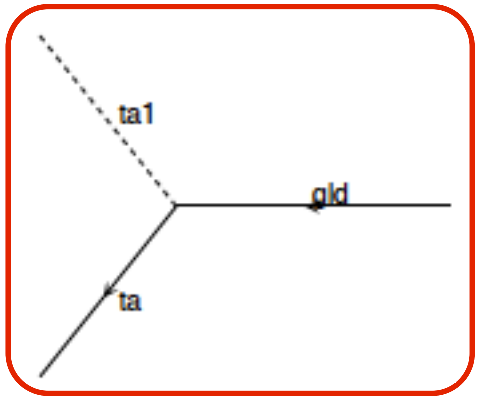

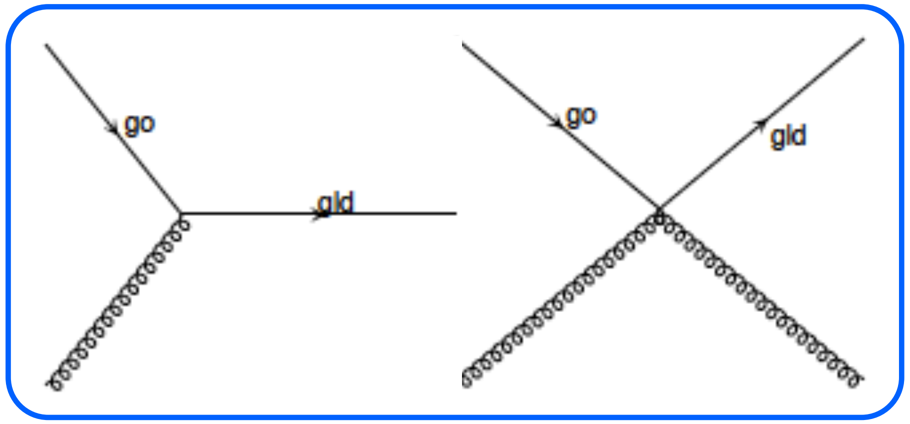

  - The ψ-f-ϕ-A_μ vertex is absent.
  - The couplings are proportional to the mass splitting inside the supermultiplet.
  - The couplings are inversely proportional to the SUSY-breaking scale through the gravitino mass

$$m_{3/2} = \langle F \rangle / \sqrt{3}\,\overline{M}_{\rm Pl}$$

Checking our codes by the goldstino equivalence theorem

- MG/ME w/ gravitinos
  [arXiv:1010.4255]

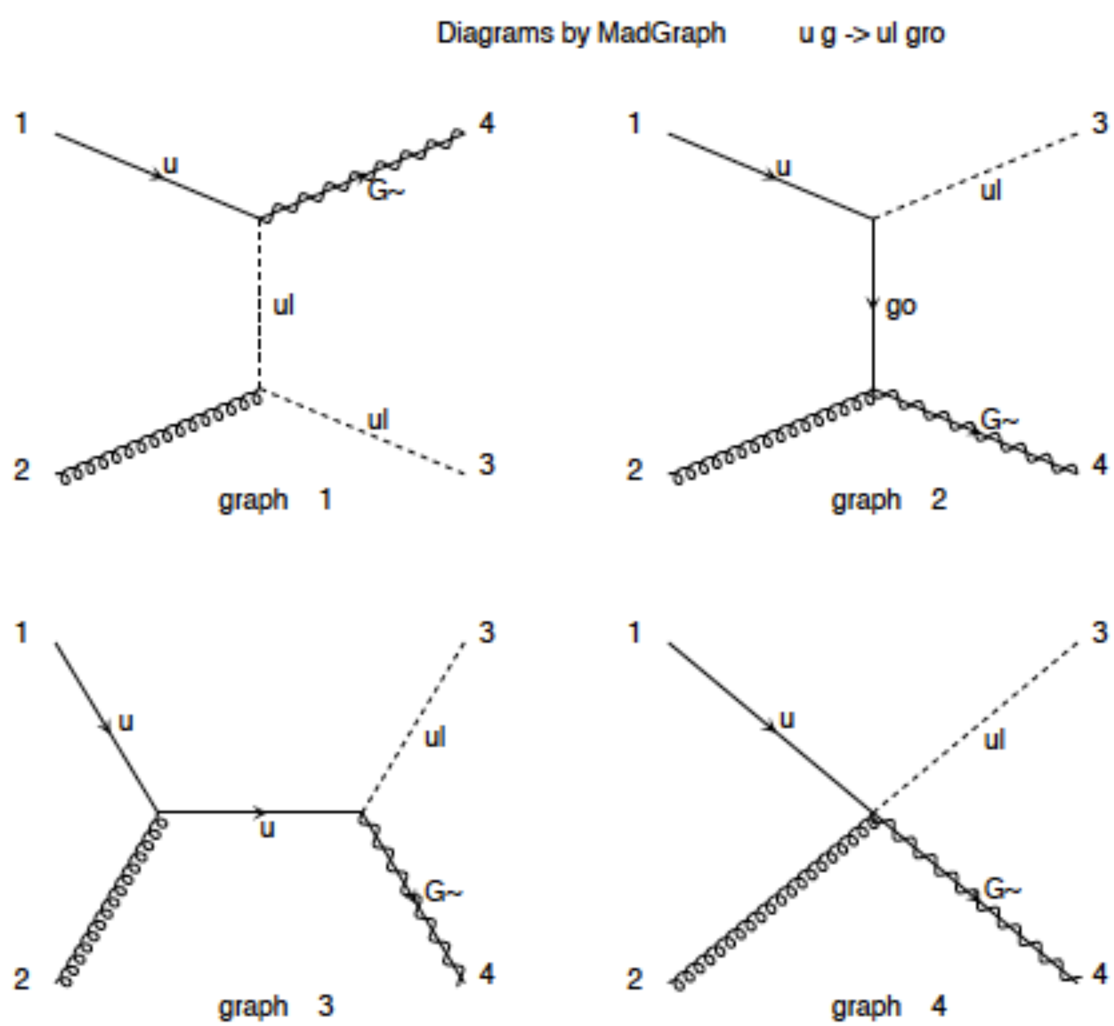

- MG/ME w/ goldstinos
  [arXiv:1101.1289]

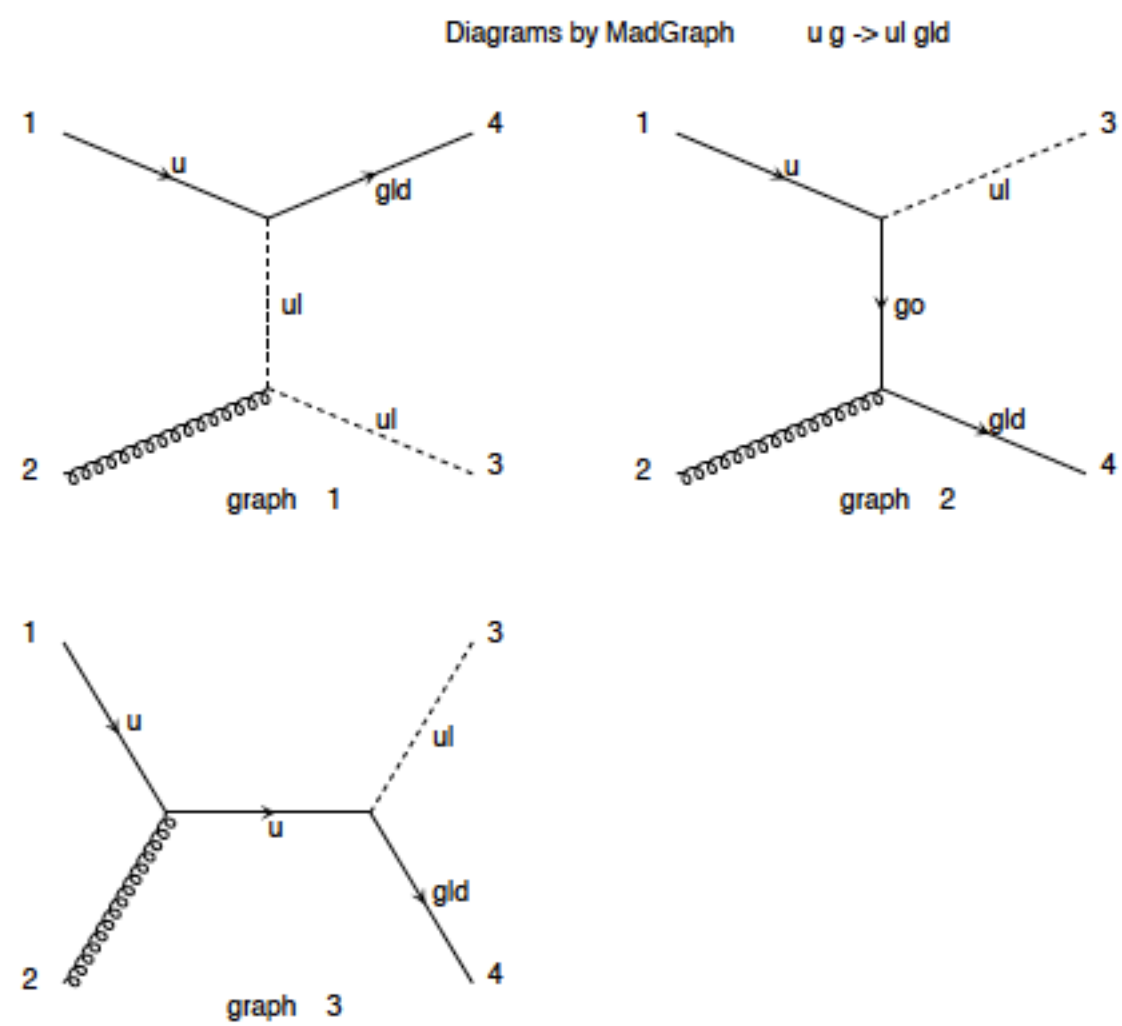

The gravitino-goldstino equivalence

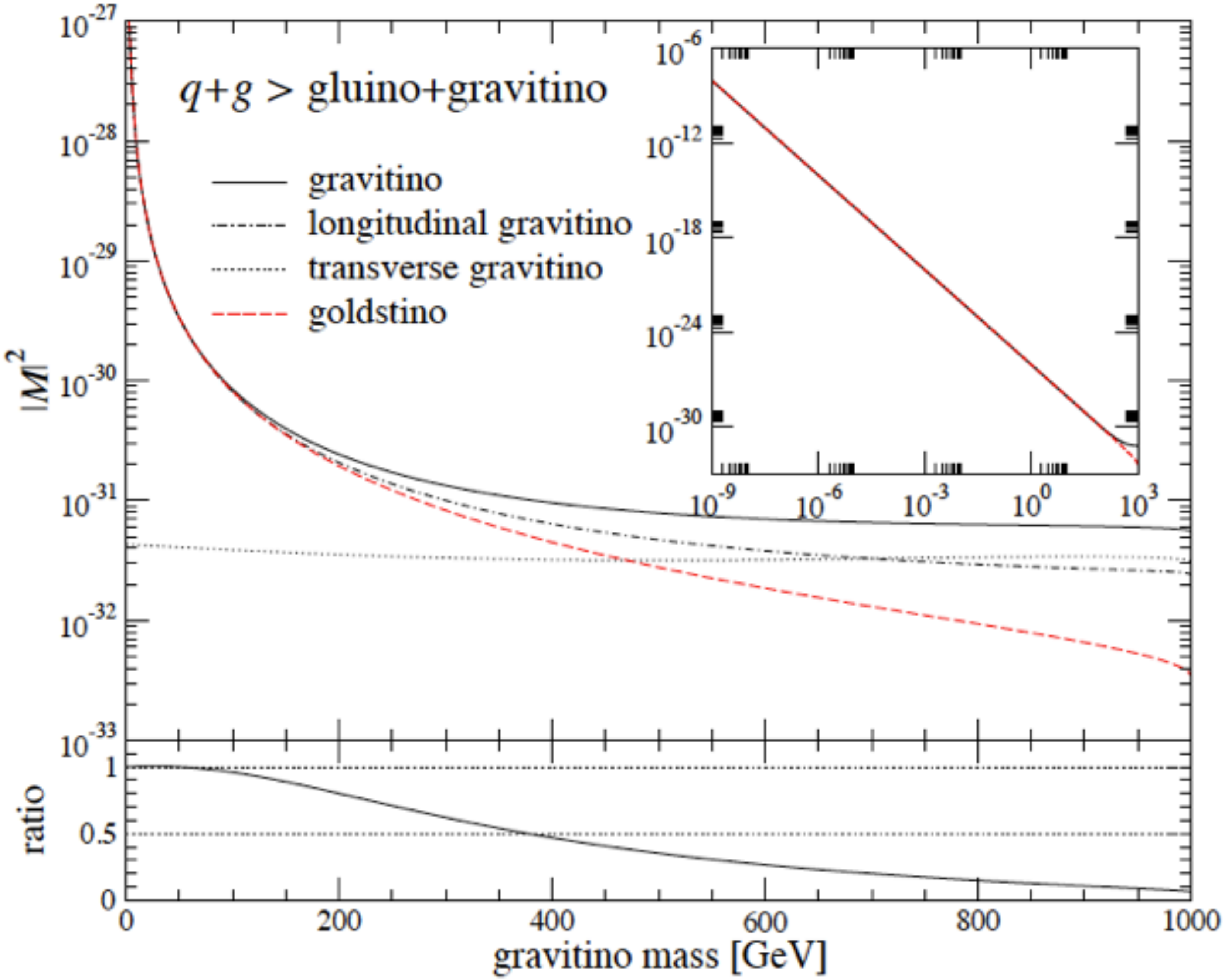

at $\sqrt{\hat{s}} = 2$ TeV and $\cos\hat{\theta} = 0.5$ as a function of the gravitino mass, where the squark and gluino masses are fixed at 1 TeV. The ratios of the squared matrix elements are also shown.

- In the region of the small gravitino mass, or in the high energy region, both amplitudes agree well each other.
- The longitudinal modes (or the goldstino) become dominant in the high energy region, while the contributions from the transverse modes do not depend on the energy.
- The squared matrix elements are proportional to $(m_{3/2})^{-2}$.

Collider signatures for a gravitino LSP

1. Gluino NLSP
2. Neutralino NLSP
3. Slepton NLSP
4. Stau NLSP
5. ...

1. Gluino NLSP

- If gluinos are the NLSP and light enough, those productions can be explored in the early LHC data as well as in the Tevatron.

- Associated gravitino productions with a gluino (or a squark) lead to characteristic signals of monojet plus missing energy when a produced gluino (squark) promptly decays into a gluon (quark) and a LSP gravitino.

$$pp \to \tilde{g}\tilde{G} \to g\tilde{G}\tilde{G} \Rightarrow \text{jet} + \not{E}$$

*The associated productions for SPS7 and 8 studied by Klasen and Pignor (2007)

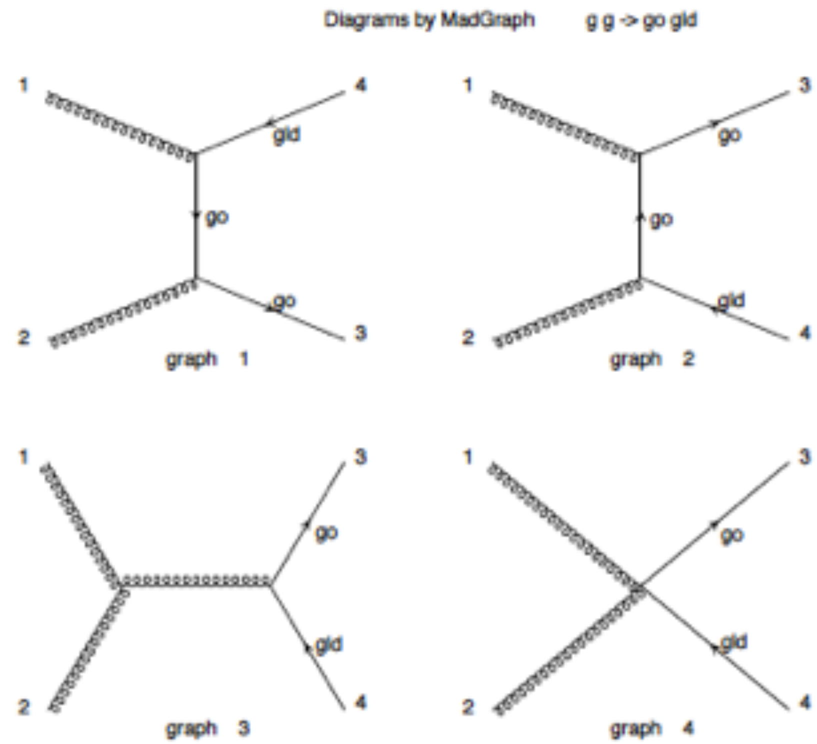

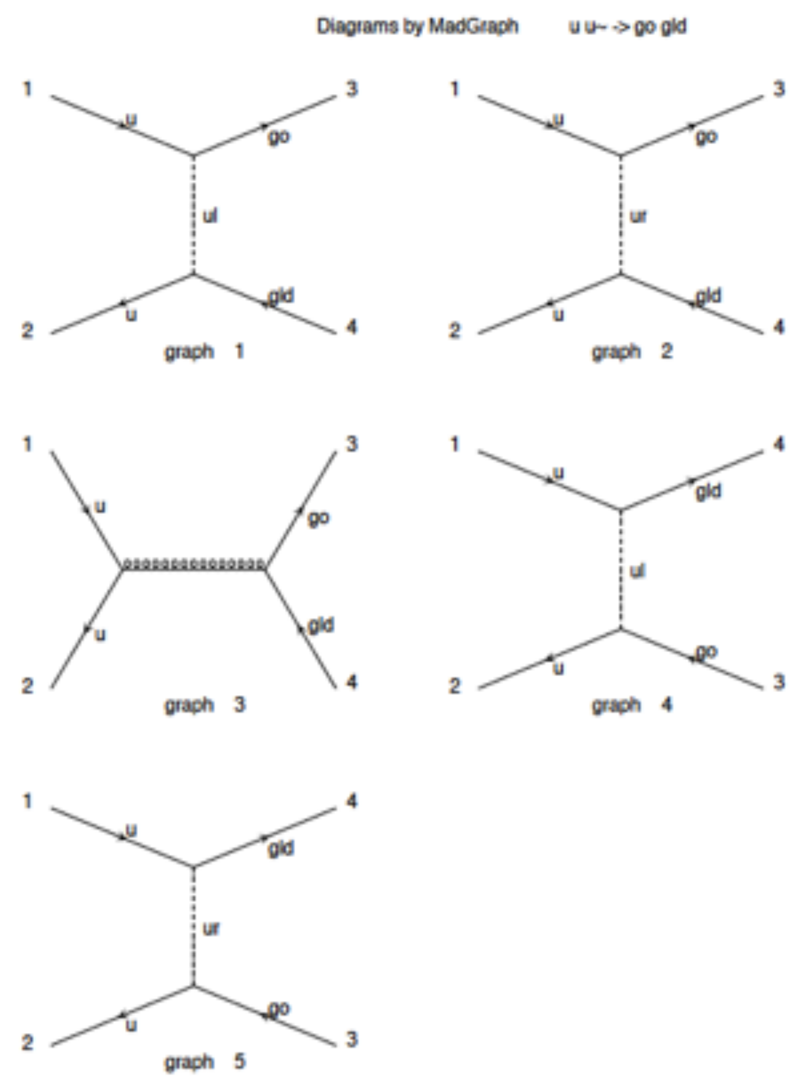

Associated gravitino productions with a gluino

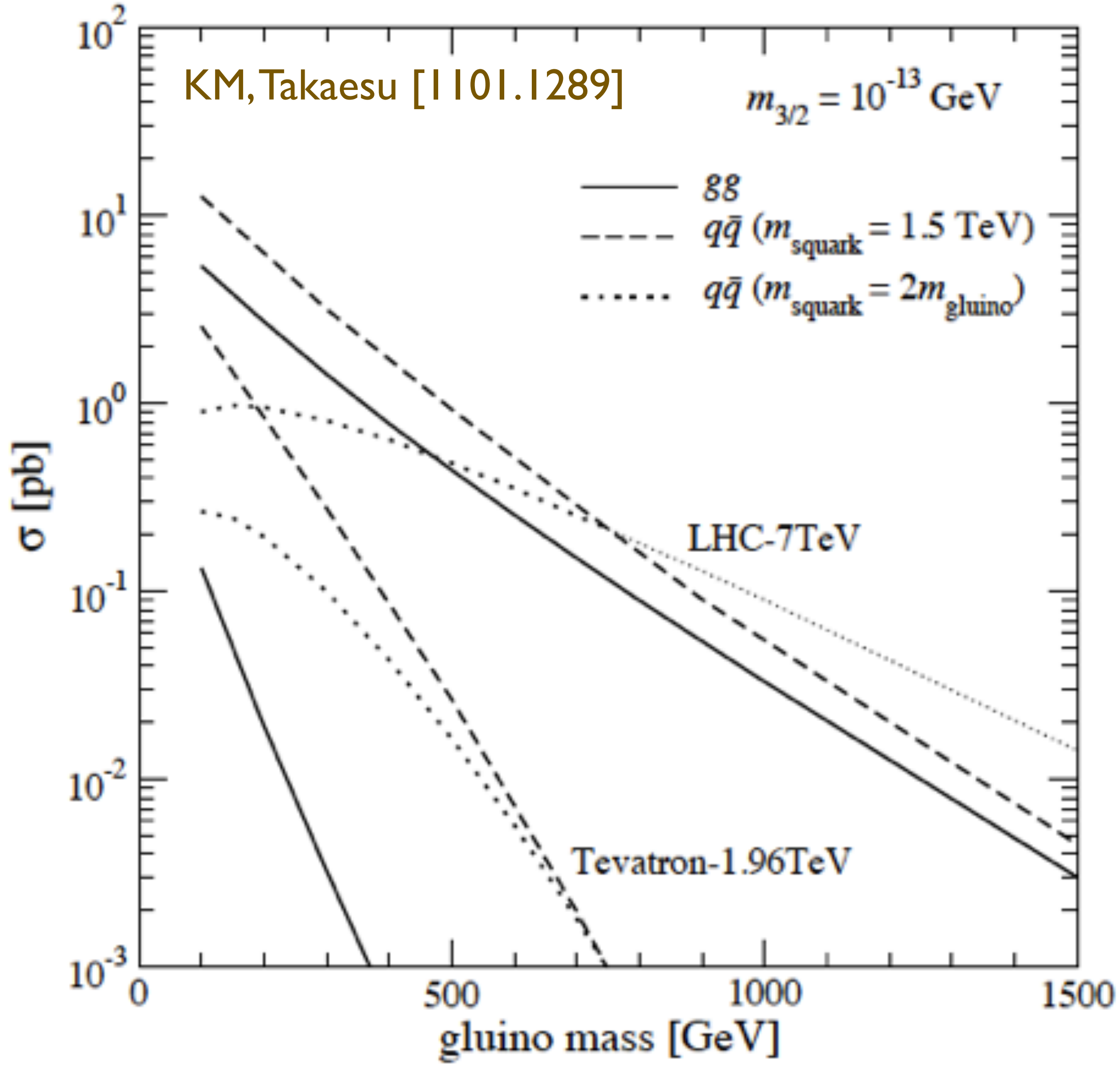

Fig. 3. Total cross sections of each subprocess of associated gravitino productions with a gluino, $p\bar{p}/pp \to \tilde{g}\tilde{G}$, at the Tevatron-1.96TeV/LHC-7TeV for $m_{3/2} = 10^{-13}$ GeV as a function of the gluino mass. The squark masses are fixed at 1.5 TeV (dashed) and $2m_{\tilde{g}}$ (dotted) for the $q\bar{q}$ subprocesses, where the cross section in the $\Gamma_{\tilde{q}\to q\tilde{G}} > m_{\tilde{q}}/2$ region is shown with a thin dotted line.

Associated gravitino productions with a gluino

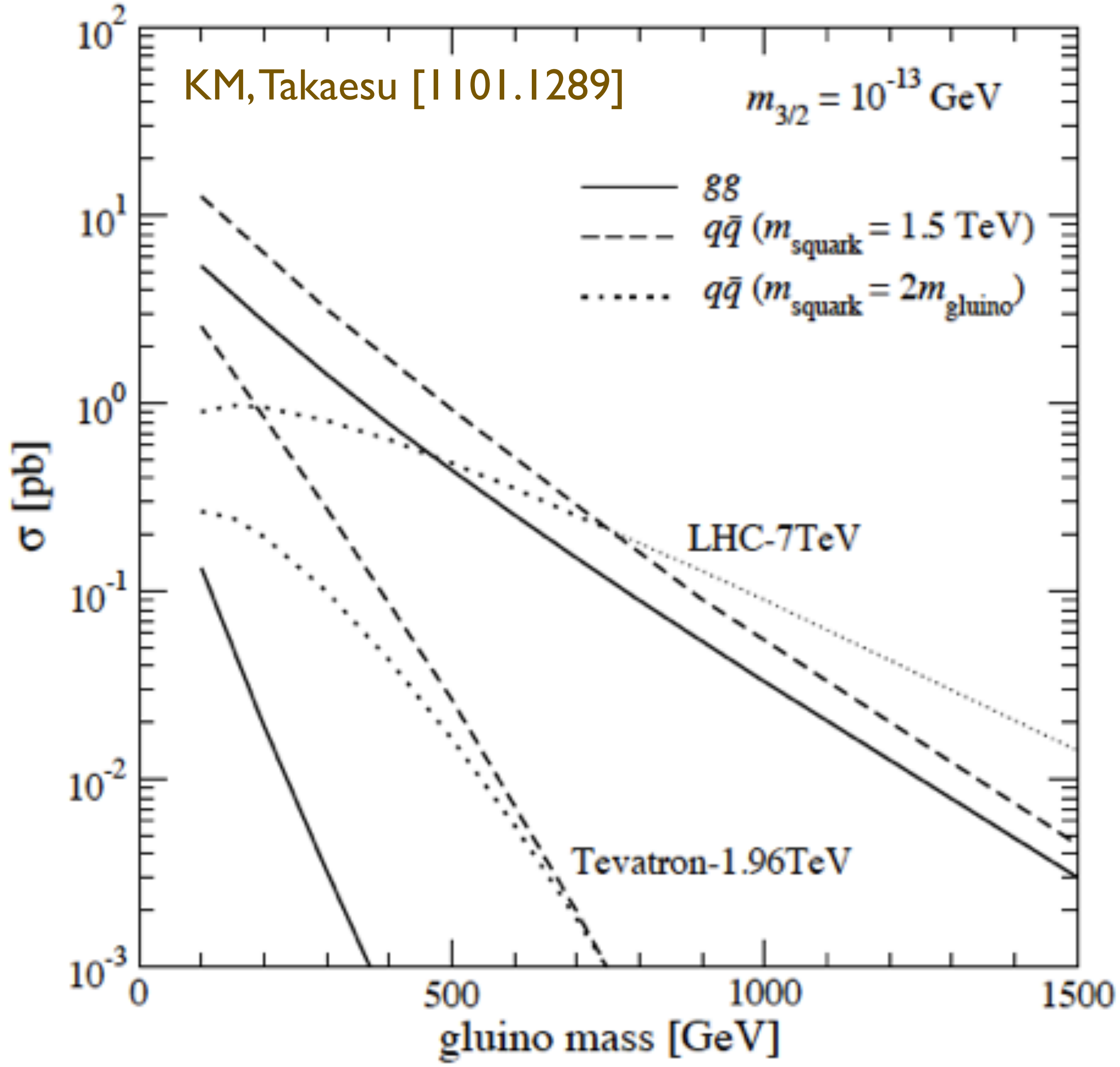

Fig. 3. Total cross sections of each subprocess of associated gravitino productions with a gluino, $p\bar{p}/pp \to \tilde{g}\tilde{G}$, at the Tevatron-1.96TeV/LHC-7TeV for $m_{3/2} = 10^{-13}$ GeV as a function of the gluino mass. The squark masses are fixed at 1.5 TeV (dashed) and $2m_{\tilde{g}}$ (dotted) for the $q\bar{q}$ subprocesses, where the cross section in the $\Gamma_{\tilde{q}\to q\tilde{G}} > m_{\tilde{q}}/2$ region is shown with a thin dotted line.

- The cross sections of all the subprocesses scale with $(m_{3/2})^{-2}$.

➡ The lighter gravitinos enhance the monojet signals, which can be interpreted as the direct lower bound for the gravitino mass.
(Note that the dijet signals produced through gluino-pair productions do not depend on the gravitino mass.)

Associated gravitino productions with a gluino

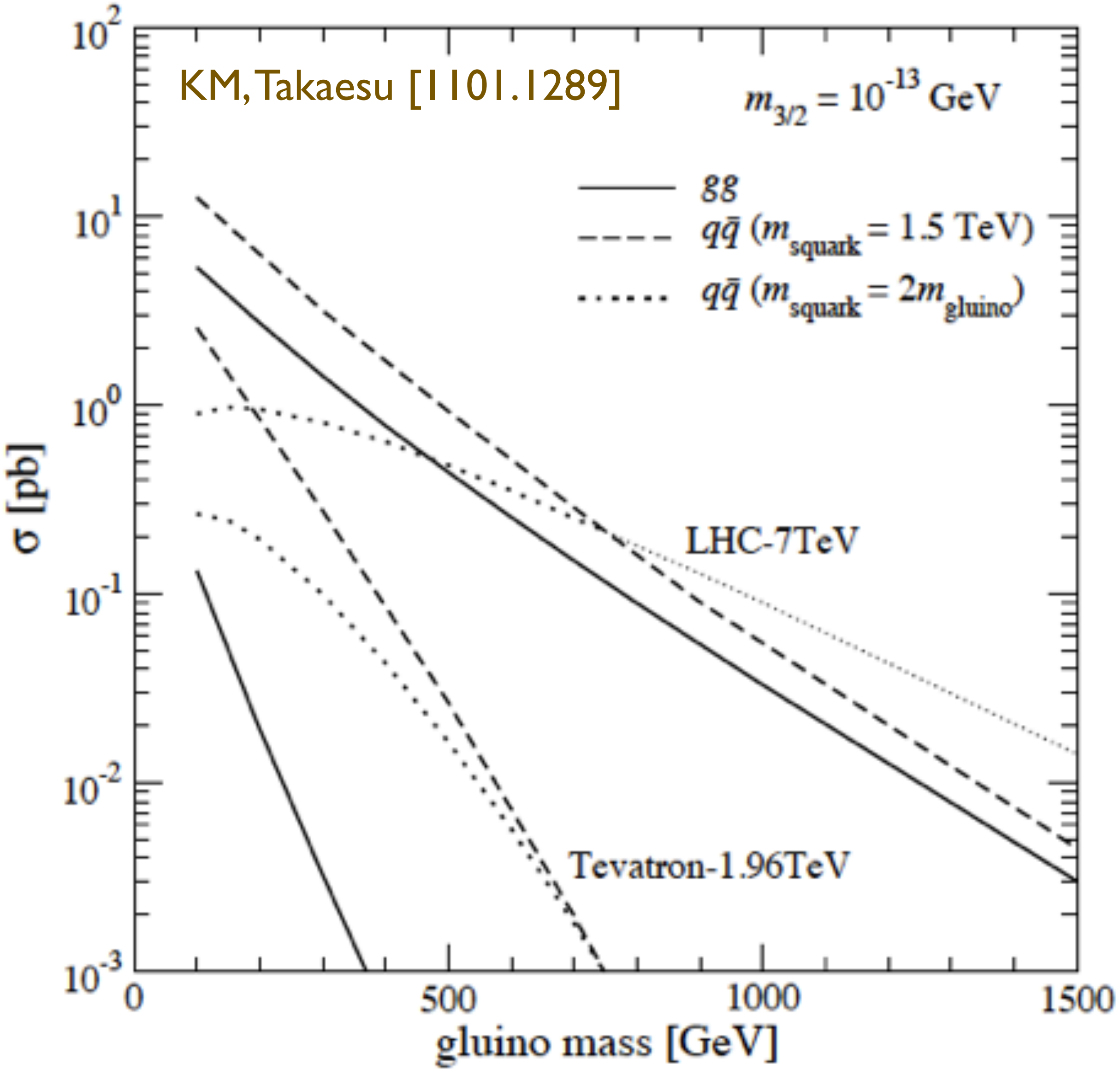

Fig. 3. Total cross sections of each subprocess of associated gravitino productions with a gluino, $p\bar{p}/pp \to \tilde{g}\tilde{G}$, at the Tevatron-1.96TeV/LHC-7TeV for $m_{3/2} = 10^{-13}$ GeV as a function of the gluino mass. The squark masses are fixed at 1.5 TeV (dashed) and $2m_{\tilde{g}}$ (dotted) for the $q\bar{q}$ subprocesses, where the cross section in the $\Gamma_{\tilde{q}\to q\tilde{G}} > m_{\tilde{q}}/2$ region is shown with a thin dotted line.

- The cross sections of all the subprocesses scale with $(m_{3/2})^{-2}$.

➡ The lighter gravitinos enhance the monojet signals, which can be interpreted as the direct lower bound for the gravitino mass.
(Note that the dijet signals produced through gluino-pair productions do not depend on the gravitino mass.)

- The t- and u- channel squark masses are quite sensitive to the cross section, and the heavier squark exchange increases the cross section because $g_{\tilde{G}q\tilde{q}} \propto m_{\tilde{q}}^2$.

➡ The cross section of the qqbar channel can be larger than that of the gg channel even for the LHC.

Associated gravitino productions with a squark

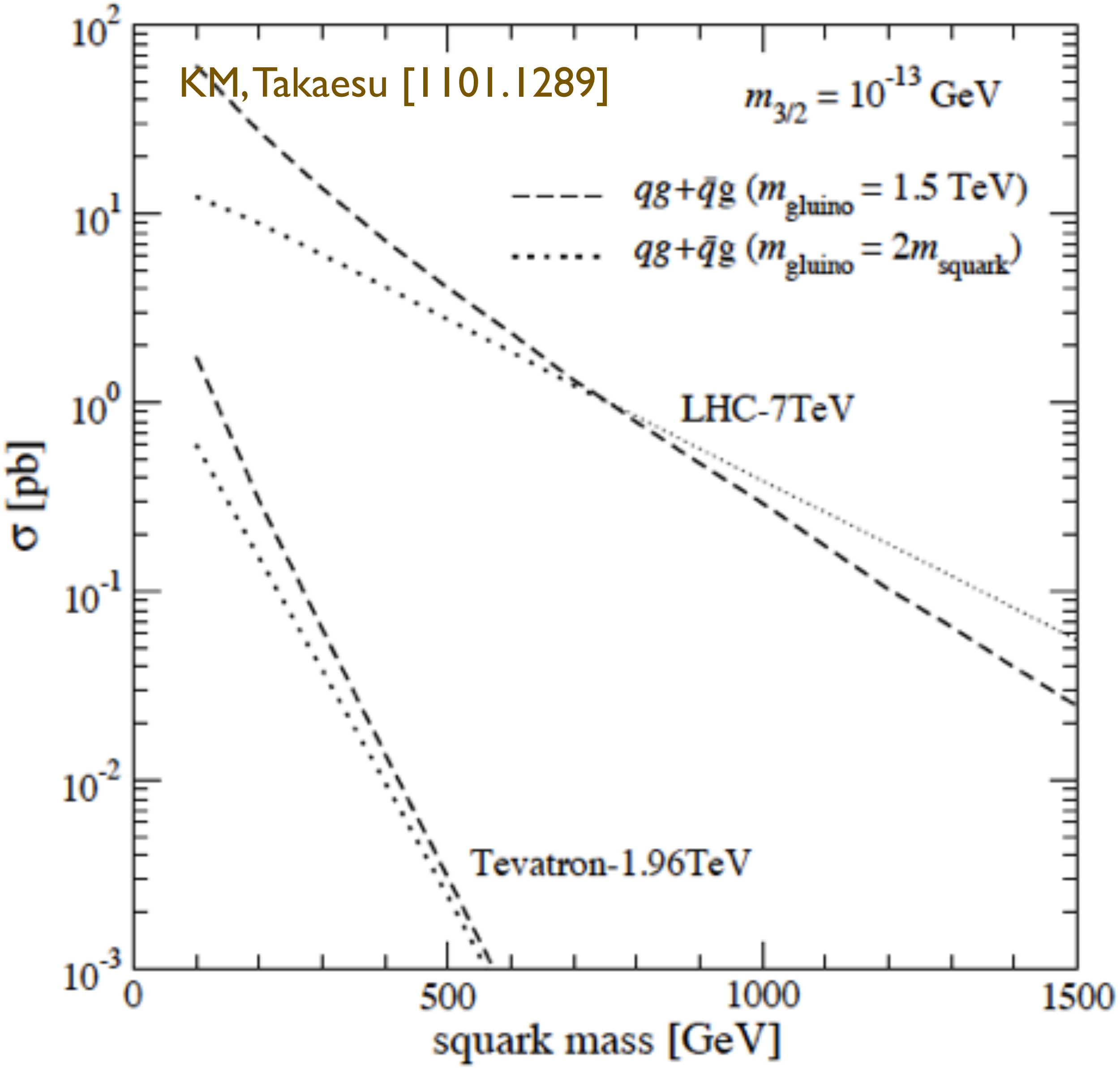

Fig. 4. Total cross sections of associated gravitino productions with a squark, $p\bar{p}/pp \to \tilde{q}\tilde{G}$, at the Tevatron-1.96TeV/LHC-7TeV for $m_{3/2} = 10^{-13}$ GeV as a function of the squark mass. The gluino masses are fixed at 1.5 TeV (dashed) and $2m_{\tilde{q}}$ (dotted), where the cross section in the $\Gamma_{\tilde{g}\to g\tilde{G}} > m_{\tilde{g}}/2$ region is shown with a thin dotted line.

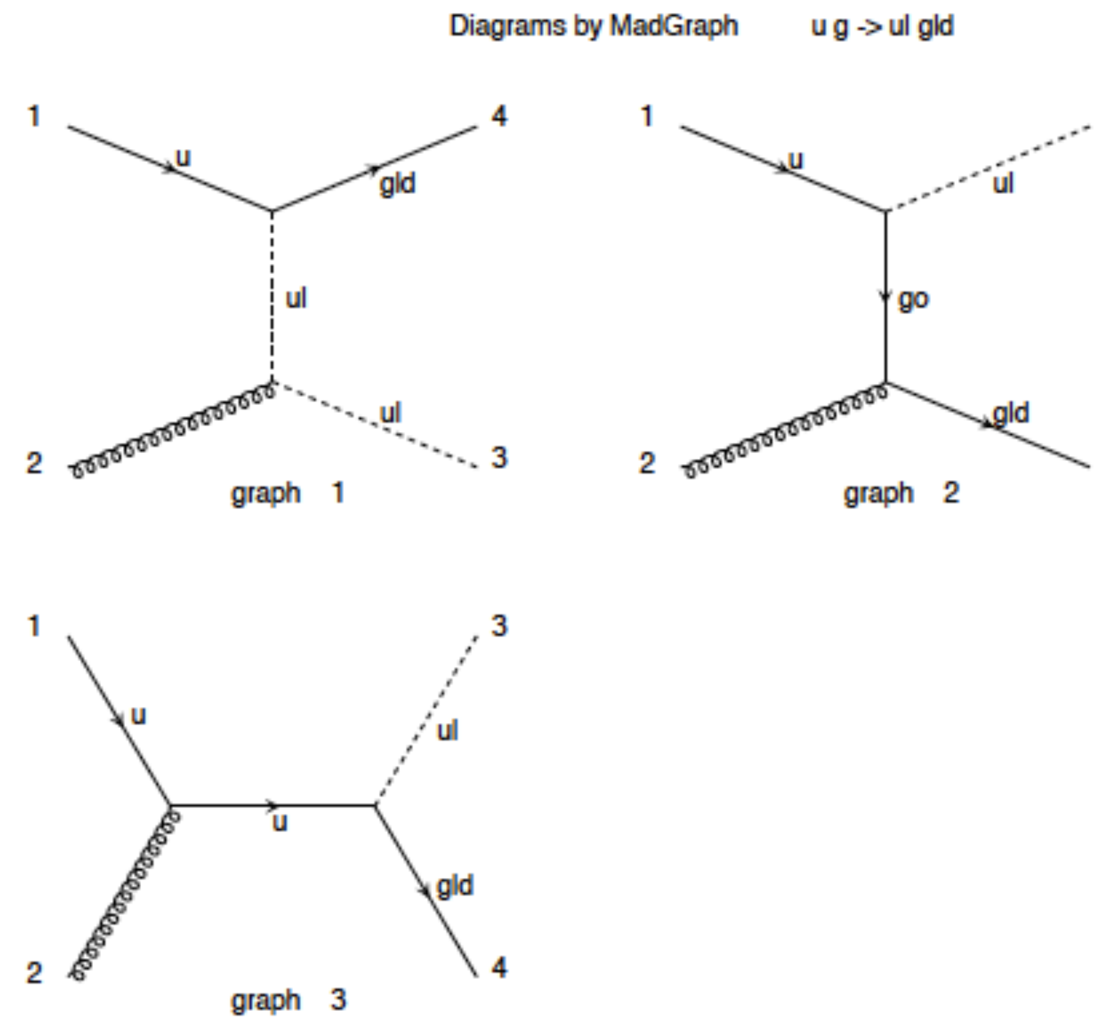

- Similar to the gluino productions, the heavy gluino increases the cross section.

Fayet (1986)
Lopez, Nanopoulos, Zichichi (1996)

2.1 Neutralino NLSP (mono-photon)

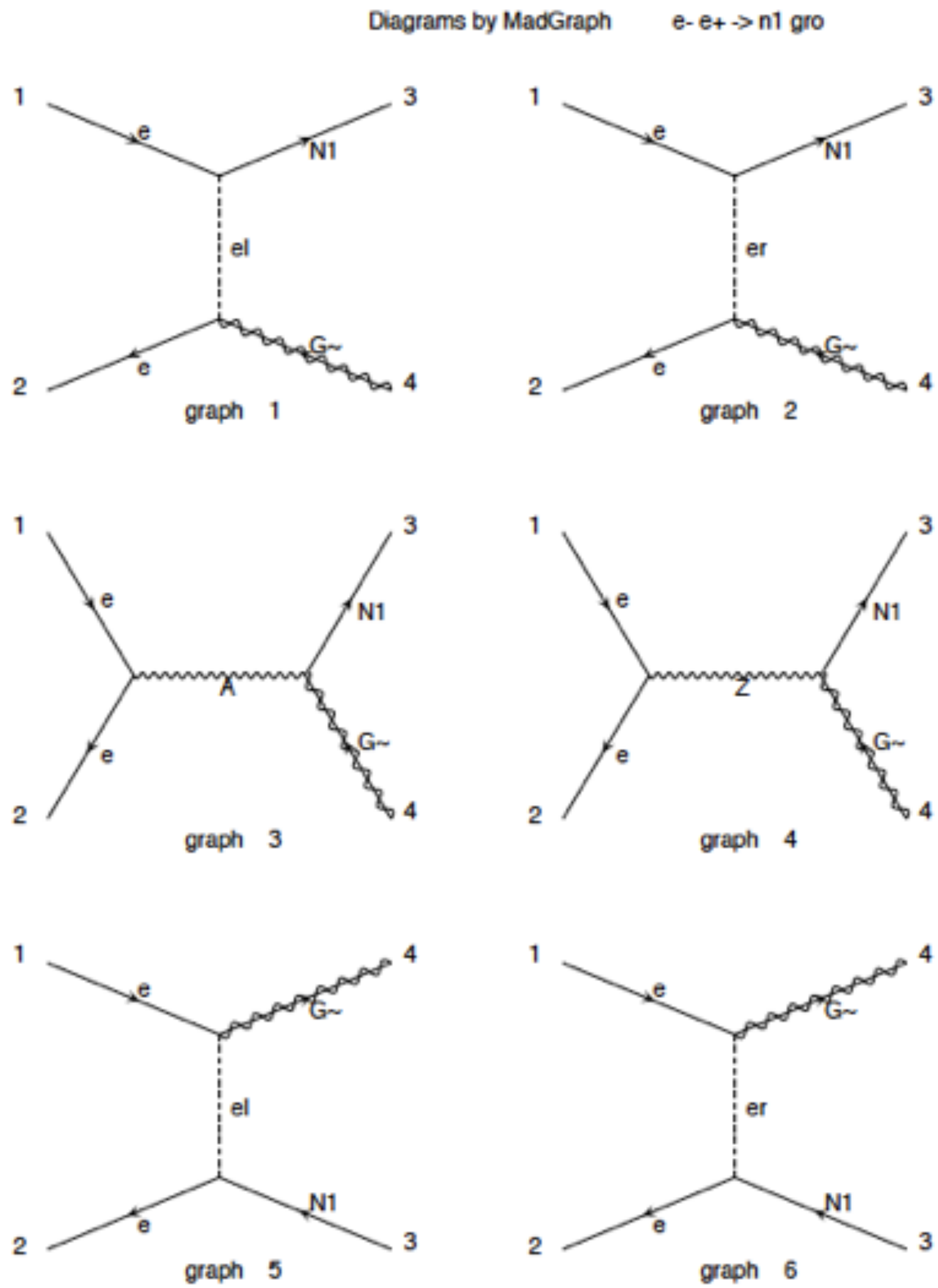

$$e^-\left(p_1,\frac{\lambda_1}{2}\right)+e^+\left(p_2,\frac{\lambda_2}{2}\right)\to\tilde{\chi}_1^0\left(p_3,\frac{\lambda_3}{2}\right)+\tilde{G}\left(p_4,\frac{\lambda_4}{2}\right)$$

$$\mathcal{M}_{\lambda,\lambda_3\lambda_4}=\mathcal{M}^{s_\lambda}+\mathcal{M}^{t_\lambda}+\mathcal{M}^{u_\lambda}\qquad\text{with }\lambda=\lambda_1=-\lambda_2$$

$$\mathcal{M}^{s}_{\lambda,\lambda_3\lambda_4}=\frac{-e\,C^s_\lambda\,m_{\tilde{\chi}^0_1}}{2\sqrt{6}\,\overline{M}_{\rm Pl}m_{3/2}}\frac{1}{s}\,\bar{v}(p_2,-\lambda)\gamma^\mu u(p_1,\lambda)$$
$$\times\,\bar{u}(p_4,\lambda_4)[\not{p}_3+\not{p}_4,\gamma_\mu]v(p_3,\lambda_3),$$

$$\mathcal{M}^{t_\lambda}_{\lambda,\lambda_3\lambda_4}=\frac{\sqrt{2}\,e\,C^{\tilde{e}*}_\lambda\,m^2_{\tilde{e}_\lambda}}{\sqrt{3}\,\overline{M}_{\rm Pl}m_{3/2}}\frac{1}{t-m^2_{\tilde{e}_\lambda}}$$
$$\times\,\bar{u}(p_3,\lambda_3)u(p_1,\lambda)\,\bar{v}(p_2,-\lambda)v(p_4,\lambda_4),$$

$$\mathcal{M}^{u_\lambda}_{\lambda,\lambda_3\lambda_4}=\frac{-\sqrt{2}\,e\,C^{\tilde{e}}_\lambda\,m^2_{\tilde{e}_\lambda}}{\sqrt{3}\,\overline{M}_{\rm Pl}m_{3/2}}\frac{1}{u-m^2_{\tilde{e}_\lambda}}$$
$$\times\,\bar{u}(p_4,\lambda_4)u(p_1,\lambda)\,\bar{v}(p_2,-\lambda)v(p_3,\lambda_3),$$

$$C^s_\lambda=C^\gamma+\frac{s}{s-m_Z^2+im_Z\Gamma_Z}g_\lambda C^Z$$
$$C^\gamma=U_{11}\cos\theta_W+U_{21}\sin\theta_W,$$
$$C^Z=-U_{11}\sin\theta_W+U_{21}\cos\theta_W,$$
$$C^{\tilde{e}}_\pm=T^{\tilde{e}}_\pm\frac{U_{21}}{\sin\theta_W}+Y^{\tilde{e}}_\pm\frac{U_{11}}{\cos\theta_W},$$

$$e^+e^-\to\tilde{\chi}_1^0\tilde{G}\to\gamma\tilde{\chi}_1^0\tilde{\chi}_1^0\Rightarrow\gamma+\not{E}$$

Helicity amplitudes

$$\mathcal{M}_{\lambda,\lambda_3\lambda_4} = \frac{-e}{\sqrt{6}\,\overline{M}_{\rm Pl} m_{3/2}} \sqrt{\beta}\, s\, \hat{\mathcal{M}}_{\lambda,\lambda_3\lambda_4}$$

KM, Oexl, Takaesu

λ	$\lambda_3\lambda_4$			$\hat{\mathcal{M}}^s$	$\hat{\mathcal{M}}^t$	$\hat{\mathcal{M}}^u$	
$\pm$	$\pm\mp$	$(1+\cos\theta)$	[	$\frac{m_{\tilde{\chi}}^2}{s} C_\pm^s$		$+\frac{m_{\tilde{e}_\pm}^2}{u-m_{\tilde{e}_\pm}^2} C_\pm^{\tilde{e}}$	]
$\pm$	$\mp\pm$	$-(1-\cos\theta)$	[	$\frac{m_{\tilde{\chi}}^2}{s} C_\pm^s$	$+\frac{m_{\tilde{e}_\pm}^2}{t-m_{\tilde{e}_\pm}^2} C_\pm^{\tilde{e}}$		]
$\pm$	$\pm\pm$	$\pm\frac{m_{\tilde{\chi}}}{\sqrt{s}}\sin\theta$	[	$C_\pm^s$	$+\frac{m_{\tilde{e}_\pm}^2}{t-m_{\tilde{e}_\pm}^2} C_\pm^{\tilde{e}}$		]
$\pm$	$\mp\mp$	$\mp\frac{m_{\tilde{\chi}}}{\sqrt{s}}\sin\theta$	[	$C_\pm^s$		$+\frac{m_{\tilde{e}_\pm}^2}{u-m_{\tilde{e}_\pm}^2} C_\pm^{\tilde{e}}$	]

Table 1. The reduced helicity amplitudes $\hat{\mathcal{M}}_{\lambda,\lambda_3\lambda_4}$ for $e^-_\lambda e^+_{-\lambda} \to \tilde{\chi}^0_{1\lambda_3} \tilde{G}_{\lambda_4}$.

- The overall angular dependence is dictated by the J=1 d-function as
$$\mathcal{M}_{\lambda,\lambda_3\lambda_4} \propto d^1_{\lambda,(\lambda_3-\lambda_4)/2}(\theta)$$
- The t- and u-amplitudes become dominant as the selectron mass increases.
- The cross sections for $\lambda_3=\lambda_4$ are very small.

Total cross sections (the collision energy)

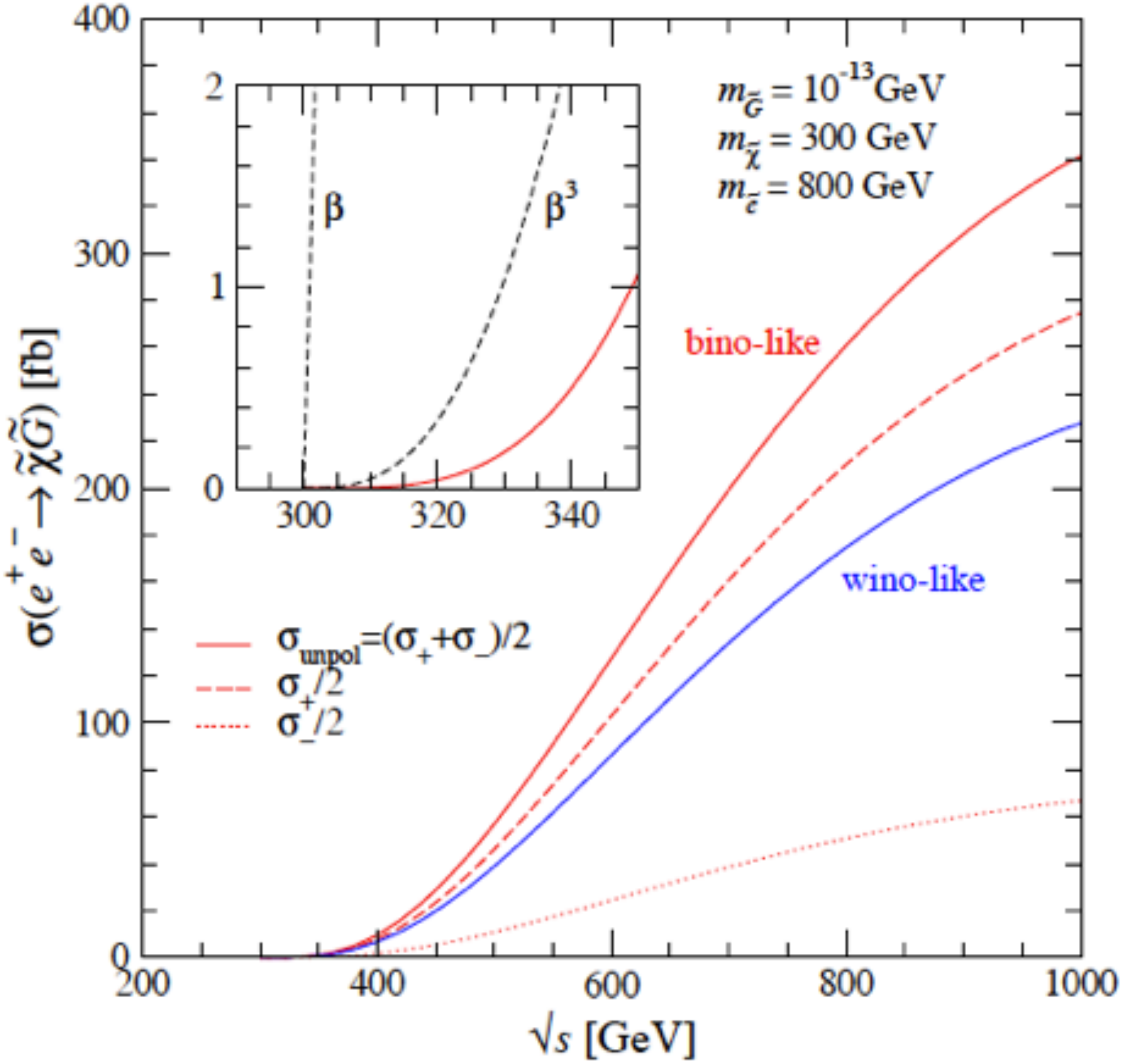

Fig. 2. Total cross sections of associated gravitino productions with a bino-/wino-like neutralino in e^+e^- collisions, $e^+e^- \to \tilde{\chi}^0_1\tilde{G}$, for $m_{3/2} = 10^{-13}$ GeV as a function of the collision energy. The neutralino and selectron masses are fixed at 300 GeV and 800 GeV, respectively. The threshold region is enlarged and the hypothetical dependence $\sigma \sim \beta$ and β^3 with the same cofficient is also shown.

- The initial-helicity (λ) dependent cross section

$$d\sigma_\lambda = \frac{1}{2s}\frac{1}{2}\sum_{\lambda_{3,4}} |\mathcal{M}_{\lambda,\lambda_3\lambda_4}|^2 d\Phi_2$$

- The cross section scales with $(m_{3/2})^{-2}$.
- The threshold excitation is $\sigma \sim \beta^4$.
- The ratio of the polarized and unpolarized cross sections is roughly given by

$$\frac{\sigma_\pm}{2\sigma_{\rm unpol}} \sim \frac{|C^{\tilde{e}}_\pm|^2}{|C^{\tilde{e}}_+|^2 + |C^{\tilde{e}}_-|^2}$$

→ neutralino mixing

Total cross sections (the neutralino mass)

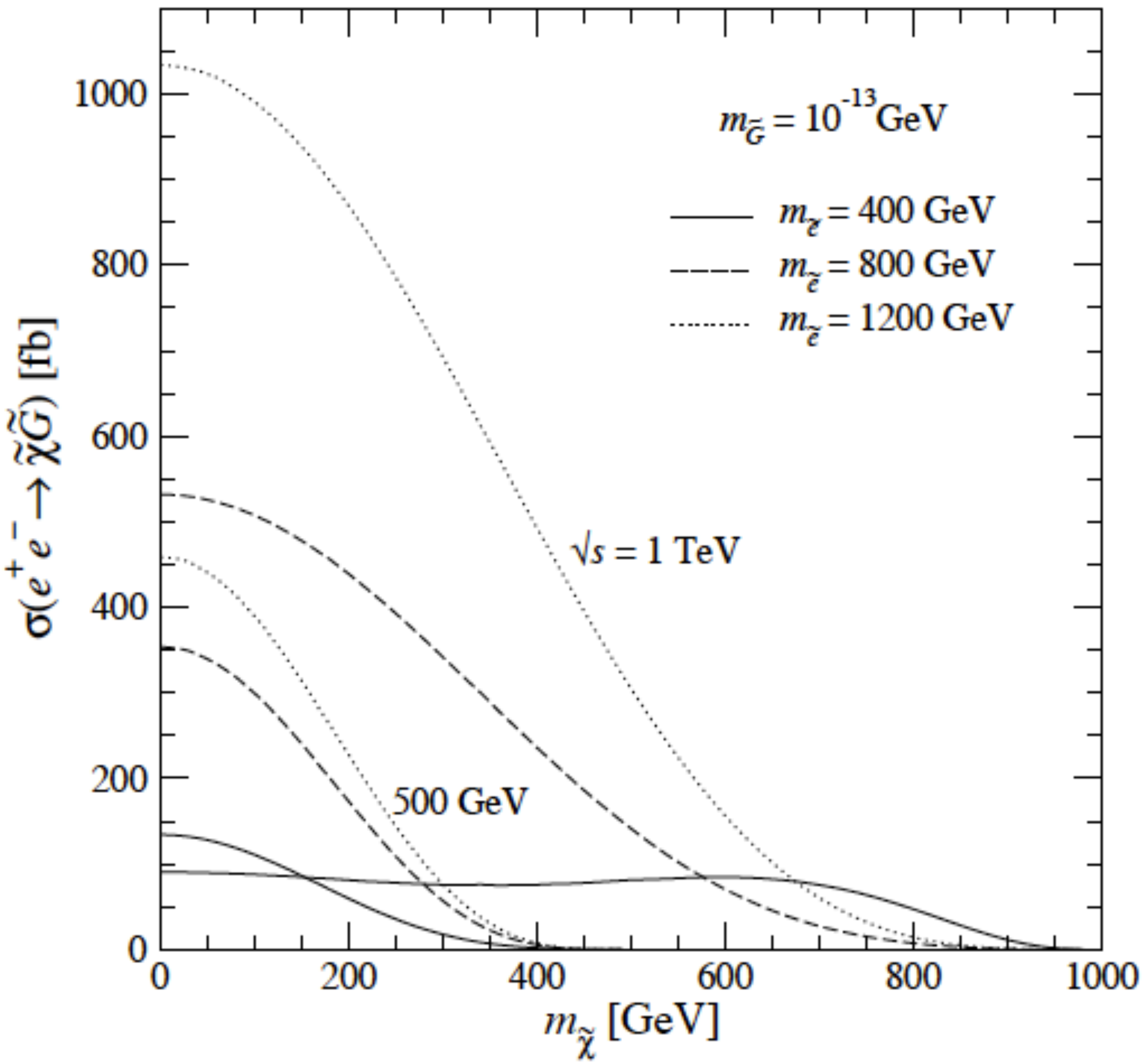

Fig. 3. Total cross sections of $e^+e^- \to \tilde{\chi}_1^0\tilde{G}$ at $\sqrt{s} = 500$ GeV and 1 TeV for $m_{3/2} = 10^{-13}$ GeV as a function of the neutralino mass. The selectron masses are fixed at 400 (solid), 800 (dashed) and 1200 (dotted) GeV, respectively.

- The cross sections are strongly suppressed as the neutralino mass is approaching the collider energy.
- The cross sections are quite sensitive to the selectron masses, even if the collider energy cannot reach them.

Angular distributions

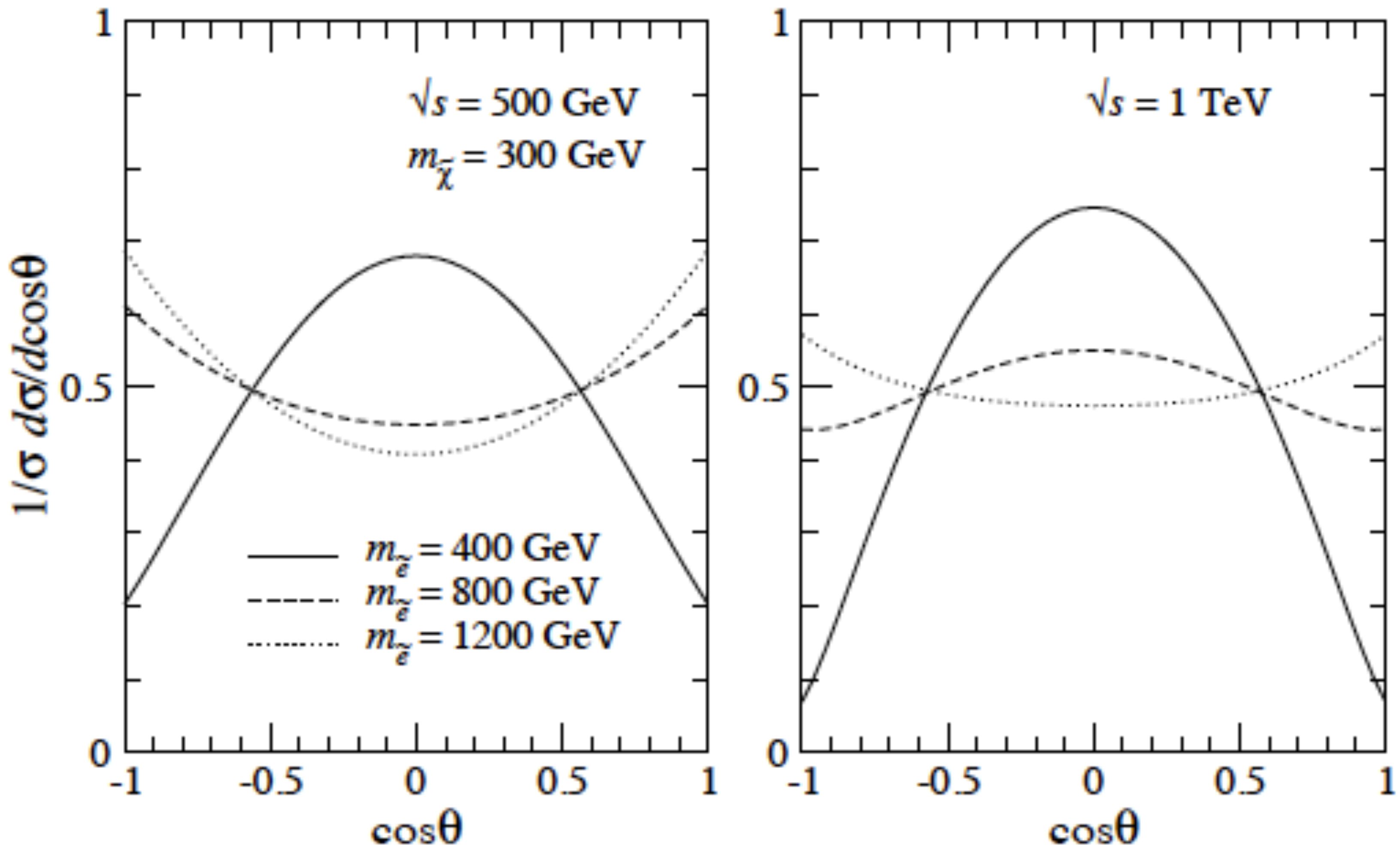

Fig. 4. Normalized angular distributions of neutralinos in $e^+e^- \rightarrow \tilde{\chi}_1^0 \tilde{G}$ at $\sqrt{s}$ = 500 GeV (left) and 1 TeV (right) for $m_{\tilde{\chi}_1^0}$ = 300 GeV, where the selectron masses are taken to be 400, 800 and 1200 GeV.

- Not only the cross section but also the angular distribution is sensitive to the selectron masses.

Single-photon + missing energy

σ [fb]		$(P_{e^-}, P_{e^+}) =$	$(0,0)$	$(0.9,0)$	$(0.9,-0.6)$
$\sqrt{s} = 500$ GeV	$m_{\tilde{e}} = 400$ GeV		15	23	37
	800 GeV		48	75	119
	1200 GeV		64	100	159
	SM background		1592	178	94
$\sqrt{s} = 1$ TeV	$m_{\tilde{e}} = 400$ GeV		72	112	177
	800 GeV		320	494	785
	1200 GeV		642	1002	1582
	SM background		1443	149	65

Table 2. Cross sections in fb for the signal $e^+e^- \to \tilde{\chi}_1^0\tilde{G} \to \gamma\tilde{G}\tilde{G}$, assuming $B(\tilde{\chi}_1^0 \to \gamma\tilde{G}) = 1$, with $m_{\tilde{G}} = 10^{-13}$ GeV and $m_{\tilde{\chi}_1^0} = 300$ GeV and for the SM background $e^+e^- \to \gamma\nu\bar{\nu}$ at $\sqrt{s} = 500$ GeV and 1 TeV, with different beam polarizations. The minimal cuts in (19) and the Z-peak cut in (20) are taken into account.

- The kinematical cuts:

$$E_\gamma > 0.03\sqrt{s}, \quad |\eta_\gamma| < 2, \text{ (19)} \qquad E_\gamma < \frac{s - m_Z^2}{2\sqrt{s}} - 5\Gamma_Z, \text{ (20)}$$

- The cross section with beam polarizations:

$$\sigma(P_{e^-}, P_{e^+}) = 2\sum_\lambda \left(\frac{1 + P_{e^-}\lambda}{2}\right)\left(\frac{1 - P_{e^+}\lambda}{2}\right)\sigma_\lambda$$

- With beam polarizations, the signal is enhanced, while the background coming from the t-channel W-exchange can be reduced.

Mono-photon distributions (energy)

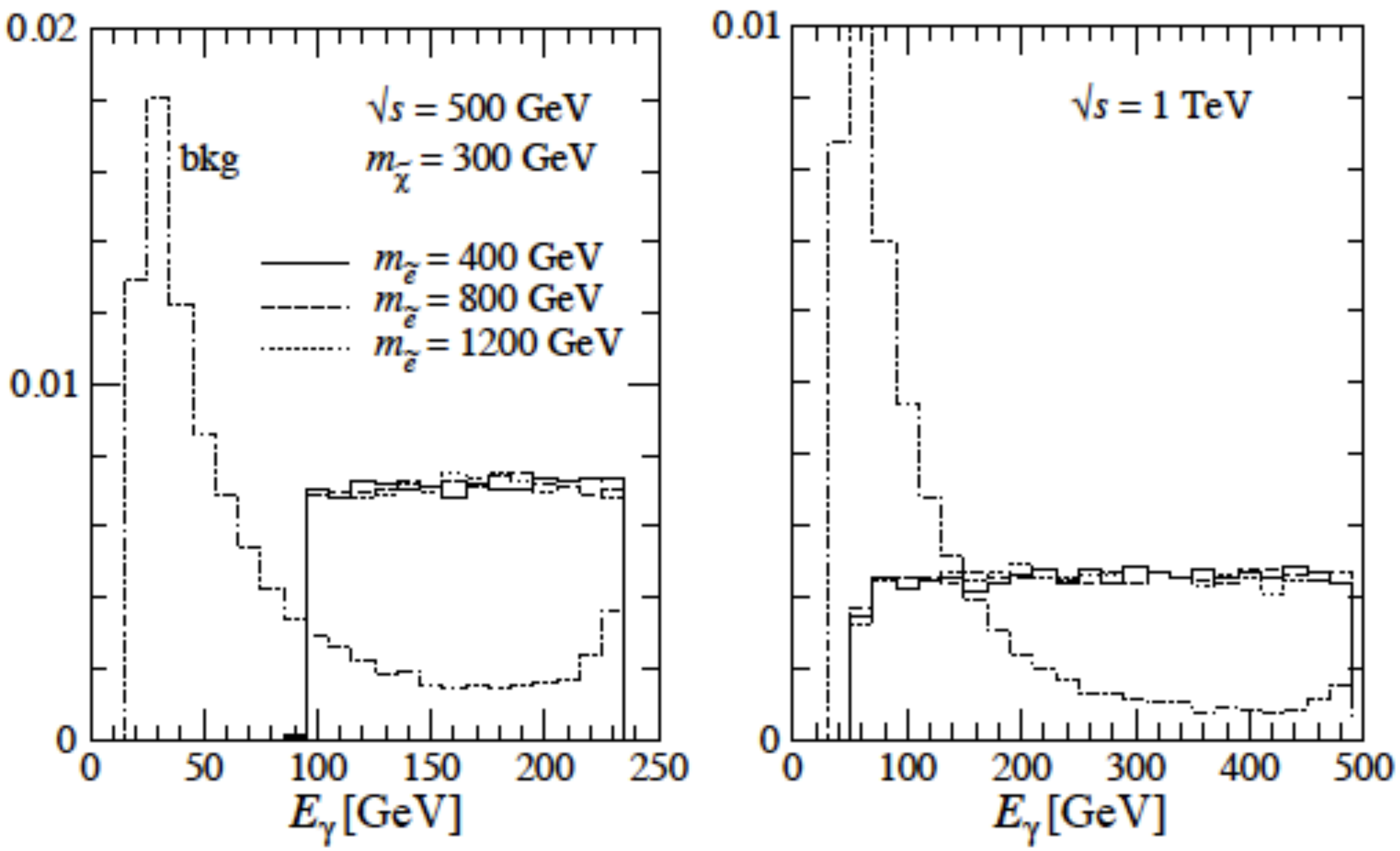

Fig. 5. Normalized photon energy distributions in $e^+e^- \to \tilde{\chi}_1^0 \tilde{G} \to \gamma \tilde{G} \tilde{G}$ at $\sqrt{s}$ = 500 GeV (left) and 1 TeV (right) for $m_{\tilde{\chi}_1^0}$ = 300 GeV, where $m_{\tilde{e}}$ = 400 (solid), 800 (dashed) and 1200 (dotted) GeV, respectively, with all the kinematical cuts and the beam polarizations as table 2. Those of the SM background are also shown by dot-dashed lines.

- The neutralino decays into a photon and a gravitino is isotropic in the neutralino rest frame.
- The range of the energy is

$$\frac{m_{\tilde{\chi}}^2}{2\sqrt{s}} < E_\gamma < \frac{\sqrt{s}}{2}$$

→ neutralino mass

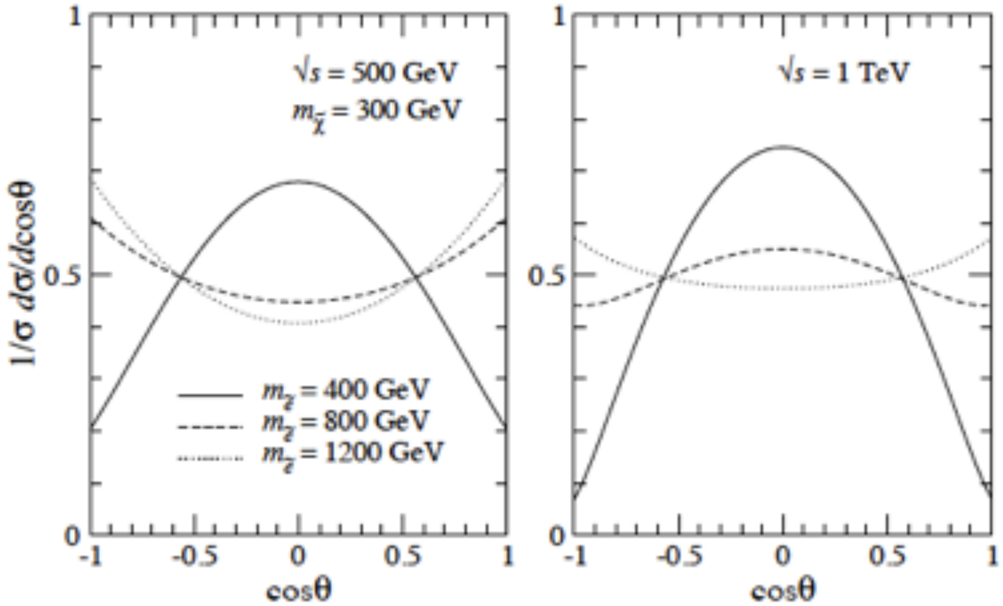

Mono-photon distributions (angle)

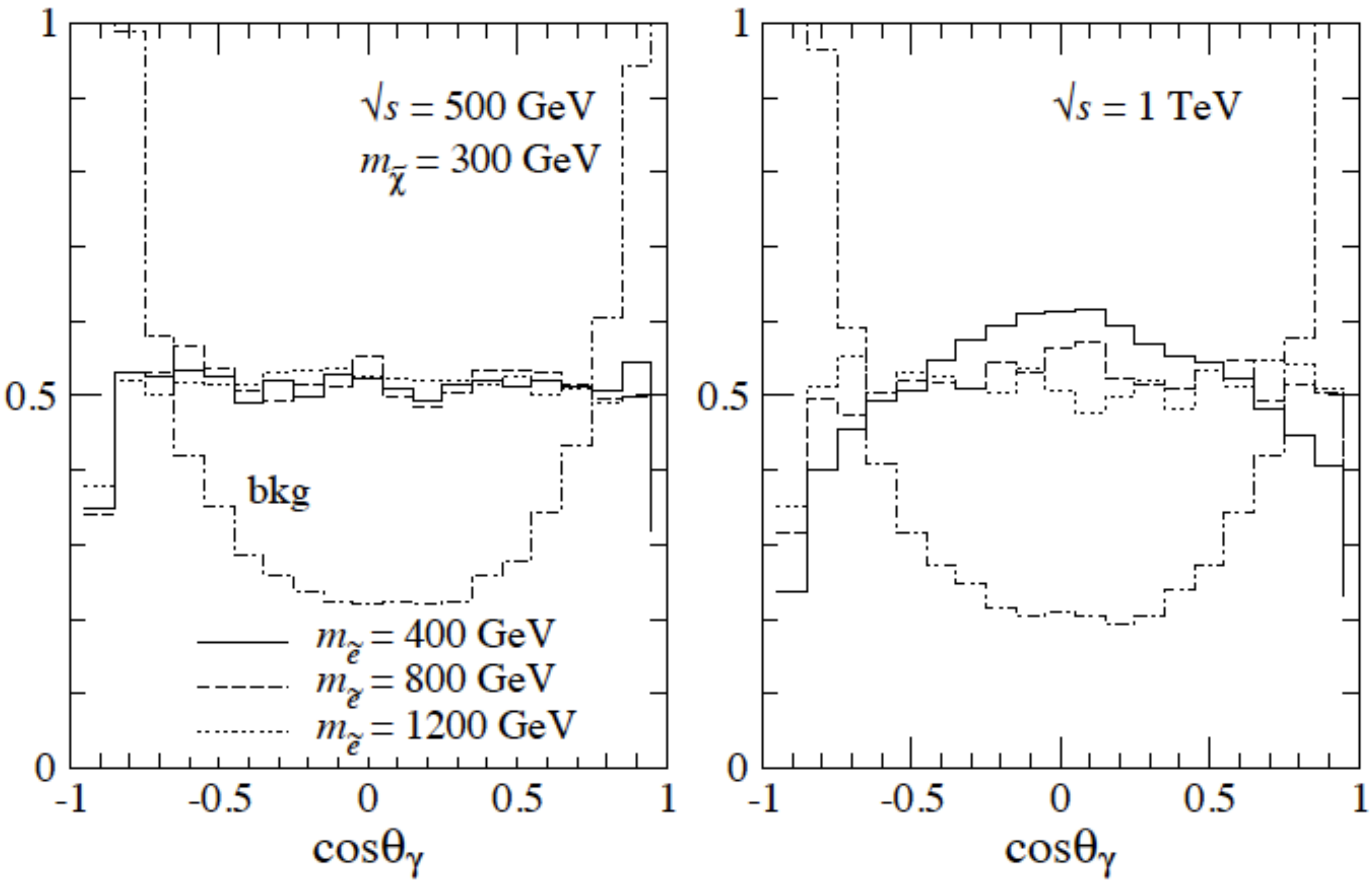

- When $\beta \to 1$, the original neutralino directions can survive.
  → selectron mass

2. I Neutralino NLSP (mono-photon)

- Single photon + missing energy at LEP
  - The cross section proportional to $(m_{3/2})^{-2}$.

EPJC38(2005)395

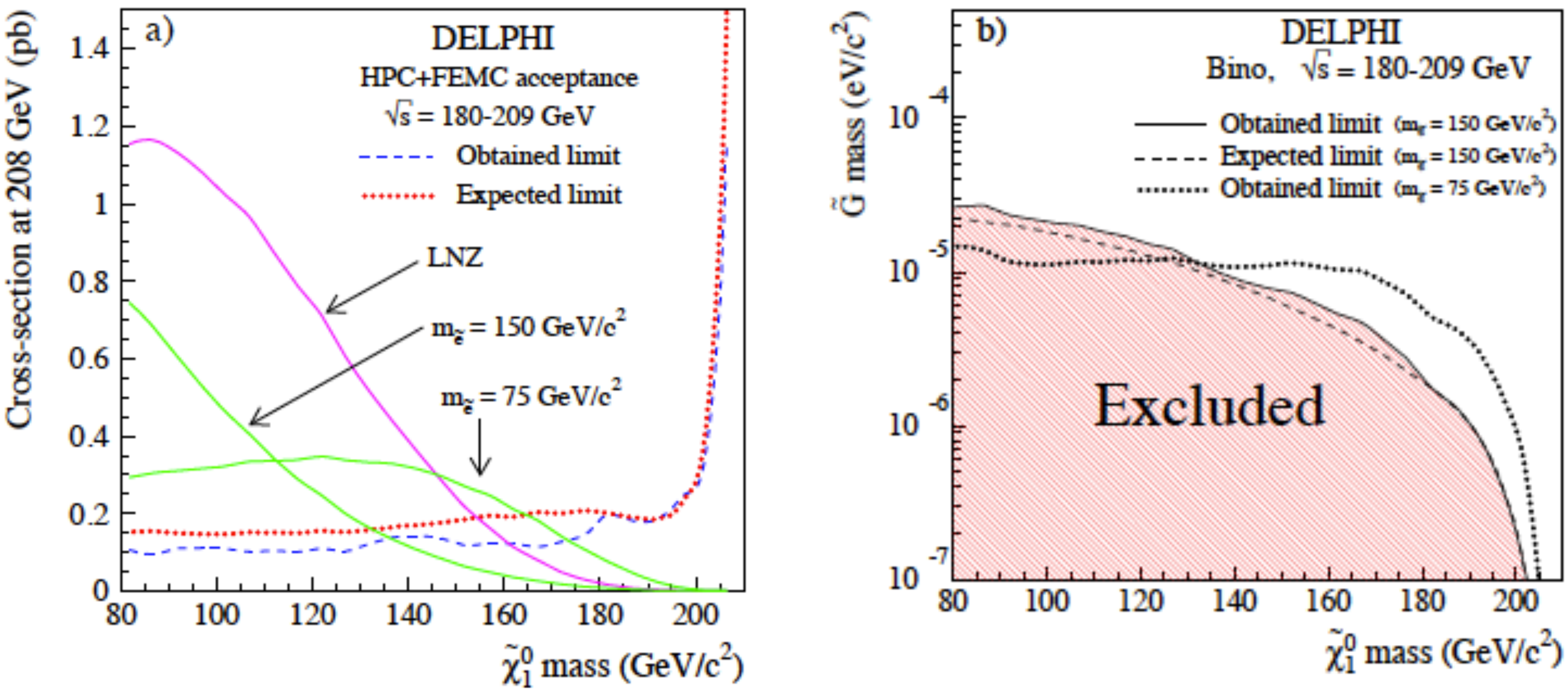

Figure 9: a) Upper limit at 95% C.L. on the cross-section at $\sqrt{s}$ =208 GeV of the process $e^+e^- \rightarrow \tilde{G}\tilde{\chi}_1^0 \rightarrow \tilde{G}\tilde{G}\gamma$ as a function of the $\tilde{\chi}_1^0$ mass. The predicted cross-sections under the assumption that the neutralino is a Bino or as described by the LNZ-model are also shown for $m_{\tilde{G}} = 1 \times 10^{-5}$ eV/c^2. b), c) Exclusion plots in the $m_{\tilde{\chi}_1^0}$-$m_{\tilde{G}}$ mass plane.

2. 1 Neutralino NLSP (mono-photon)

- Single photon + missing energy at LEP
  - The cross section proportional to $(m_{3/2})^{-2}$.

EPJC38(2005)395

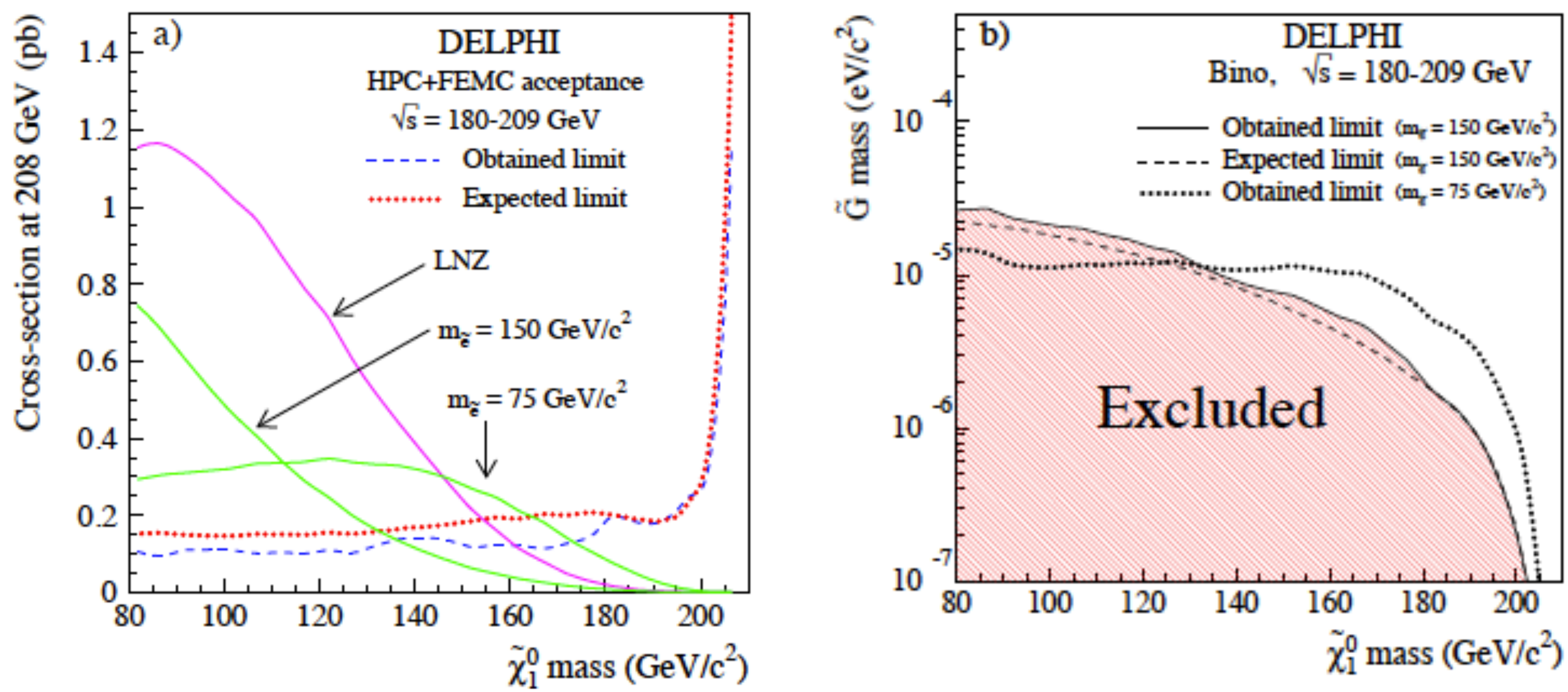

Figure 9: a) Upper limit at 95% C.L. on the cross-section at $\sqrt{s}$ =208 GeV of the process $e^+e^- \to \tilde{G}\tilde{\chi}_1^0 \to \tilde{G}\tilde{G}\gamma$ as a function of the $\tilde{\chi}_1^0$ mass. The predicted cross-sections under the assumption that the neutralino is a Bino or as described by the LNZ-model are also shown for $m_{\tilde{G}} = 1 \times 10^{-5}$ eV/c^2. b), c) Exclusion plots in the $m_{\tilde{\chi}_1^0}$-$m_{\tilde{G}}$ mass plane.

$$\boxed{\begin{array}{l} m_{\tilde{G}} > 1.09 \cdot 10^{-5}\ \mathrm{eV/c^2} \\ |F|^{\frac{1}{2}} > 214\ \mathrm{GeV} \end{array}}$$

2.2 Neutralino NLSP (di-photon)

- Two-photon + missing energy at LEP

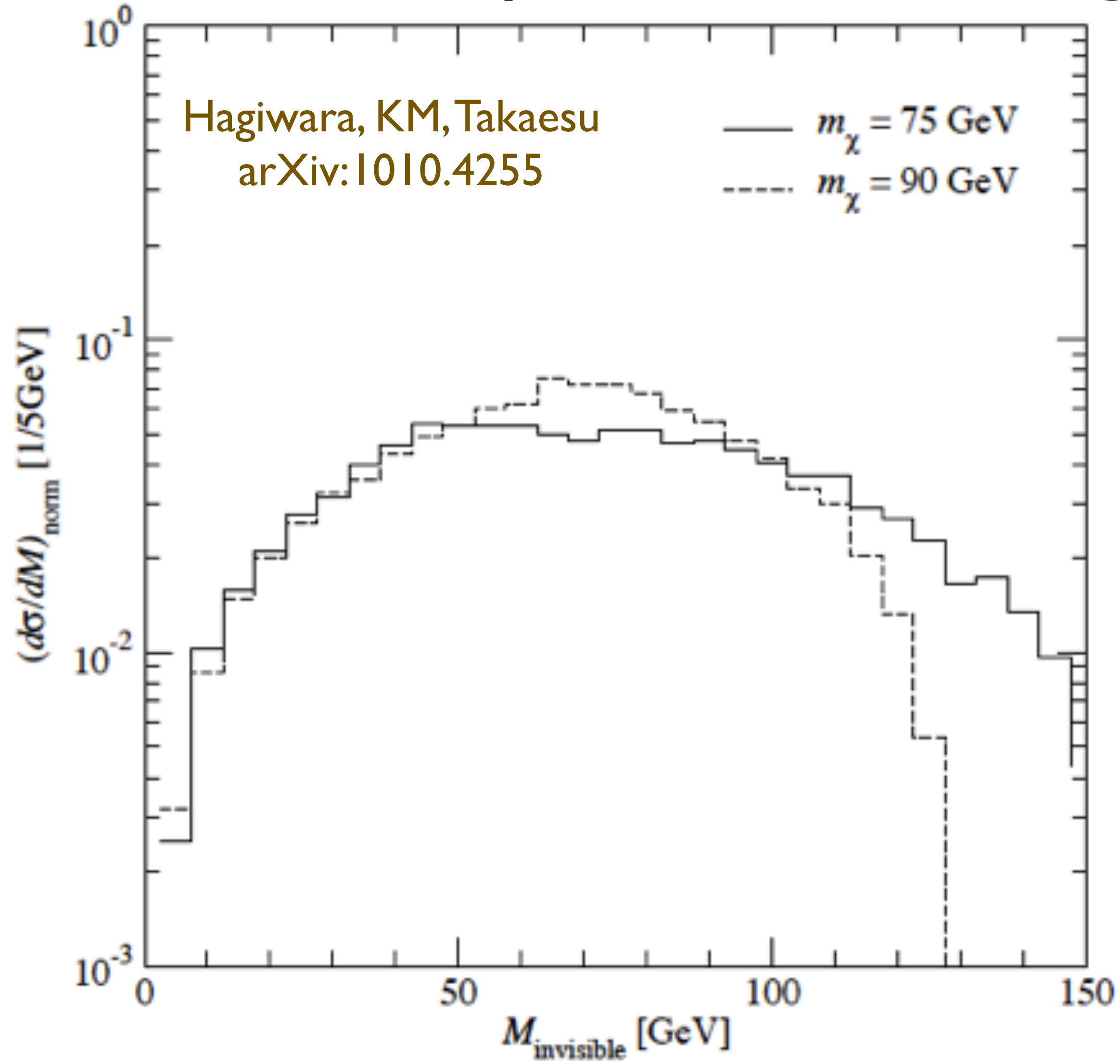

Fig. 4. Missing invariant mass distributions for $e^+e^- \to \tilde{\chi}_1^0\tilde{\chi}_1^0 \to \gamma\gamma\tilde{G}\tilde{G}$ at $\sqrt{s} = 190$ GeV. The cases for the neutralino mass $m_\chi = 75$ and 90 GeV are shown as a solid and dashed line, respectively, with the normalized cross section after kinematical cuts of (121).

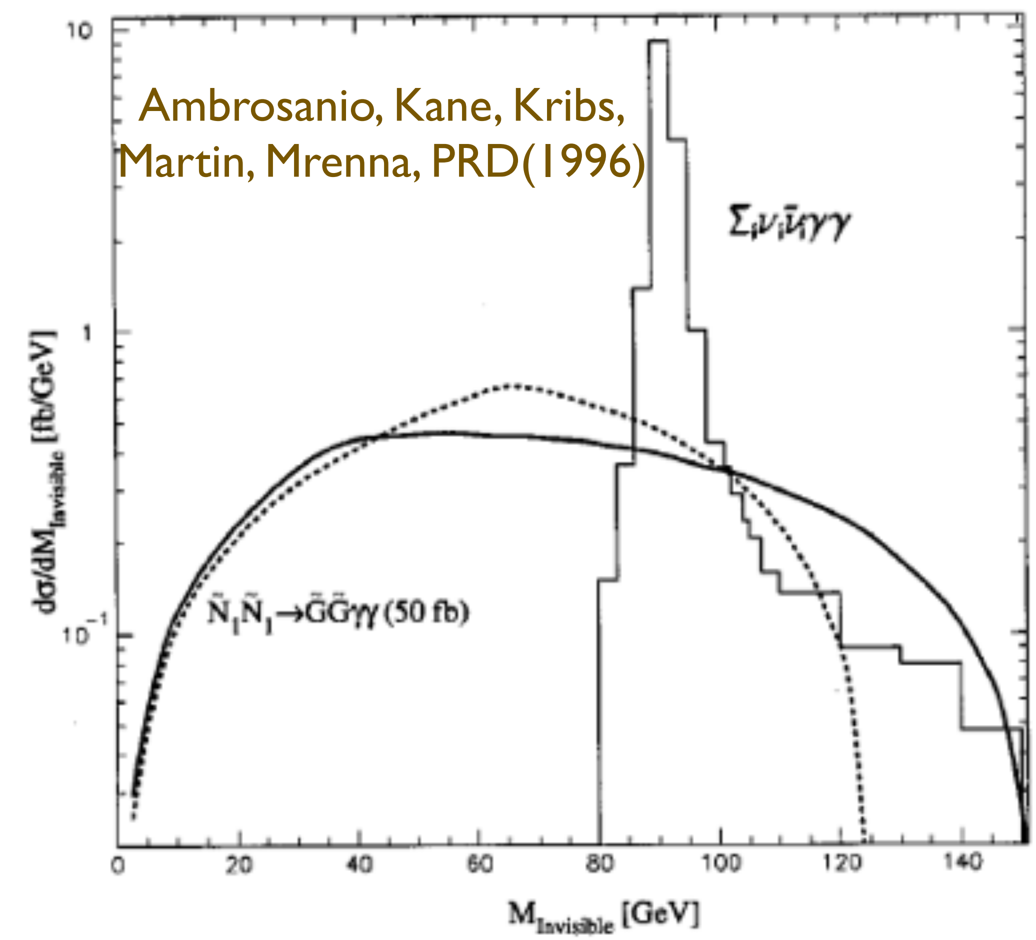

FIG. 16. Distribution of the missing invariant mass in $\gamma\gamma E$ events at LEP with $\sqrt{s}=190$ GeV. Angular and photon energy cuts have been applied as described in the text. The lighter solid line is the remaining total background (56 fb) for all three neutrino species. The signals for $m_{\tilde{N}_1}=75$ and 90 GeV are the solid and dashed lines, respectively, with an arbitrary choice of 50 fb for the signal before cuts in each case.

2.2 Neutralino NLSP (di-photon)

- Two-photon + missing energy at LEP

Hagiwara, KM, Takaesu
arXiv:1010.4255

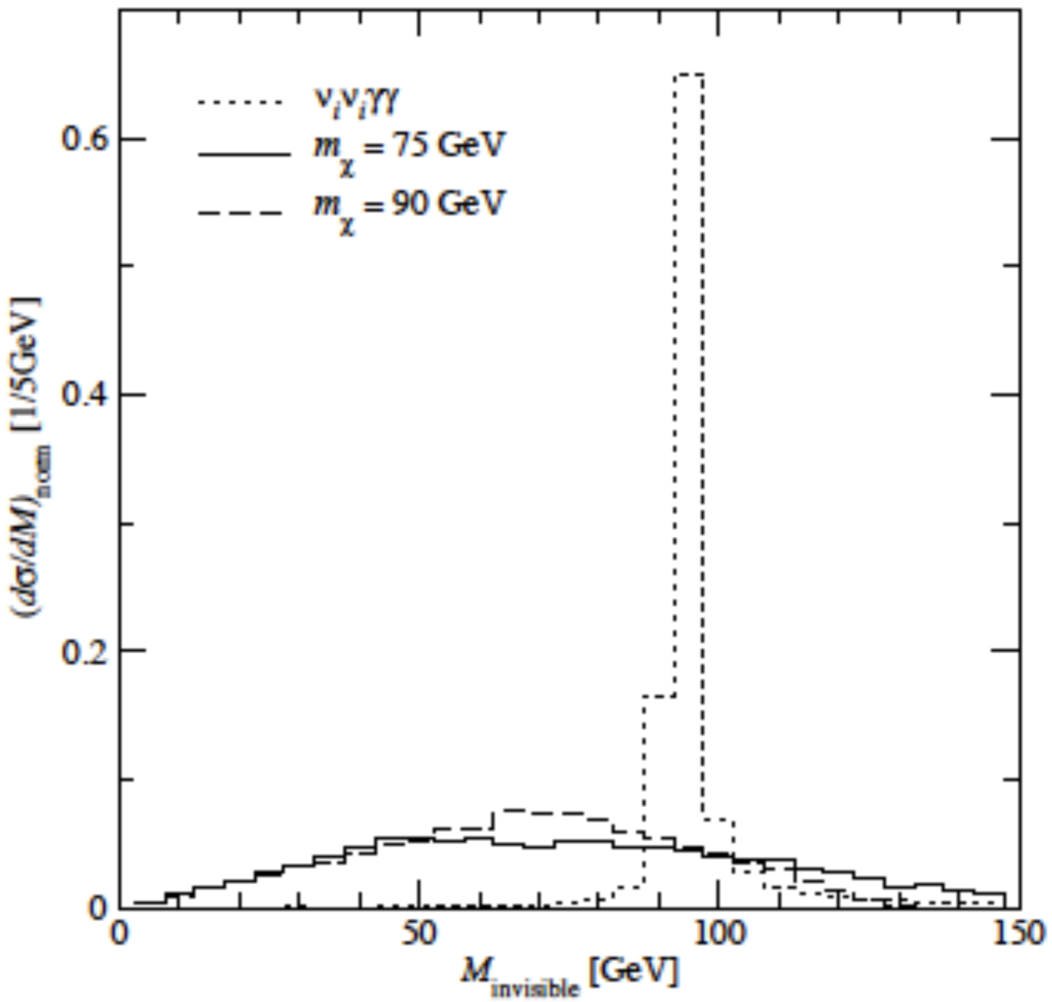

EPJC38(2005)395

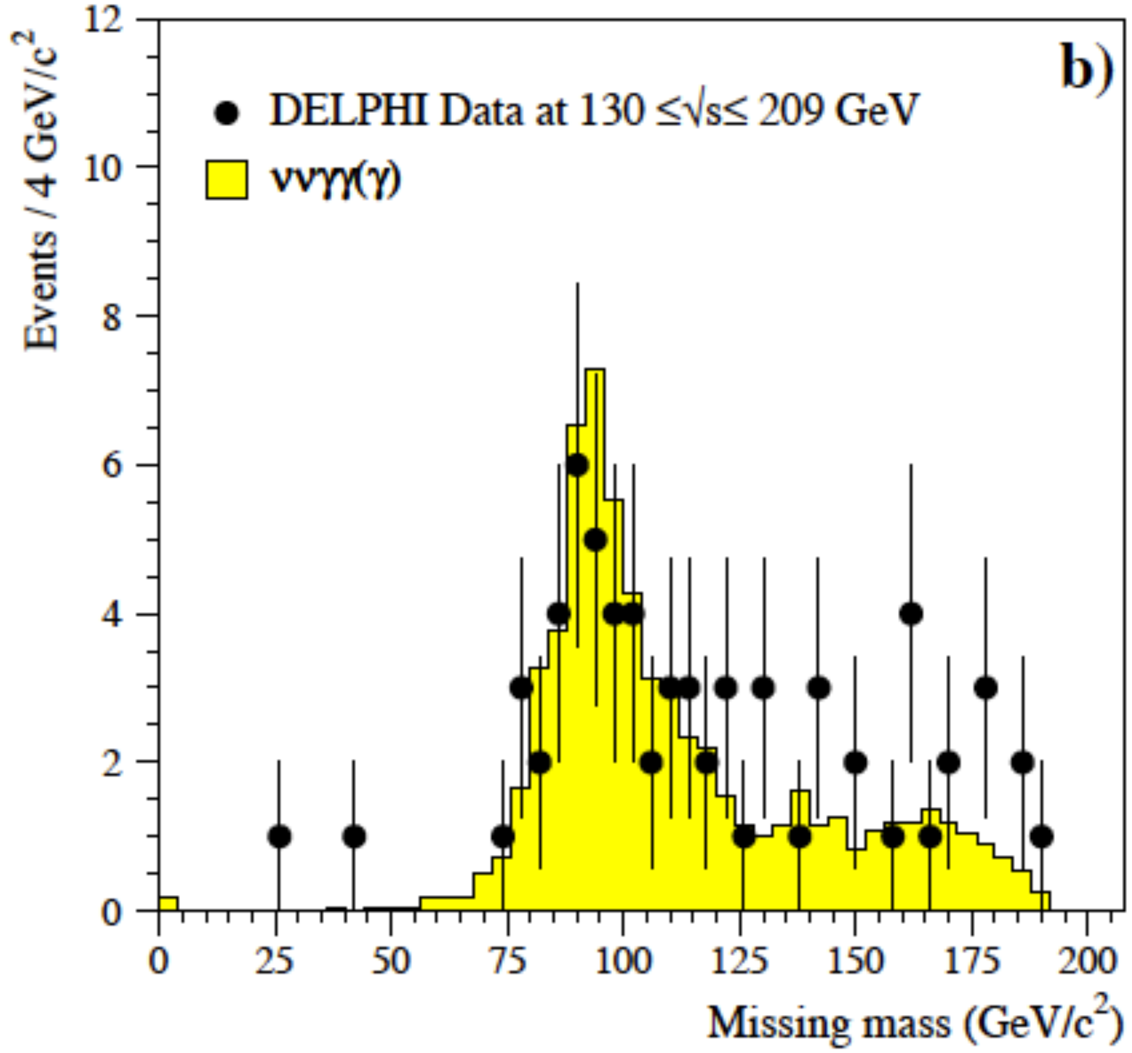

2.2 Neutralino NLSP (di-photon)

- Two-photon + missing energy at LEP
  - The cross section does not depend on $m_{3/2}$.

EPJC38(2005)395

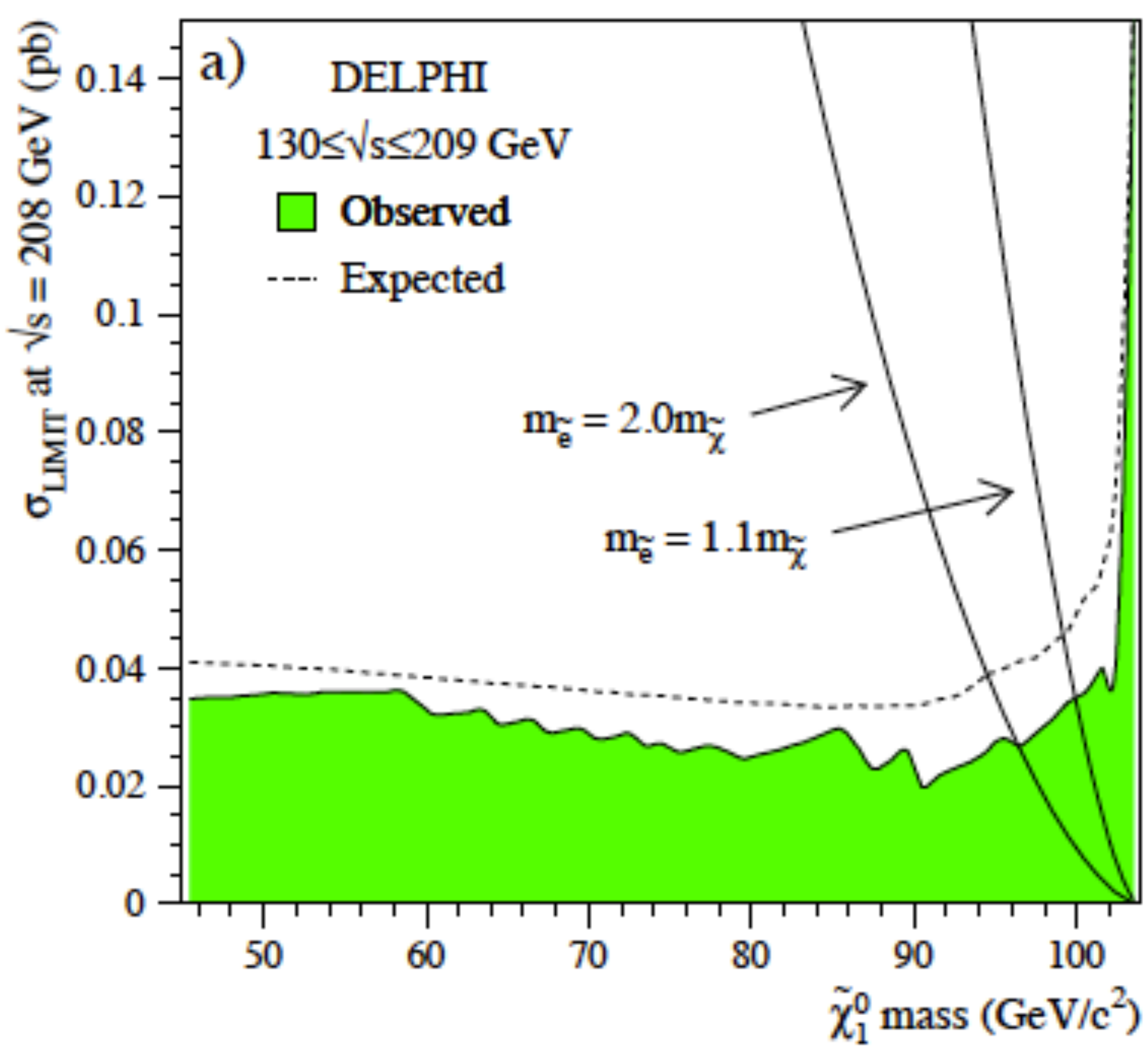

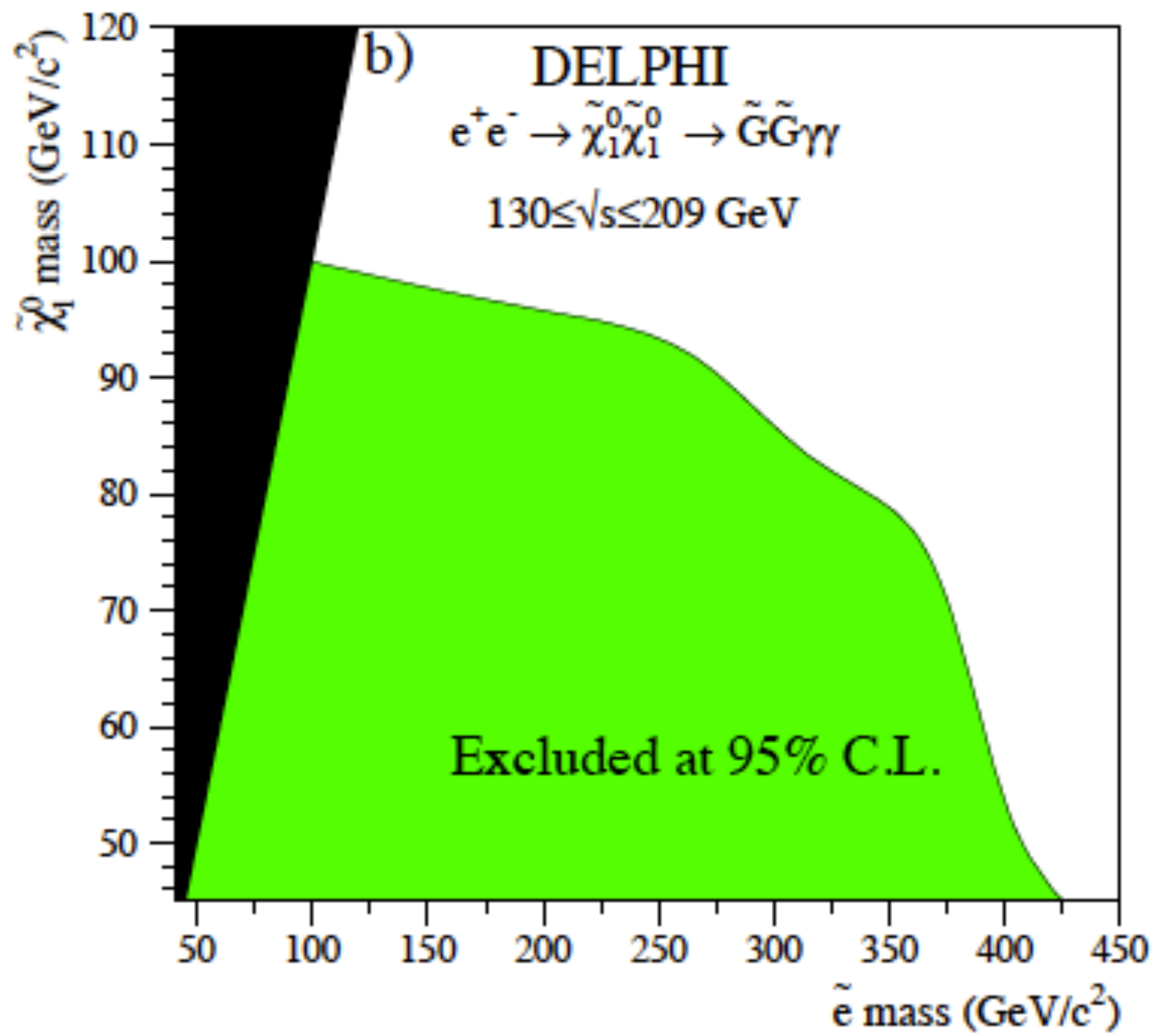

2.3 Neutralino NLSP (di-photon) at LHC

Search for Supersymmetry in pp Collisions at $\sqrt{s} = 7$ TeV in Events with Two Photons and Missing Transverse Energy

The CMS Collaboration*

Abstract

A search for supersymmetry in the context of general gauge-mediated (GGM) breaking with the lightest neutralino as the next-to-lightest supersymmetric particle and the gravitino as the lightest is presented. The data sample corresponds to an integrated luminosity of 36 pb^{-1} recorded by the CMS experiment at the LHC. The search is performed using events containing two or more isolated photons, at least one hadronic jet, and significant missing transverse energy. No excess of events at high missing transverse energy is observed. Upper limits on the signal cross section for GGM supersymmetry between 0.3 and 1.1 pb at the 95% confidence level are determined for a range of squark, gluino, and neutralino masses, excluding supersymmetry parameter space that was inaccessible to previous experiments.

2.3 Neutralino NLSP (di-photon) at LHC

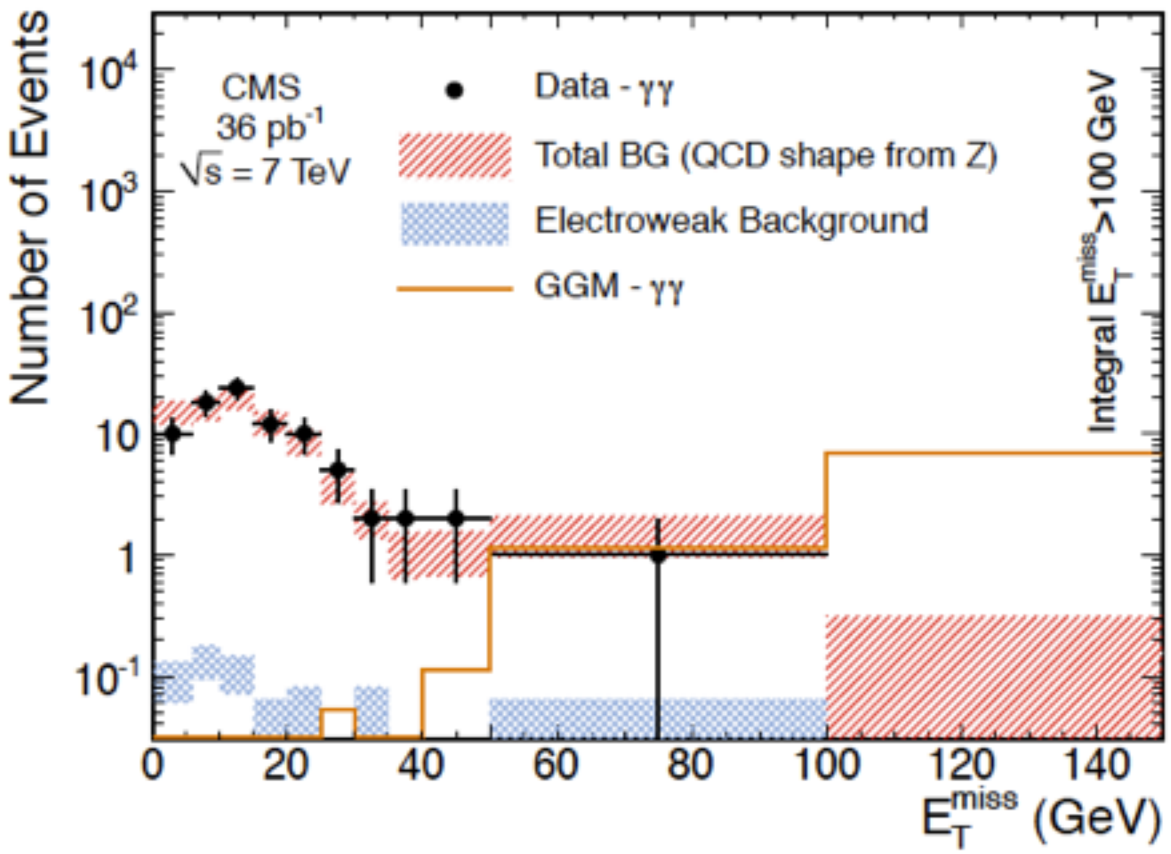

Figure 1: E_T^{miss} distribution for $\gamma\gamma$ data compared with backgrounds and a possible GGM SUSY signal. The solid circles with error bars represent the data. The double-hatched blue band represents the contribution of the electroweak background. The single-hatched red band shows the sum of the electroweak background with the QCD E_T^{miss} prediction obtained from the $Z \to ee$ sample. The widths of the bands correspond to the sum of the statistical and systematic uncertainties on the backgrounds. The prediction of the GGM SUSY sample point described in the text is shown in the plot as the solid line histogram.

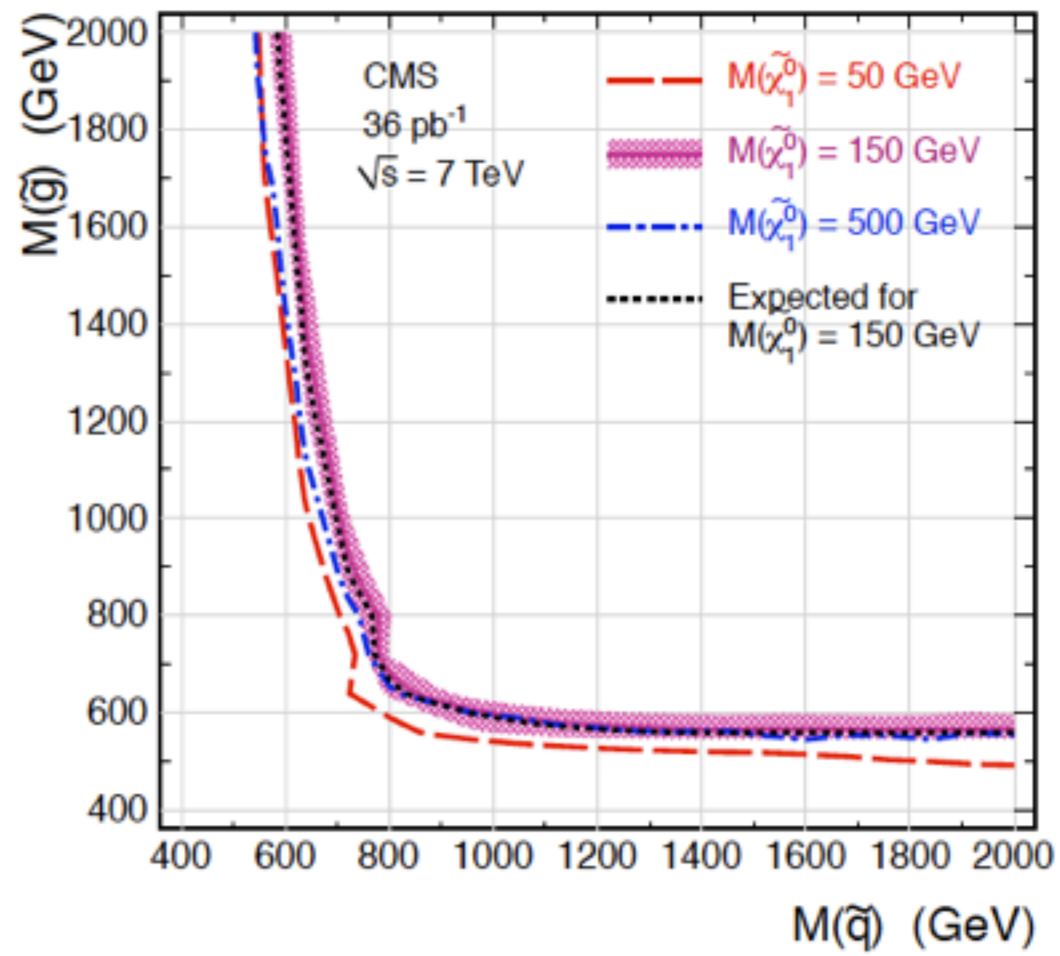

Figure 4: Lower 95% CL exclusion limits on the squark ($\tilde{q}$) and gluino ($\tilde{g}$) masses in the GGM benchmark model for 50, 150, and 500 GeV neutralino ($\tilde{\chi}_1^0$) masses. The areas below and to the left of the lines are excluded. The expected exclusion limit for 150 GeV neutralino mass is shown by the dashed line. The shaded band represents ± 1 standard deviation of theoretical uncertainty on the GGM cross section.

3.1 Selectron NLSP (mono-electron)

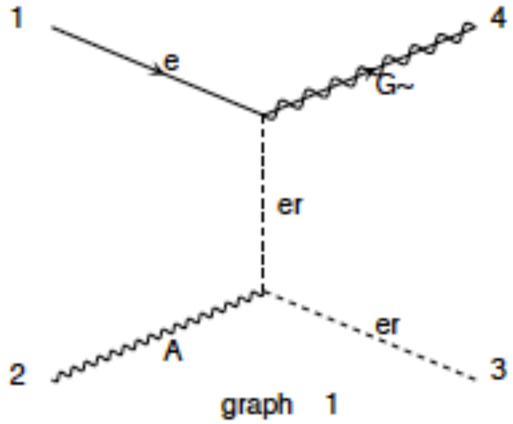

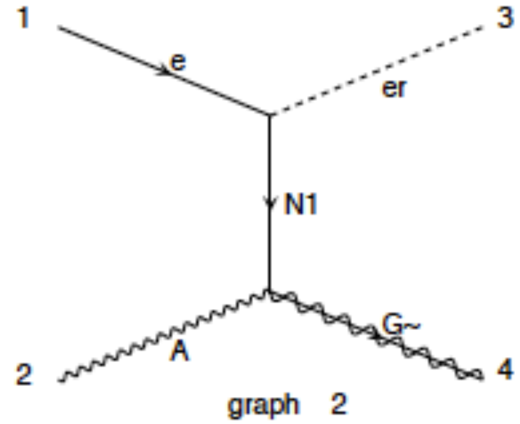

$$e^-\gamma \to \tilde{e}_R^-\tilde{G} \to e^-\tilde{G}\tilde{G} \Rightarrow e^- + \not{E}$$

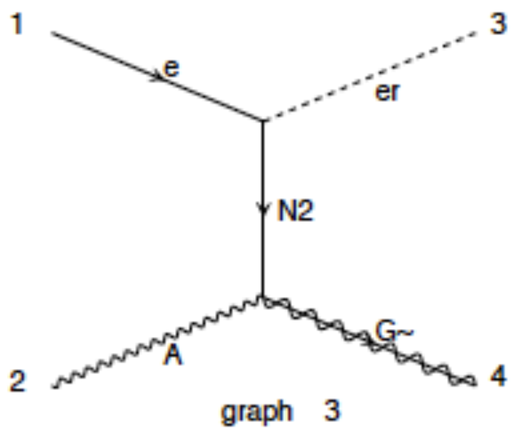

$\lambda_1\lambda$	λ_4			$\hat{\mathcal{M}}^s$	$\hat{\mathcal{M}}^t$	$\hat{\mathcal{M}}^u$	
$++$	$-$	$-2\sin\frac{\theta}{2}$	[	$\frac{m_{\tilde{e}}^2}{s}$	$+\sum_i C_i^\gamma C_i^{\tilde{e}} \frac{m_{\tilde{\chi}_i}^2}{t-m_{\tilde{\chi}_i}^2}$	$+\frac{m_{\tilde{e}}^2}{u-m_{\tilde{e}}^2}\beta\cos^2\frac{\theta}{2}$	]
$+-$	$+$	$-\sin\theta\sin\frac{\theta}{2}$	[		$\sum_i C_i^\gamma C_i^{\tilde{e}} \frac{\sqrt{s}m_{\tilde{\chi}_i}}{t-m_{\tilde{\chi}_i}^2}\beta$		]
$+-$	$-$	$\sin\theta\cos\frac{\theta}{2}$	[			$\frac{m_{\tilde{e}}^2}{u-m_{\tilde{e}}^2}\beta$	]

Table 3. The reduced helicity amplitudes $\hat{\mathcal{M}}_{\lambda_1\lambda,\lambda_4}$ for $e^-_{\lambda_1}\gamma_\lambda \to \tilde{e}_R^-\tilde{G}_{\lambda_4}$.

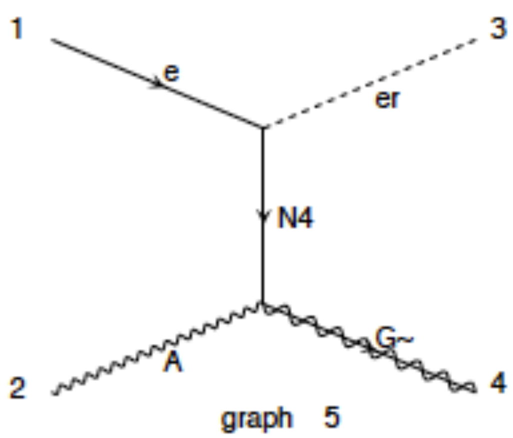

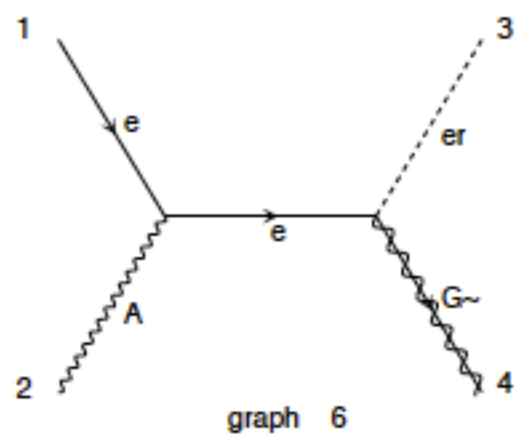

Total cross sections with P(hoton)DF

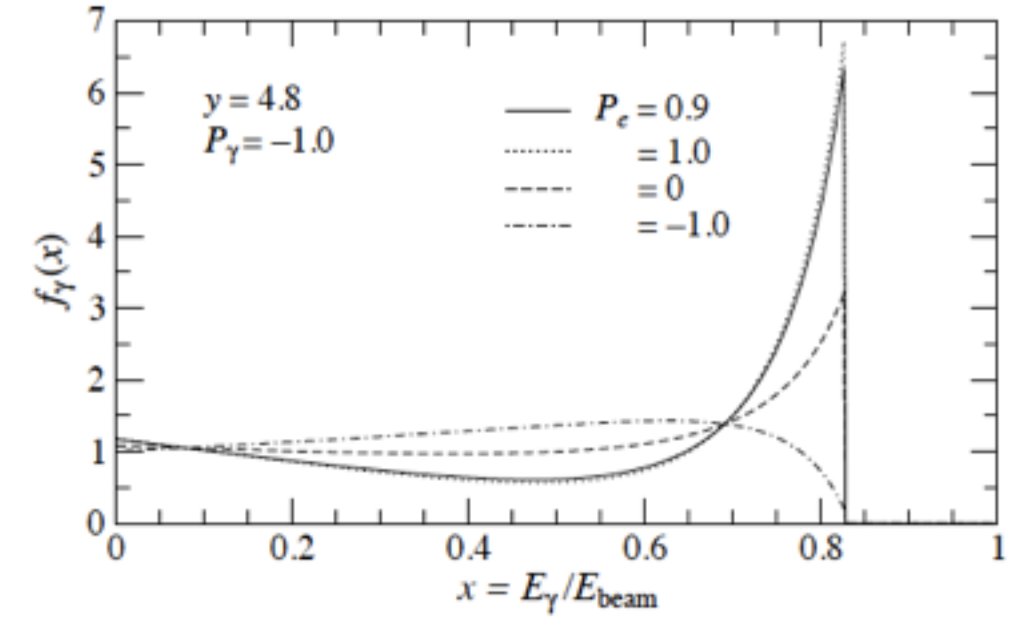

Fig. 8. The distribution functions of the Compton backward scattered photons for different electron beam polarizations.

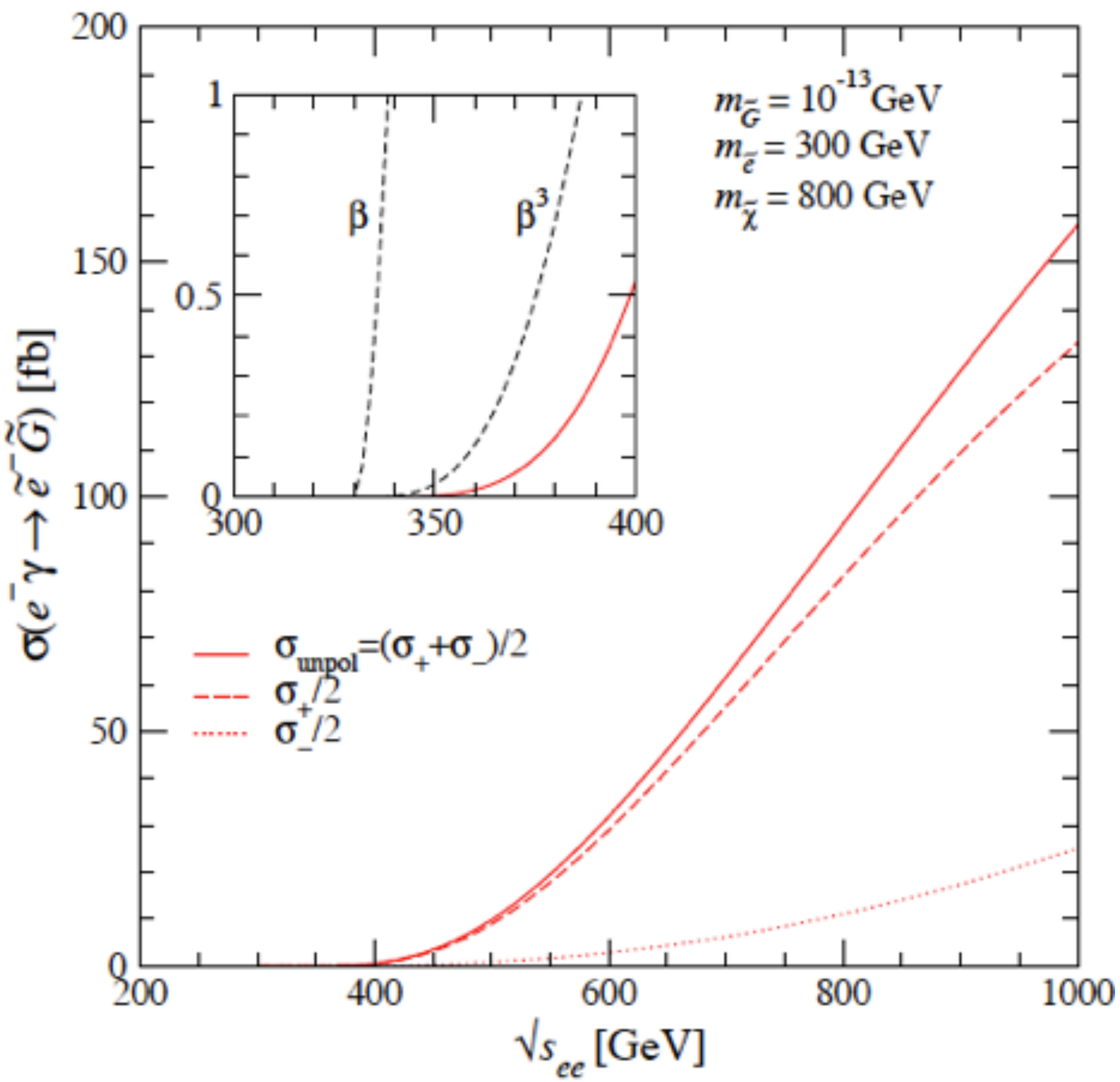

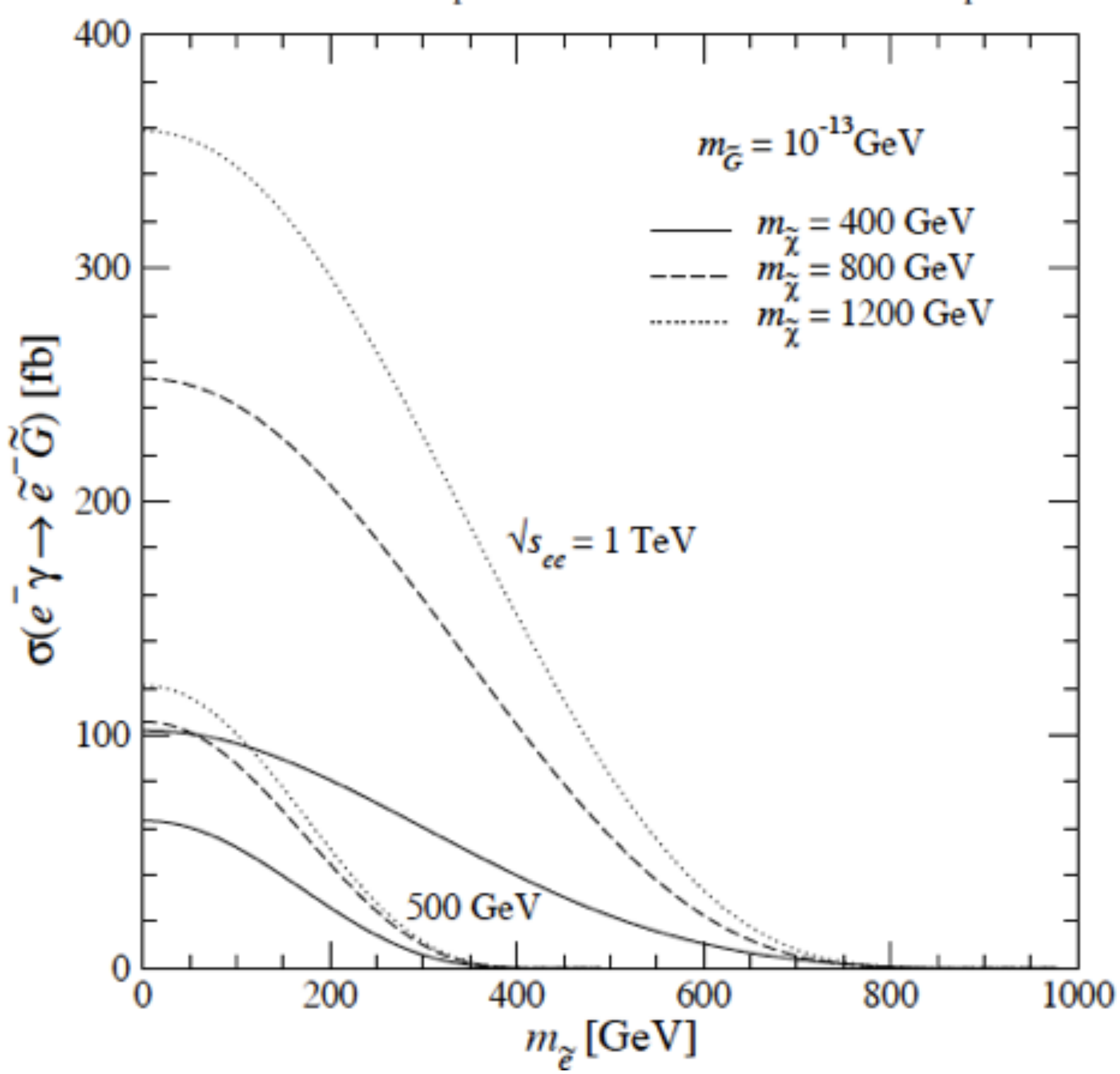

Single-electron + missing energy

σ [fb]		$(P_{e^-}, P_\gamma) =$	$(0,0)$	$(0.9,0)$
$\sqrt{s_{ee}} = 500$ GeV	$m_{\tilde{\chi}} = 400$ GeV		5	9
	800 GeV		9	16
	1200 GeV		10	18
	SM background		2594	284
$\sqrt{s_{ee}} = 1$ TeV	$m_{\tilde{\chi}} = 400$ GeV		58	110
	800 GeV		152	289
	1200 GeV		220	416
	SM background		2796	290

Table 4. Cross sections in fb for the signal $e^-\gamma \to \tilde{e}_R^-\tilde{G} \to e^-\tilde{G}\tilde{G}$, assuming $B(\tilde{e}_R \to e\tilde{G}) = 1$, with $m_{\tilde{G}} = 10^{-13}$ GeV and $m_{\tilde{e}_R} = 300$ GeV and for the SM background $e^-\gamma \to e^-\nu\bar{\nu}$ at $\sqrt{s_{ee}} = 500$ GeV and 1 TeV, with different electron beam polarizations. The minimal cuts in (29) and the Z-peak cut in (30) are taken into account.

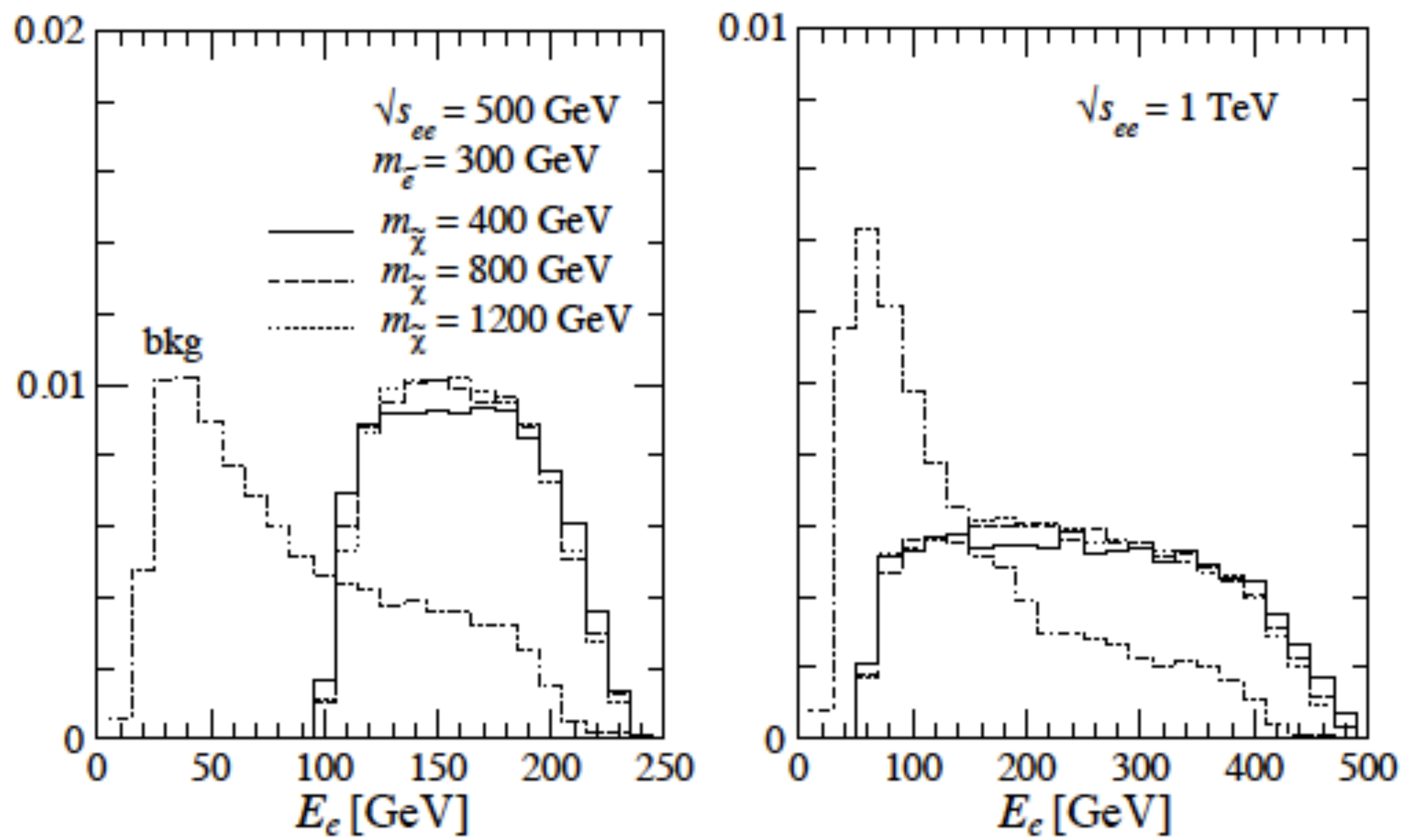

Mono-electron distributions (angle)

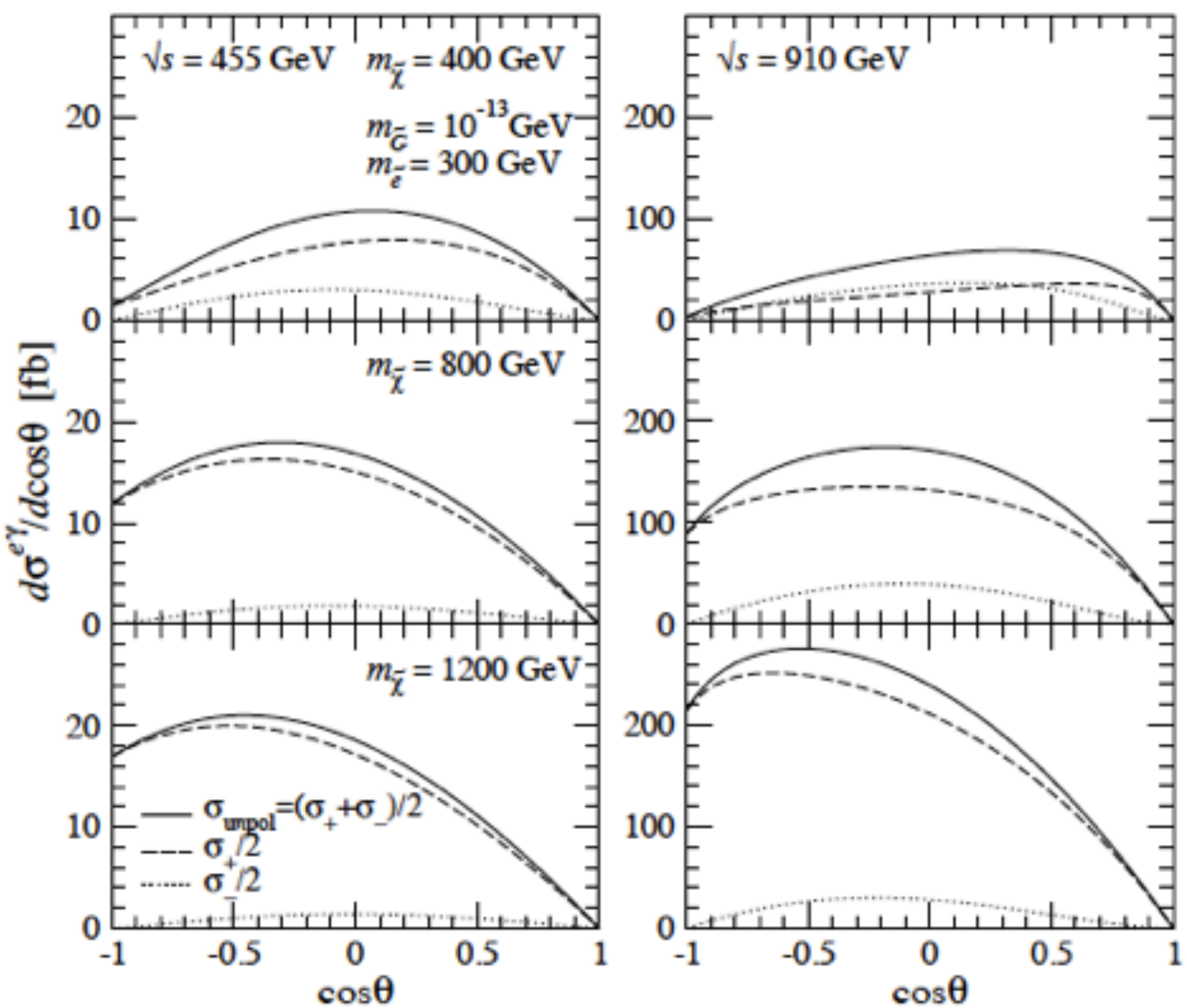

Fig. 11. Angular distributions of selectrons for the process $e^-\gamma \to \tilde{e}_R^- \tilde{G}$ at $\sqrt{s} = 455$ (left) and 910 (right) GeV in the CM frame of the $e^-\gamma$ collisions, with $m_{3/2} = 10^{-13}$ GeV and $m_{\tilde{e}_R} = 300$ GeV. The neutralino masses are taken to be 400 (top), 800 (middle) and 1200 (bottom) GeV, respectively.

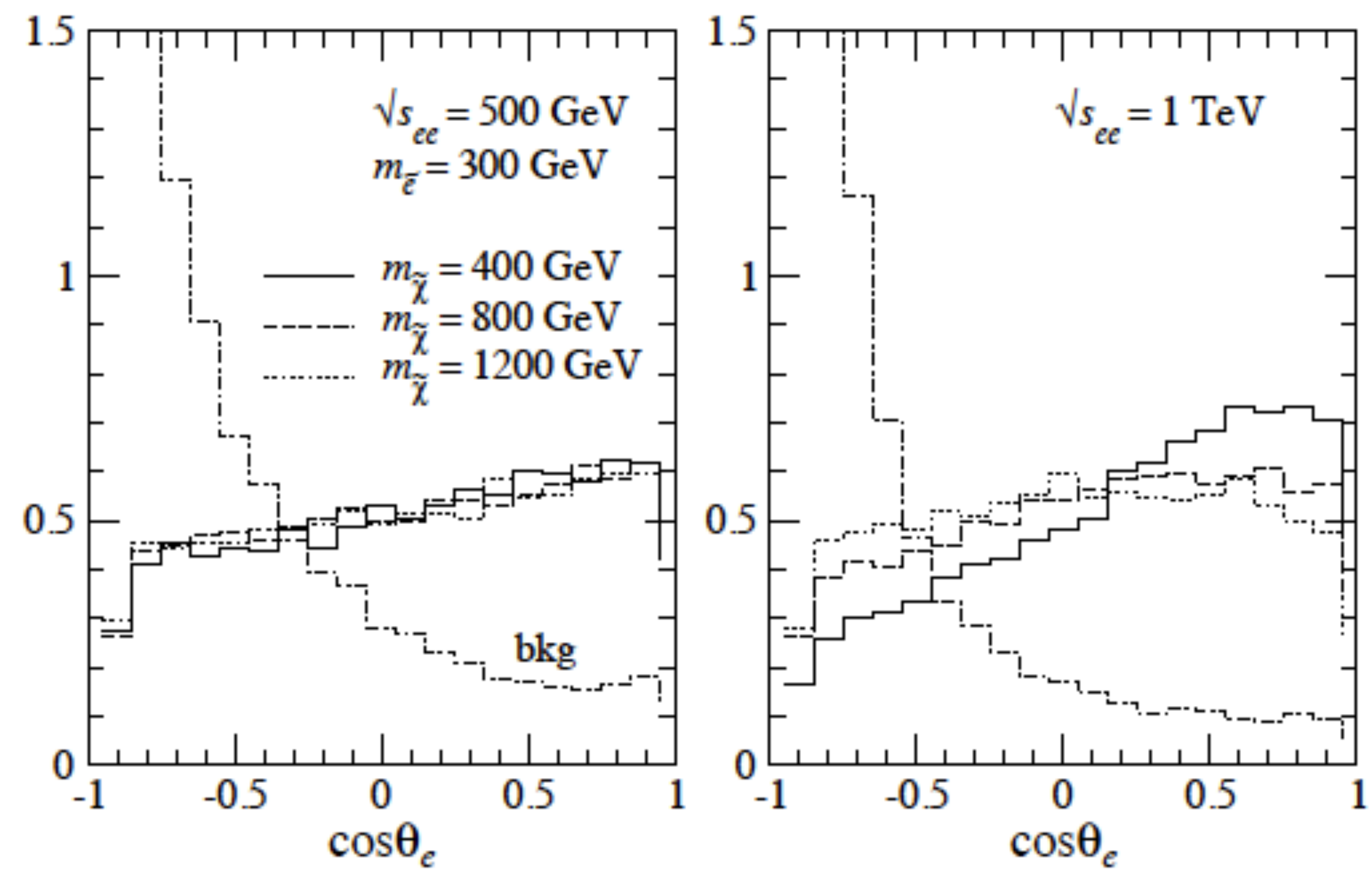

Fig. 13. The same as fig. 12, but for the electron angular distributions in the e^-e^- laboratory frame.

4. Stau NLSP

Buchmuller, Hamaguchi, Ratz, Yanagida, PLB(2004)

- Radiative stau decays to study the spin-3/2 nature of the gravitino

$$\tilde{\tau}_R^- \to \tau^- \tilde{G}\gamma \quad \text{vs.} \quad \tilde{\tau}_R^- \to \tau^- \tilde{\chi}_1^0 \gamma$$

- Photon polarization by means of Stokes parameters

$$\frac{d\rho_{\lambda\lambda'}}{dE_\gamma \, d\cos\theta} = \frac{1}{2}\left(1 + \sum_{i=1}^{3} P_i \sigma_i\right)_{\lambda\lambda'} \cdot \frac{d\Gamma_{\rm sum}}{dE_\gamma \, d\cos\theta}$$

- The photon density matrix

$$d\rho_{\lambda\lambda'} = \frac{1}{2m_{\tilde{\tau}}} \sum \mathcal{M}_\lambda \mathcal{M}^*_{\lambda'} \, d\Phi_3$$

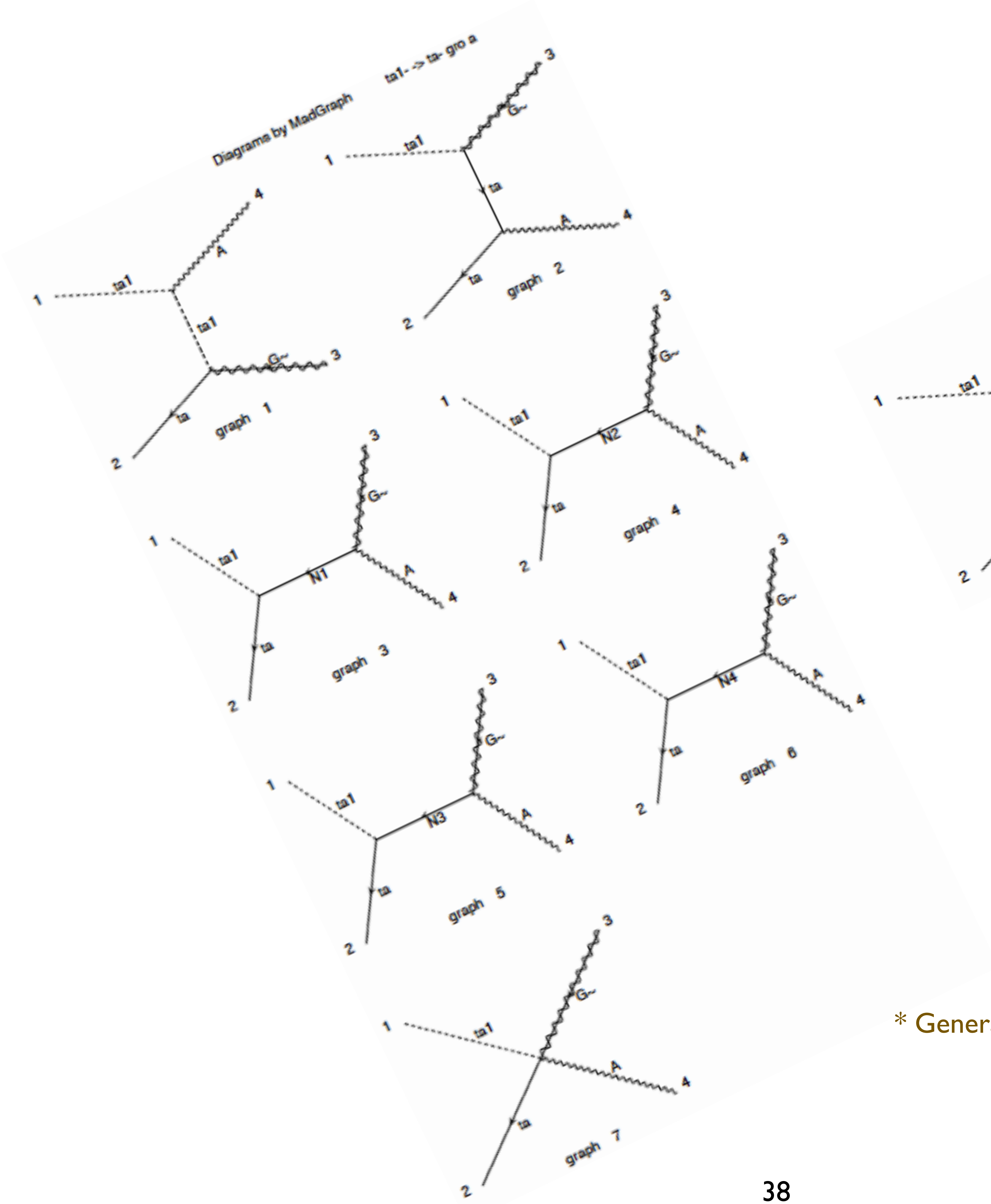

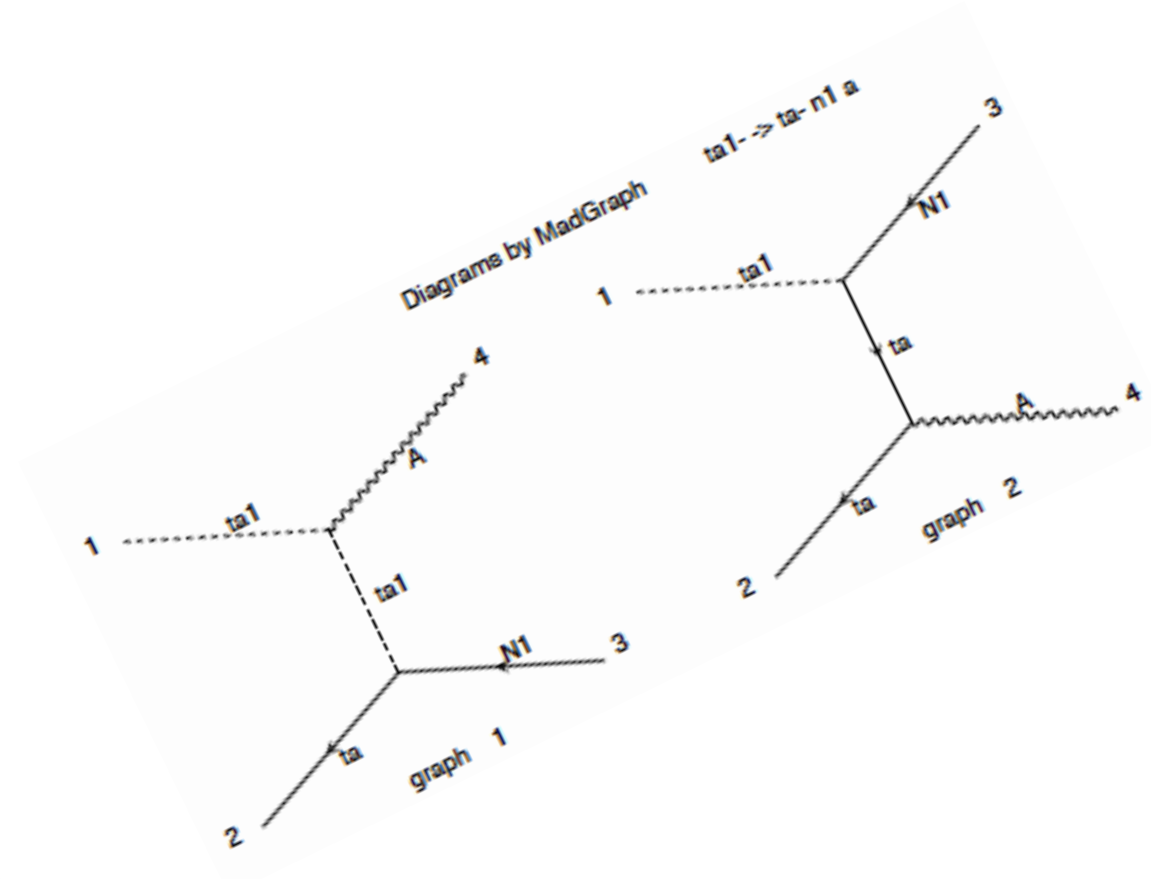

* Generated by MG/ME with gravitinos.

spin-3/2 vs. spin-1/2

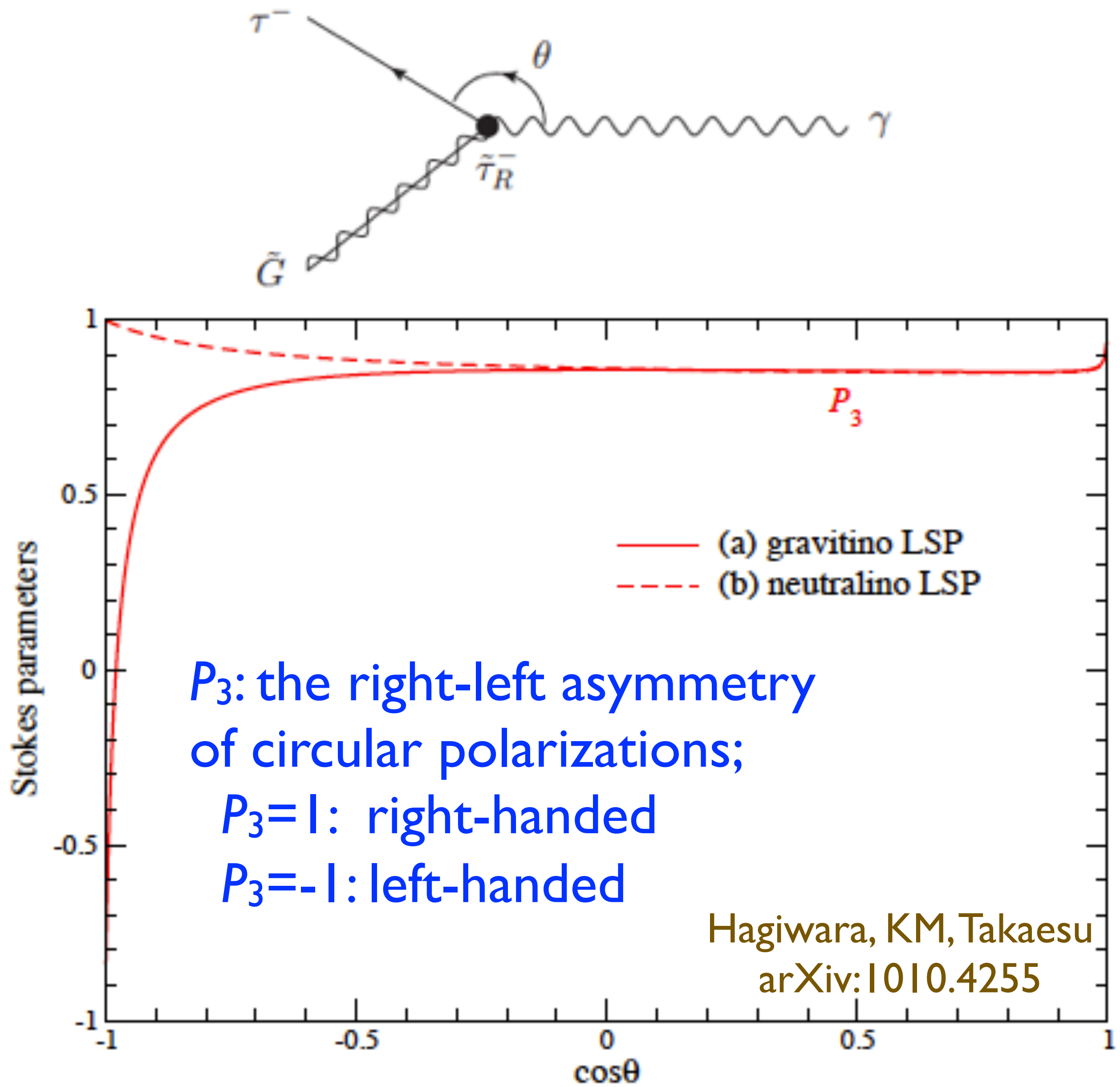

Fig. 3. Angular dependence of the Stokes parameters of the radiated photon for the $\tilde{\tau}$ decay process, $\tilde{\tau}_R \to \tau\tilde{G}\gamma$ (a) and $\tilde{\tau}_R \to \tau\tilde{\chi}_1^0\gamma$ (b), where θ is the decay angle between the photon and the tau-lepton. We set $m_{\tilde{\tau}} = 150$ GeV, $m_{\rm LSP} = 75$ GeV and $E_\gamma = 40$ GeV.

- cosθ>0: the photon bremsstrahlung is dominant, and only 1/2 helicities of the gravitino are allowed.
- cosθ<0: the neutralino propagating amplitudes and the 4-point interaction amplitude become important.
- cosθ~-1: The left-handed photon is only allowed for spin-3/2 LSP, i.e. gravitino.

spin-3/2 vs. spin-1/2

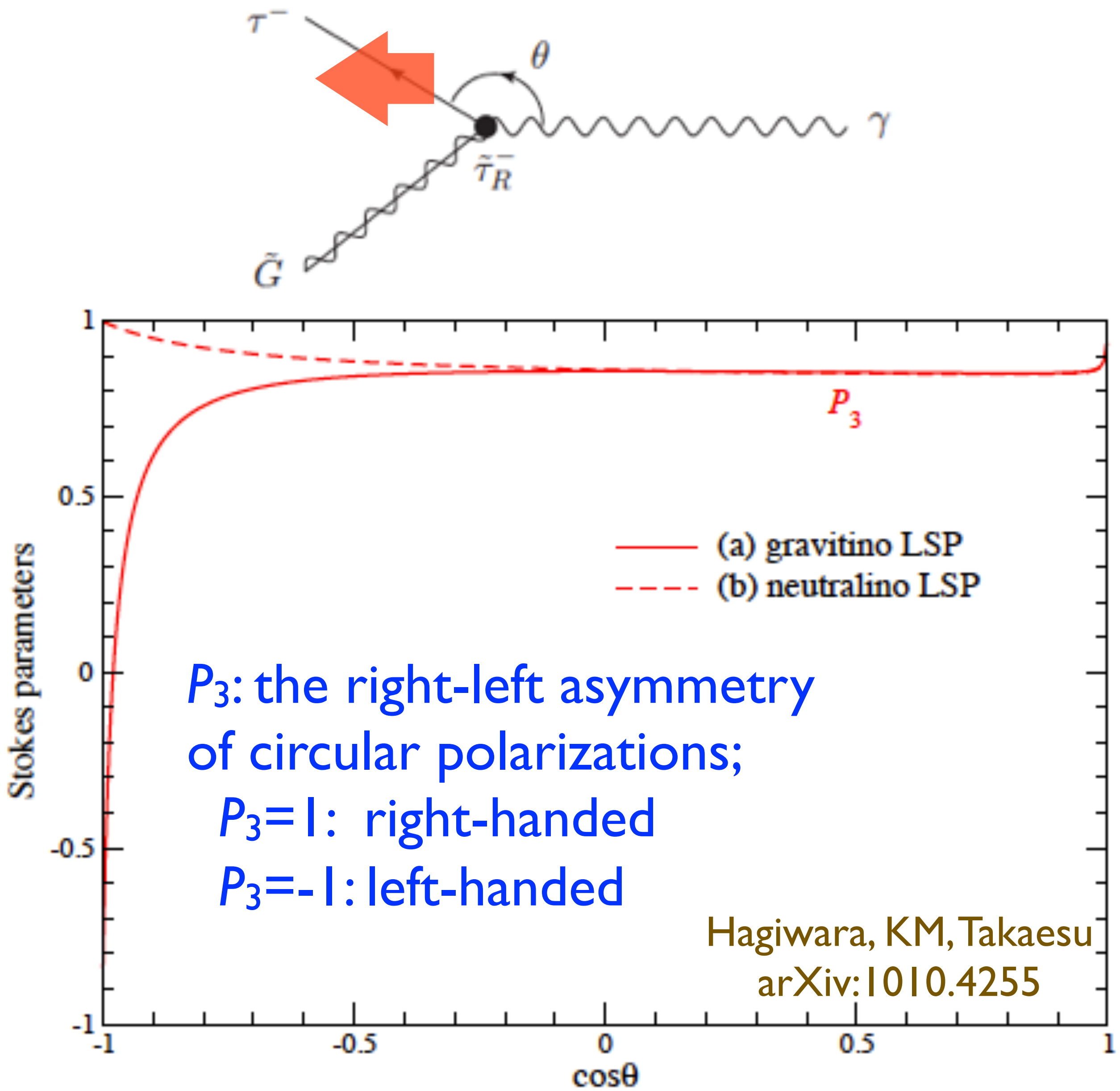

Fig. 3. Angular dependence of the Stokes parameters of the radiated photon for the $\tilde{\tau}$ decay process, $\tilde{\tau}_R \to \tau\tilde{G}\gamma$ (a) and $\tilde{\tau}_R \to \tau\tilde{\chi}_1^0\gamma$ (b), where θ is the decay angle between the photon and the tau-lepton. We set $m_{\tilde{\tau}} = 150$ GeV, $m_{\rm LSP} = 75$ GeV and $E_\gamma = 40$ GeV.

- $\cos\theta>0$: the photon bremsstrahlung is dominant, and only 1/2 helicities of the gravitino are allowed.
- $\cos\theta<0$: the neutralino propagating amplitudes and the 4-point interaction amplitude become important.
- $\cos\theta\sim-1$: The left-handed photon is only allowed for spin-3/2 LSP, i.e. gravitino.

spin-3/2 vs. spin-1/2

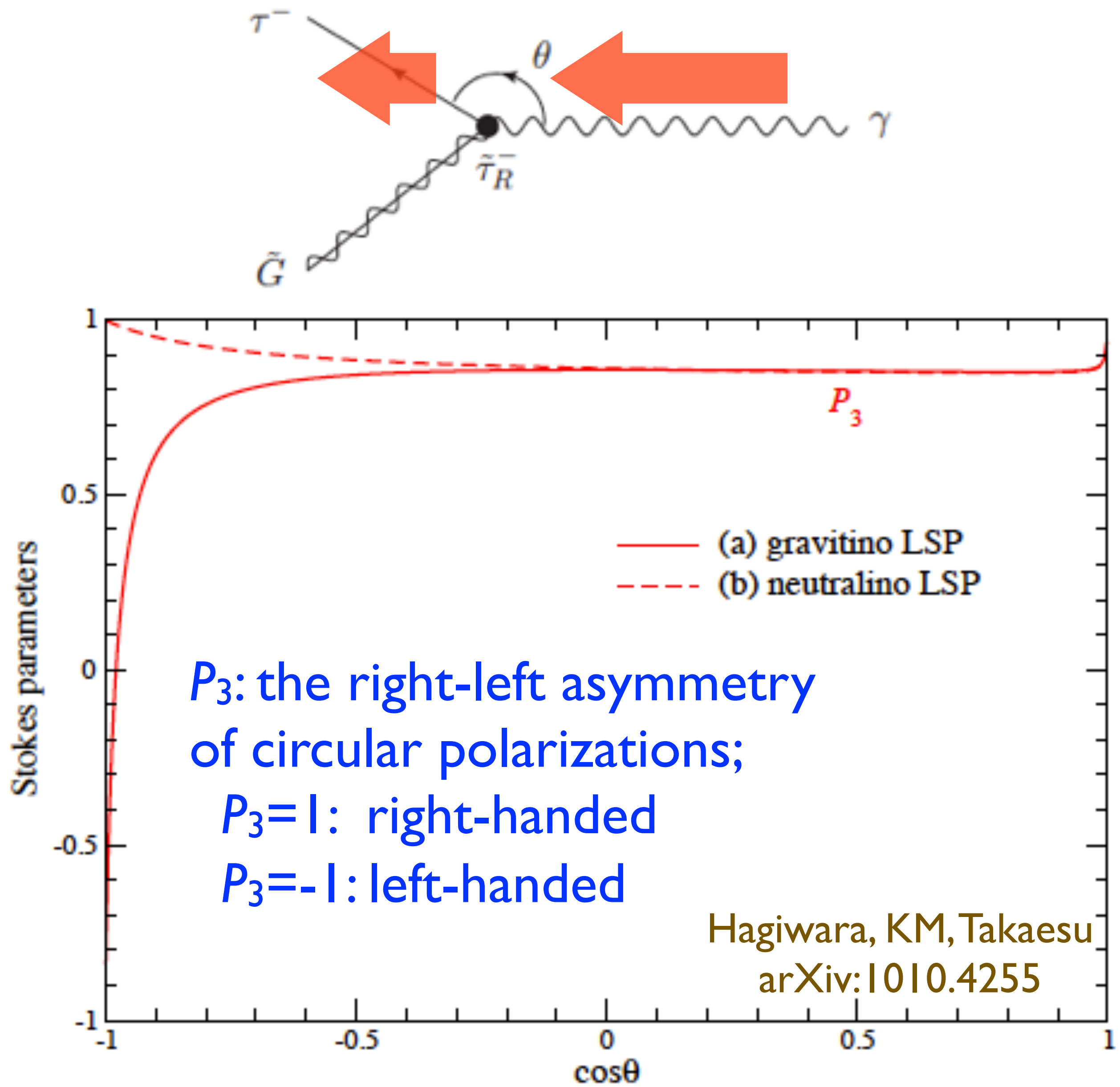

Fig. 3. Angular dependence of the Stokes parameters of the radiated photon for the $\tilde{\tau}$ decay process, $\tilde{\tau}_R \to \tau \tilde{G} \gamma$ (a) and $\tilde{\tau}_R \to \tau \tilde{\chi}_1^0 \gamma$ (b), where θ is the decay angle between the photon and the tau-lepton. We set $m_{\tilde{\tau}} = 150$ GeV, $m_{\rm LSP} = 75$ GeV and $E_\gamma = 40$ GeV.

- $\cos\theta > 0$: the photon bremsstrahlung is dominant, and only 1/2 helicities of the gravitino are allowed.
- $\cos\theta < 0$: the neutralino propagating amplitudes and the 4-point interaction amplitude become important.
- $\cos\theta \sim -1$: The left-handed photon is only allowed for spin-3/2 LSP, i.e. gravitino.

spin-3/2 vs. spin-1/2

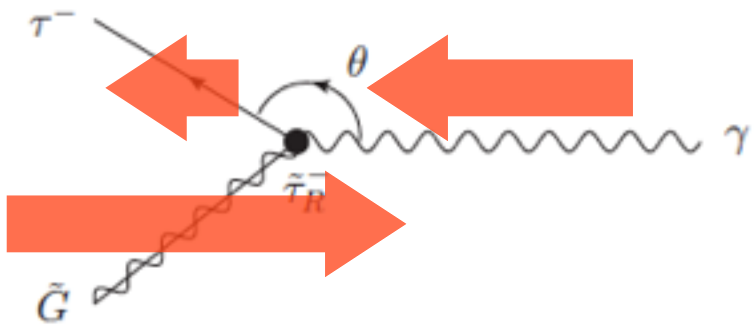

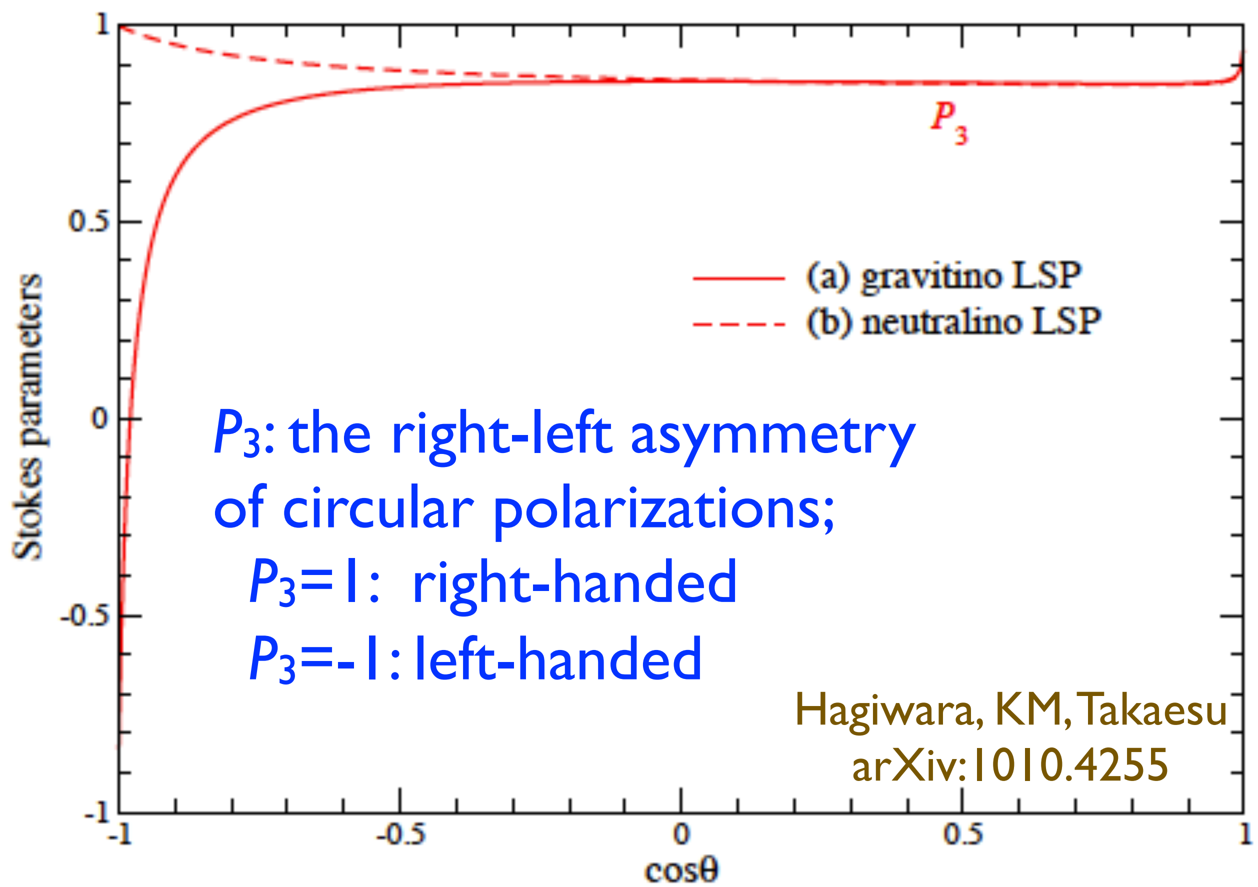

Fig. 3. Angular dependence of the Stokes parameters of the radiated photon for the $\tilde{\tau}$ decay process, $\tilde{\tau}_R \to \tau\tilde{G}\gamma$ (a) and $\tilde{\tau}_R \to \tau\tilde{\chi}_1^0\gamma$ (b), where θ is the decay angle between the photon and the tau-lepton. We set $m_{\tilde{\tau}} = 150$ GeV, $m_{\rm LSP} = 75$ GeV and $E_\gamma = 40$ GeV.

- $\cos\theta>0$: the photon bremsstrahlung is dominant, and only 1/2 helicities of the gravitino are allowed.
- $\cos\theta<0$: the neutralino propagating amplitudes and the 4-point interaction amplitude become important.
- $\cos\theta\sim-1$: The left-handed photon is only allowed for spin-3/2 LSP, i.e. gravitino.

Summary

- Gravitinos can provide rich phenomenology in particle physics as well as in cosmology, and especially play an important role in collider signatures when it is the LSP. The phenomenology really depends on what is the NLSP.
- We (Hagiwara, KM, Takaesu [1010.4255], KM, Takaesu [1101.1289])
  - added new HELAS fortran subroutines to calculate helicity amplitudes with massive gravitinos/goldstinos.
  - coded them in such a way that arbitrary amplitudes with external gravitinos/goldstinos can be generated automatically by MadGraph. (Our implementation was officially supported by MG/MEv4.5, and will be available in MG5 soon.)
  - tested our codes carefully by using the goldstino equivalence theorem as well as the gauge invariance.
- We just started to enjoy "gravitino phenomenology at the LHC" !

back-up

Wavefunction of a spin-3/2 particle

- Rarita-Schwinger wavefunction
- expressed by using the vector boson wavefunctions and the spinor wavefunctions:

$$
\begin{aligned}
\psi_u^\mu(p,+3/2) &= \epsilon^\mu(p,+)\,u(p,+),\\
\psi_u^\mu(p,+1/2) &= \sqrt{\frac{2}{3}}\,\epsilon^\mu(p,0)\,u(p,+)\\
&\quad+\sqrt{\frac{1}{3}}\,\epsilon^\mu(p,+)\,u(p,-)\,e^{i\phi},\\
\psi_u^\mu(p,-1/2) &= \sqrt{\frac{1}{3}}\,\epsilon^\mu(p,-)\,u(p,+)\\
&\quad+\sqrt{\frac{2}{3}}\,\epsilon^\mu(p,0)\,u(p,-)\,e^{i\phi},\\
\psi_u^\mu(p,-3/2) &= \epsilon^\mu(p,-)\,u(p,-)\,e^{i\phi},
\end{aligned}
$$

HELAS

- HELicity Amplitude Subroutines
  - by H. Murayama, I. Watanabe, K. Hagiwara (1992)
  - a set of FORTRAN77 subroutines which enable us to compute the helicity amplitudes of an arbitrary tree-level Feynman diagram with a simple sequence of CALL SUBROUTINE statements.
- e.g., stau_R- > tau- + gravitino

$$i\mathcal{M}_{\sigma_1\sigma_2} = ig\,\bar{u}(p_1,\sigma_1)\,P_L\gamma^\mu\gamma^\nu\,\psi_\mu(p_2,\sigma_2)\,k_\nu$$

• $\tilde{\tau}_R \to \tau + \psi_{3/2}$

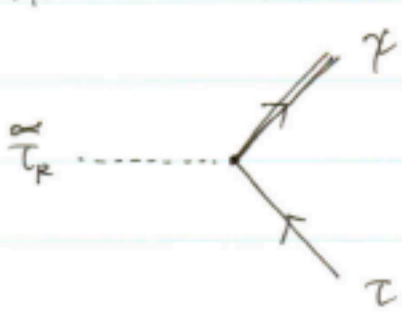

$$\begin{cases} k^\mu = M(1,0,0,0) \\ p_1^\mu = \frac{M}{2}\beta(1,\ \sin\theta\cos\phi,\ \sin\theta\sin\phi,\ \cos\theta) \\ p_2^\mu = \frac{M}{2}\left(1+\frac{m^2}{M^2},\ -\beta\sin\theta\cos\phi,\ -\beta\sin\theta\sin\phi,\ -\beta\cos\theta\right) \end{cases}$$

$$\beta = 1-\frac{m^2}{M^2},\quad E_2+|\vec{p}_2| = M,\quad E_2-|\vec{p}_2| = \frac{m^2}{M}$$

$$\mathcal{M}_{\sigma_1\sigma_2} = g\,\bar{\psi}_\mu(p_2,\sigma_2)\gamma^\nu\gamma^\mu P_R v(p_1,\sigma_1)k_\nu \qquad \left(g=\frac{1}{\sqrt{2}M_{pl}}\right)$$

$$= gM\,\bar{\psi}_\mu(p_2,\sigma_2)\gamma^0\underbrace{\gamma^\mu P_R}_{=\begin{pmatrix}0&\sigma^\mu\\ \bar{\sigma}^\mu&0\end{pmatrix}\begin{pmatrix}0&0\\0&1\end{pmatrix}=\begin{pmatrix}0&\sigma^\mu\\0&0\end{pmatrix}} v(p_1,\sigma_1)$$

$$J^\mu_{\sigma_1\sigma_2'} = u^\dagger(p_2,\sigma_2')\begin{pmatrix}0&\sigma^\mu\\0&0\end{pmatrix}v(p_1,\sigma_1)$$

• $$J^\mu_{-+} = -\sqrt{M\beta}\sqrt{\frac{m^2}{M}}\left(\sin\frac{\theta}{2},\ -\cos\frac{\theta}{2}e^{i\phi}\right)\left[\begin{pmatrix}1&0\\0&1\end{pmatrix},\begin{pmatrix}0&1\\1&0\end{pmatrix},\begin{pmatrix}0&-i\\i&0\end{pmatrix},\begin{pmatrix}1&0\\0&-1\end{pmatrix}\right]\begin{pmatrix}\cos\frac{\theta}{2}\\ \sin\frac{\theta}{2}e^{i\phi}\end{pmatrix}$$

$$= -\sqrt{\beta}m\left[0,\ \sin^2\frac{\theta}{2}e^{i\phi}-\cos^2\frac{\theta}{2}e^{-i\phi},\ -i\left(\sin^2\frac{\theta}{2}e^{i\phi}+\cos^2\frac{\theta}{2}e^{-i\phi}\right),\ 2\sin\frac{\theta}{2}\cos\frac{\theta}{2}\right]$$

$$= -\sqrt{\beta}m\left[0,\ -\cos\theta\cos\phi+i\sin\phi,\ -\cos\theta\sin\phi-i\cos\phi,\ \sin\theta\right]$$

• $$J^\mu_{--} = -\sqrt{M\beta}\sqrt{M}\left(\cos\frac{\theta}{2}e^{i\phi},\ \sin\frac{\theta}{2}\right)\sigma^\mu\begin{pmatrix}\cos\frac{\theta}{2}\\ \sin\frac{\theta}{2}e^{i\phi}\end{pmatrix}$$

$$= -\sqrt{\beta}M\left[e^{i\phi},\ \sin\frac{\theta}{2}\cos\frac{\theta}{2}\left(e^{2i\phi}+1\right),\ -i\sin\frac{\theta}{2}\cos\frac{\theta}{2}\left(e^{2i\phi}-1\right),\ e^{i\phi}\left(\cos^2\frac{\theta}{2}-\sin^2\frac{\theta}{2}\right)\right]$$

$$= -\sqrt{\beta}Me^{i\phi}\left[1,\ \sin\theta\cos\phi,\ \sin\theta\sin\phi,\ \cos\theta\right]$$

$p \to p_2$ i.e. $\phi \to \phi + \pi$
$\therefore e^{i\phi} \to -e^{i\phi}$

$$\cdot\ \psi^\mu(p, -\tfrac{1}{2}) = \sqrt{\tfrac{2}{3}}\, \varepsilon^\mu(p, 0)\, u(p, -)\, e^{i\phi} + \sqrt{\tfrac{1}{3}}\, \varepsilon^\mu(p, -)\, u(p, +)$$

$$\therefore\ \underset{--}{\mathcal{M}_{\sigma_1\sigma_2}} = g M \left[-\sqrt{\tfrac{2}{3}}\, \varepsilon_\mu^*(p_2, 0)\, J^\mu_{--}\, e^{-i\phi} + \sqrt{\tfrac{1}{3}}\, \varepsilon_\mu^*(p_2, -)\, J^\mu_{-+} \right]$$

$$\begin{aligned}
\varepsilon^*(p_2, 0) \cdot J_{--} &= -\sqrt{\beta}\, M\, e^{+i\phi}\, \frac{E_2}{m} \left[\frac{|\vec{p}_2|}{E_2} + 1 \right] \\
&= -\sqrt{\beta}\, M\, e^{i\phi}\, \frac{1}{m} \cdot M \\
&= -\sqrt{\beta}\, \frac{M^2}{m}\, e^{i\phi}
\end{aligned}$$

$$\begin{aligned}
\varepsilon^*(p_2, -) \cdot J_{-+} &= +\sqrt{\beta}\, m\, \frac{1}{\sqrt{2}} \Big[(\cos\theta\cos\phi + i\sin\phi)(-\cos\theta\cos\phi + i\sin\phi) \\
&\qquad + (\cos\theta\sin\phi - i\cos\phi)(-\cos\theta\sin\phi - i\cos\phi) \\
&\qquad - \sin^2\theta \Big] \\
&= -\frac{\sqrt{\beta}}{\sqrt{2}}\, m \left[\cos^2\theta\cos^2\phi + \sin^2\phi + \cos^2\theta\sin^2\phi + \cos^2\phi + \sin^2\theta \right] \\
&= -\sqrt{2\beta}\, m
\end{aligned}$$

$$\begin{aligned}
\therefore\ \mathcal{M}_{--} &= g M \left[+\sqrt{\tfrac{2}{3}}\, \sqrt{\beta}\, \frac{M^2}{m} - \sqrt{\tfrac{2}{3}}\, \sqrt{\beta}\, m \right] \\
&= +\sqrt{\tfrac{2}{3}}\, \sqrt{\beta}\, \frac{M}{m}\, g\, (M^2 \pm m^2)
\end{aligned}$$

$$|\mathcal{M}_{--}|^2 = \frac{2}{3}\, \beta\, g^2\, \frac{M^2}{m^2}\, (M^2 \pm m^2)^2$$

$$\begin{aligned}
\therefore\ \Gamma &= \frac{1}{2M}\, |\mathcal{M}|^2\, d\Phi_2 \\
&= \frac{1}{2M}\, \frac{\beta}{8\pi}\, \frac{2}{3}\, \beta\, \frac{1}{2M_{Pl}^2}\, \frac{M^2}{m^2}\, (M^2 \pm m^2)^2 \\
&= \frac{M^5}{48\pi M_{Pl}^2 m^2} \left(1 - \frac{m^2}{M^2}\right)^2 \left(1 \pm \frac{m^2}{M^2}\right)^2 \\
&= \frac{M^5}{48\pi M_{Pl}^2 m^2} \left(1 - \frac{m^2}{M^2}\right)^4
\end{aligned}$$

$p\to P_2$ i.e. $\phi\to\phi+\pi$ $\therefore e^{i\phi}\to -e^{i\phi}$

$$\cdot\ \Psi^\mu(P,-\tfrac12) = \sqrt{\tfrac23}\,\varepsilon^\mu(P,0)\,u(P,-)\,e^{i\phi} + \sqrt{\tfrac13}\,\varepsilon^\mu(P,-)\,u(P,+)$$

$$\therefore \mathcal{M}_{\underset{--}{\sigma_1\sigma_2}} = gM\left[-\sqrt{\tfrac23}\,\varepsilon^*_\mu(P_2,0)\,J^\mu_{--}\,e^{-i\phi} + \sqrt{\tfrac13}\,\varepsilon^*_\mu(P_2,-)\,J^\mu_{-+}\right]$$

$$\begin{aligned}\varepsilon^*(P_2,0)\cdot J_{--} &= -\sqrt{\beta}\,M\,e^{+i\phi}\,\frac{E_2}{m}\left[\frac{|\vec{P}_2|}{E_2}+1\right]\\ &= -\sqrt{\beta}\,M\,e^{i\phi}\,\frac{1}{m}\cdot M\\ &= -\sqrt{\beta}\,\frac{M^2}{m}\,e^{i\phi}\end{aligned}$$

$$\begin{aligned}\varepsilon^*(P_2,-)\cdot J_{-+} &= +\sqrt{\beta}\,m\,\frac{1}{\sqrt2}\Big[(\cos\theta\cos\phi+i\sin\phi)(-\cos\theta\cos\phi+i\sin\phi)\\ &\qquad + (\cos\theta\sin\phi-i\cos\phi)(-\cos\theta\sin\phi-i\cos\phi)\\ &\qquad - \sin^2\theta\Big]\\ &= -\frac{\sqrt{\beta}}{\sqrt2}\,m\left[\cos^2\theta\cos^2\phi+\sin^2\phi+\cos^2\theta\sin^2\phi+\cos^2\phi+\sin^2\theta\right]\\ &= -\sqrt{2\beta}\,m\end{aligned}$$

$$\begin{aligned}\therefore \mathcal{M}_{--} &= gM\left[+\sqrt{\tfrac23}\sqrt{\beta}\,\frac{M^2}{m} - \sqrt{\tfrac23}\sqrt{\beta}\,m\right]\\ &= +\sqrt{\tfrac23}\sqrt{\beta}\,\frac{M}{m}\,g\,(M^2\pm m^2)\end{aligned}$$

$$|\mathcal{M}_{--}|^2 = \frac23\,\beta\,g^2\,\frac{M^2}{m^2}\,(M^2\pm m^2)^2$$

$$\begin{aligned}\therefore \Gamma &= \frac{1}{2M}\,|\mathcal{M}|^2\,d\Phi_2\\ &= \frac{1}{2M}\,\frac{\beta}{8\pi}\,\frac{2}{3}\,\beta\,\frac{1}{2M_{Pl}^2}\,\frac{M^2}{m^2}\,(M^2\pm m^2)^2\\ &= \frac{M^5}{48\pi M_{Pl}^2 m^2}\left(1-\frac{m^2}{M^2}\right)^2\left(1\pm\frac{m^2}{M^2}\right)^2\\ &= \frac{M^5}{48\pi M_{Pl}^2 m^2}\left(1-\frac{m^2}{M^2}\right)^4\end{aligned}$$

➡ Reliable tools to generate amplitudes and to calculate them automatically are needed!

HELAS

- HELicity Amplitude Subroutine
- e.g., stau1- > tau- + gravitino

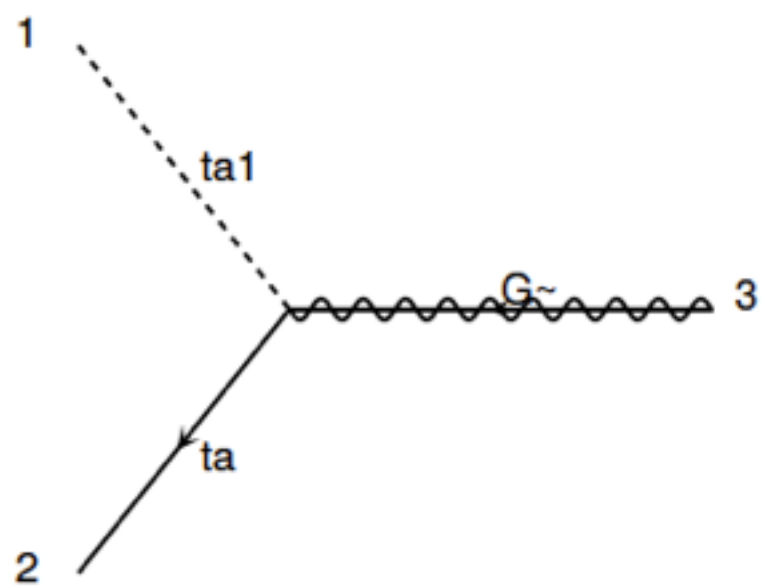


```
CALL SXXXXX(P1,                    -1,  W1)
CALL OXXXXX(P2, MST1, HEL2, +1,  W2)
CALL IRXXXX(P3, MGRO, HEL3, -1,  W3)

CALL IROSXX(W3, W2, W1, GFRS,    AMP)
```

MadGraph/MadEvent

- A software that allows you to generate amplitudes and events for any process in any model.
  - MG by T. Stelzer and W.F. Long (1994)
  - ME by F. Maltoni and T. Stelzer (2003)
- Put your process, e.g., p p > go gro (proton+proton > gluino+gravitino)
  ./bin/newprocess
- MG automatically draws all possible Feynman diagrams and writes corresponding HELAS codes.
- Set your parameters, e.g., masses, couplings, collider energy, kinematical cuts, ...
  ./bin/generate_events
- ME gives you cross sections and distributions.